



HAL
open science

Cellulose II aerogels: a review

Tatiana Budtova

► **To cite this version:**

Tatiana Budtova. Cellulose II aerogels: a review. *Cellulose*, 2019, 26 (1), pp.81-121. 10.1007/s10570-018-2189-1 . hal-02419114

HAL Id: hal-02419114

<https://hal.science/hal-02419114>

Submitted on 20 Mar 2023

HAL is a multi-disciplinary open access archive for the deposit and dissemination of scientific research documents, whether they are published or not. The documents may come from teaching and research institutions in France or abroad, or from public or private research centers.

L'archive ouverte pluridisciplinaire **HAL**, est destinée au dépôt et à la diffusion de documents scientifiques de niveau recherche, publiés ou non, émanant des établissements d'enseignement et de recherche français ou étrangers, des laboratoires publics ou privés.

1 *Submitted to Cellulose 13 September 2018*

2 *Submitted revised version 19 November 2018*

3

4

Cellulose II aerogels: a review

5

6

Tatiana Budtova

7

8 MINES ParisTech, PSL Research University, Center for Materials Forming (CEMEF), UMR CNRS 7635,

9

CS 10207, 06904 Sophia Antipolis, France

10

11

12

13 Corresponding author: Tatiana Budtova

14 Email: Tatiana.Budtova@mines-paristech.fr

15

16

17

18 Acknowledgements.

19 I would like to devote this review and warmly thank my PhD and Master students and post-doctoral

20 researchers without whom the progress in bio-aerogels in general and this article in particular would

21 not have been possible.

22

23
24
25
26
27
28
29
30
31
32
33
34
35
36
37
38
39
40
41
42
43
44
45
46
47
48

Table of contents

ABSTRACT

1. INTRODUCTION

2. PREPARATION PATHWAYS, MECHANISMS OF STRUCTURE FORMATION AND CHARACTERIZATION OF BIO-AEROGELS

2.1. Overall approach in making bio-aerogels and mechanisms of structure formation

2.2. Shaping, kinetics of solvent exchange and drying

2.3. Characterisation of bio-aerogels

3. CELLULOSE AEROGELS: CASE STUDIES

3.1. Aerogels from cellulose dissolved via derivatization

3.2. Aerogels from cellulose dissolved in direct aqueous solvents

3.3. Aerogels from cellulose dissolved in direct non-aqueous solvents

4. OVERVIEW ON CELLULOSE II AEROGELS STRUCTURE AND PROPERTIES

4.1. Volume change during processing

4.2. Trends in density, morphology and specific surface area

4.3. Mechanical properties of cellulose II aerogels and their composites

4.4. Thermal conductivity of cellulose II aerogels and their composites

5. POTENTIAL APPLICATIONS OF CELLULOSE II AEROGELS

5.1. Bio-medical applications

5.2. Absorption and adsorption

5.3. Composite aerogels with metal particles and quantum dots

5.4. Carbon aerogels

6. CONCLUSIONS AND PROSPECTS

49 **ABSTRACT**

50

51 Cellulose II aerogels are light-weight, open pores materials with high specific surface area. They
52 are made in the same way as bio-aerogels based on other polysaccharides, via dissolution-(gelation)-
53 solvent exchange-drying with supercritical CO₂. Gelation step is often omitted as cellulose allows
54 keeping 3D shape during solvent exchange (which leads to cellulose coagulation) and drying. Drying
55 in supercritical conditions preserves the porosity of “wet” (coagulated) cellulose.

56 There are numerous ways to vary cellulose II aerogel morphology and properties by changing
57 processing conditions and cellulose type. Together with chemical and physical modifications of
58 cellulose and possibility of making hybrid and composite materials (organic-inorganic and organic-
59 organic), it opens up a huge variety of aerogel properties and applications. On one hand, they are
60 similar to those of classical aerogels, i.e. can be used for absorption and adsorption, as catalysts and
61 catalysts support and in electro-chemistry when pyrolysed. On the other hand, because no toxic
62 compounds are involved in the preparation of cellulose aerogels, they can be used in life science
63 applications such as pharma, bio-medical, food and cosmetics.

64 The review makes an overview of results reported in literature on the structure and properties
65 of cellulose II aerogels and their applications. The reader may be surprised finding more questions
66 than answers and clear trends. The review shows that several fundamental questions still remain to
67 be answered and applications to be explored.

68

69 Keywords: cellulose; aerogel; density; structure; surface area; mechanical properties

70

71 **1. INTRODUCTION**

72 This review is devoted to cellulose II based aerogels and the term “aerogel” will be first defined as
73 literature provides different approaches. According to IUPAC Gold Book, aerogel is a “Gel comprised
74 of a microporous solid in which the dispersed phase is a gas” with examples such as “Microporous
75 silica, microporous glass and zeolites” (IUPAC. Compendium of Chemical Terminology 2014). This
76 definition is very restrictive as it includes only microporous materials, i.e. with pore sizes below 2 nm,
77 and thus excludes, for example, classical silica aerogels which have pores of some tens of
78 nanometers. Aerogel scientists now agree that aerogels are open pores solid networks with high
79 porosity (at least 90%), high specific surface area (“although no official convention really exists”
80 (Pierre 2011) and are nanostructured (mainly mesoporous with small macropores). These structural
81 properties make aerogels very attractive for various applications such as acoustic and thermal
82 insulation (some aerogels are superinsulating materials, i.e. with thermal conductivity lower than
83 that of air in ambient conditions), catalysts and catalyst supports, for adsorption and absorption,
84 particle detectors (Cerenkov counters), electrochemical when pyrolysed and as matrices for drug
85 delivery.

86 The first aerogels were synthesized via sol-gel chemistry and reported by Kistler; solvent was
87 removed from the gel by drying in super-critical conditions (Kistler 1931). In this case capillary
88 pressure, which develops during drying and is responsible for pores’ collapse, is theoretically zero as
89 no liquid–vapor interface (no meniscus) is formed in super-critical state.

90 Since that time silica aerogels, with density around 0.1 g/cm^3 and specific surface area around
91 $800\text{-}1000 \text{ m}^2/\text{g}$ and higher, became the most studied reference aerogel materials. Their major
92 industrialized application is thermal insulation materials due to ultra-low thermal conductivity,
93 around $0.012\text{-}0.014 \text{ W/m.K}$ against 0.025 W/m.K for air. It should be noted that very similar
94 properties have been obtained for hydrophobised (silylated) silica dried at ambient pressure and
95 slightly elevated temperature (around $130 - 150 \text{ }^\circ\text{C}$). However, silica gels break during drying in the
96 course of so-called “spring-back” effect, i.e. re-opening of the pores during the last stage of drying

97 due to the repulsion of the grafted groups and certain elasticity of the solid network which recovers
98 its shape after contraction. Ambient-pressure dried silica-based “xerogels” with structure and
99 properties equivalent to supercritically dried aerogels is a unique example of ambient-dried
100 lightweight thermal superinsulating mesoporous materials.

101 Next generations of aerogels developed in the 70s-80s of the last century were based on metal
102 oxides (titanium, zirconium, aluminum) and their “mixtures” with silica (Teichner 1986) and on
103 synthetic polymers (resorcinol-formaldehyde (Pekala 1989), polyurethane (Biesmans et al. 1998),
104 polyimide (Meador et al. 2015), etc.) and their hybrids with silica (Maleki et al. 2014). Polymer
105 aerogels showed improved mechanical properties, as compared to silica ones, some possessed very
106 low thermal conductivity and interesting electro-chemical properties when pyrolysed. For more
107 information on silica and synthetic polymer aerogels the reader is advised to consult Aerogels
108 Handbook (Aegerter 2011).

109 A new generation of aerogels appeared at the beginning of the 21st century: they are biomass
110 based, mainly polysaccharide-based, and are thus called bio-aerogels. Their synthesis is inspired by
111 that of classical aerogels, from polymer dissolution to solution gelation (in some case this step can be
112 omitted which is one of the specificities of polysaccharide aerogels) followed by solvent exchange
113 and drying with supercritical carbon dioxide. Compared to silica aerogels which are extremely fragile,
114 bio-aerogels do not break under compression, with plastic deformation up to 80 % strain before pore
115 wall collapse (Sescousse et al. 2011a; Rudaz et al. 2014; Pircher et al. 2016). Bio-aerogels are of low
116 density, 0.05 – 0.2 g/cm³, and rather high specific surface area, from 200 to 600 m²/g. It seems that
117 the latter strongly depends on the type of polysaccharide but why and how is an open question.

118 The preparation of bio-aerogels does not involve any toxic components. This makes bio-aerogels
119 “human-friendly” and thus very attractive in life-science applications such as matrices for controlled
120 release and scaffolds (García-González et al. 2011; Veronovski et al. 2014). Bio-aerogels also possess
121 properties similar to synthetic polymer and inorganic aerogels: some are with thermal
122 superinsulating properties (Rudaz et al. 2014, Groult and Budtova 2018a) (but cellulose aerogels are

123 not as it will be shown in Section 4), some can be used as matrices for catalysis (Chitchigrovsky et al.
124 2009), in electrochemical applications when pyrolyzed (Budarin et al. 2006; Guilminot et al. 2008) and
125 for adsorption and/or separation (Quignard et al. 2008).

126 The number of publications on polysaccharide-based aerogels strongly increased the past 10
127 years. However, not always the term “aerogel” is used for mesoporous material with high specific
128 surface area: for example, in the first publication on starch aerogels in 1995 they were called
129 “microcellular foams” (Glenn et al. 1995). Cellulose aerogels obtained in 1993 from viscose were
130 simply called “porous cellulose” (Ookuma et al. 1998), which was also the case of a recent
131 publication on cellulose aerogel made from cellulose/ionic liquid solutions (Voon et al. 2016), and
132 also “nanoporous cellulose” (Cai et al. 2009). Cellulose aerogels obtained from cellulose dissolved in
133 direct solvents are sometimes called “aerocellulose” (Gavillon and Budtova 2008) and this term is
134 extended to “aeropolysaccharides” (Rein and Cohen 2011). In our days, the term “aerogel” is
135 sometimes overused as far as porous, but not necessarily mesoporous materials, are called
136 “aerogels”. This is often the case when a polysaccharide “system” (solution or gel or suspension) is
137 freeze-dried leading to ultra-light but highly macroporous materials, thus with low specific surface
138 area. The latter should be named “foams”, as suggested for nanocellulose based low-density
139 materials (Lavoine and Bergstrom 2017). Two excellent recent reviews on nanocellulose gels,
140 aerogels and foams summarise their physical and chemical properties, functionalization routes and
141 potential applications (Lavoine and Bergstrom 2017; De France et al. 2017). A chapter on cellulose I
142 and cellulose II various porous materials makes an overview of the influence of processing conditions
143 on materials’ properties and potential applications (Liebner et al. 2016).

144 The goal of this review is to focus on cellulose aerogels obtained via dissolution route only, i.e.
145 cellulose II based aerogels and their composites. Only dry lightweight cellulose II with certain
146 mesoporosity, i.e. specific surface area higher than around 100 m²/g, will be considered. This is
147 usually the case when drying is performed with supercritical CO₂. Few exceptional cases when other

148 types of dryings, lyophilisation or ambient pressure/low vacuum drying, lead to the elevated specific
149 surface area, will also be briefly presented.

150 The preparation pathways, structure, properties and potential applications will be analysed and
151 discussed together with some problems and challenges. Despite a certain number of publications on
152 cellulose II aerogels there are still more open questions than clear trends. While the topic “cellulose II
153 aerogels” may look narrow, it contains several fundamental questions, such as the understanding of
154 structure formation during cellulose coagulation. Thanks to drying with supercritical CO₂, which
155 keeps reasonably intact the morphology of “wet” cellulose, the latter can be “seen” and analysed.
156 The understanding of the correlations between structure formation, aerogel morphology and
157 properties is the key in the successful development of cellulose II aerogels’ applications which are
158 now mainly at the level of trials and errors.

159 The review is structured as follows. First, the general pathways in the preparation of cellulose II
160 aerogels are presented, together with characterization methods. Then, “case studies” provide more
161 details on cellulose II aerogels made from different solvents; their main properties are summarized in
162 Table S1 of the Supporting Information. The next section compares structure and properties of
163 aerogels made via different pathways. Finally, potential applications are presented and discussed.

164

165 **2. PREPARATION PATHWAYS, MECHANISMS OF STRUCTURE FORMATION AND** 166 **CHARACTERIZATION OF BIO-AEROGELS**

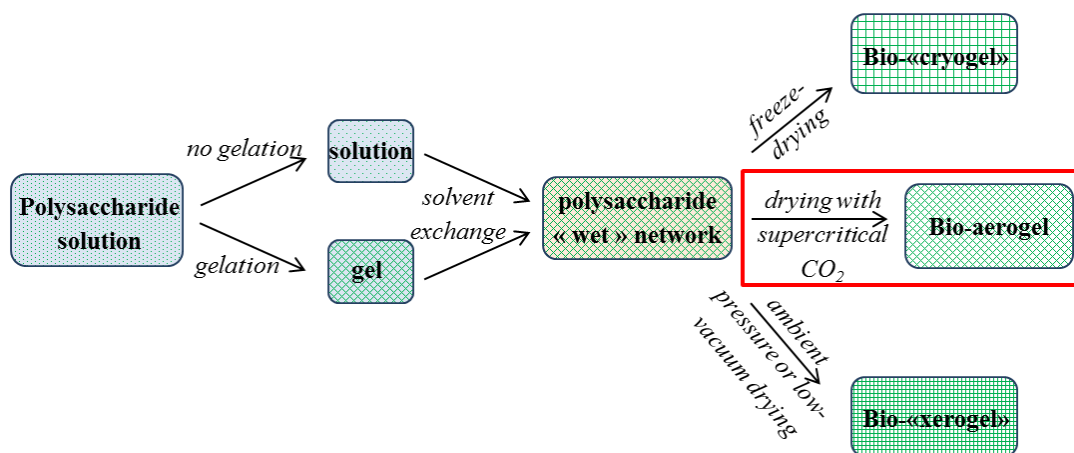
167 In this section, the general principles of bio-aerogel preparation are presented, the majority
168 being applicable to cellulose II case. The main differences with other polymer and inorganic aerogel
169 synthesis pathways are discussed. The mechanisms of aerogel structure formation are suggested.
170 The methods for bio-aerogel shaping, drying and characterization are presented.

171

172 **2.1. Overall approach in making bio-aerogels and mechanisms of structure formation**

173 Synthesis pathways for bio-aerogels are schematically presented in Figure 1. For simplicity we
 174 will call “cryogels” those that are obtained via freeze-drying and “xerogels” via ambient pressure or
 175 low vacuum drying; they are shown for having a complete overview of options and will be discussed
 176 in Section 2.2. An illustration of samples of cellulose aerogel precursor (or “wet” network with water
 177 in the pores, often called “cellulose hydrogel”) together with cellulose cryo-, aero- and xerogel made
 178 from the same solution, is presented in Figure 2.

179



180

181

Figure 1

182

Schematic presentation of bio-aerogels synthesis pathways

183



184

185

Figure 2

186

Example of “wet” cellulose aerogel precursor and aero-, cryo- and xerogel obtained from 7 wt%

187

cellulose/1-ethyl-3-methylimidazolium acetate/dimethyl sulfoxide solutions. For more details see

188

(Buchtova and Budtova 2016). Reprinted by permission from: [Springer] [Cellulose] [Buchtova N,

189

Budtova T (2016) Cellulose aero-, cryo- and xerogels: towards understanding of morphology control,

190

Cellulose 23:2585–2595], [2016]

191

192 Contrary to inorganic and synthetic polymer aerogels, the starting matter in bio-aerogels is not a
193 solution of monomers or a colloidal suspension, but a solution of “ready” polymers, here,
194 polysaccharides. No polymerization step is involved unless composite or hybrid aerogels are made
195 involving a second component (organic or inorganic) polymerized inside polysaccharide network. For
196 cellulose II aerogels it is the case, for example, of cellulose/silica interpenetrated aerogel network.

197 As follows from the name “aerogel”, it is made by replacing the solvent in a gel by air. If willing
198 to remove the solvent and preserve mesoporosity, drying with supercritical CO₂ is recommended.
199 Because in most of the cases the solvent of polysaccharide, often aqueous, is immiscible with CO₂
200 (except when aerogels are based on cellulose esters soluble in acetone), the solvent should be
201 replaced by a liquid which is miscible with both, solvent and CO₂. Acetone and alcohols are often
202 used for this purpose, all being non-solvents for the majority of natural polysaccharides, including
203 cellulose. As it will be demonstrated in the following, gelation step is not a pre-requisite in the case
204 of aerogels based on polysaccharides, and this is one of the significant differences between bio-
205 aerogels and other organic or inorganic aerogels. It is thus possible to make aerogels when the state
206 of the matter before solvent exchange is either solution or gel, as shown in Figure 1. In both cases
207 coagulated polysaccharide “wet” network is formed (with non-solvent in the pores), but the
208 mechanisms of structure formation are different.

209 When the state of the matter before solvent exchange is solution, non-solvent induced phase
210 separation occurs. This process is very similar to the formation of membranes via phase inversion
211 also known as “immersion precipitation”, but drying with supercritical CO₂ leads to highly porous
212 open-pore network with thin pore walls. Here another specificity of polysaccharides is manifesting:
213 despite certain volume shrinkage, the macromolecules do not totally collapse under solvent→non-
214 solvent exchange even if they are not gelled. Above polymer overlap concentration a 3D network is
215 formed. Chain rigidity and formation of polysaccharide networks stabilized by hydrogen bonds are
216 probably the reasons of polymer “resistance” to coagulant. To avoid packing of polymer chains into

217 dense domains, solvent→non-solvent exchange is usually performed in a gradual way, by slowly
218 increasing the fraction of non-solvent. The kinetics of phase separation probably plays a certain role
219 in structure formation.

220 When the state of the matter before solvent exchange is gel (for example, case of alginate or
221 pectin cross-linked with polyvalent metal ions or aged cellulose/(7-9)%NaOH-water), the structure of
222 future aerogel network is already pre-formed. Solvent→non-solvent exchange and drying with
223 supercritical CO₂ do not seem to strongly affect gel morphology. The examples of different aerogel
224 morphologies obtained from gelled and non-gelled pectin solutions are shown by Groult and Budtova
225 2018b. For example, aerogels from non-gelled pectin solutions are denser (0.1 – 0.15 g/cm³) and with
226 higher specific surface area (400 – 600 m²/g) as compared to their gelled counterparts (density 0.05 –
227 0.1 g/cm³ and specific surface area 250 – 500 m²/g) (Groult and Budtova 2018b).

228 Contrary to most of polysaccharide-based aerogels, the pathway to make cellulose II aerogels
229 has been, till now, via non-solvent induced phase separation, i.e. without solution physical or
230 chemical gelation. This is probably due to the traditions developed in processing of cellulose from
231 solutions: spinning fibers and casting films are made by direct coagulation or regeneration of
232 cellulose in a non-solvent (usually water). Another reason is that except cellulose/(7-9)%NaOH/water
233 solutions that are spontaneously gelling with time and temperature increase, gelling cellulose
234 solutions is not as easy as gelling other polysaccharides such as alginate, pectin or carrageenan which
235 need just a change of solution pH or addition of metal ions, or of aqueous starch pastes which are
236 gelling during retrogradation.

237

238 **2.2. Shaping, kinetics of solvent exchange and drying**

239 2.2.1. Shaping

240 Drying with supercritical CO₂ preserves the shape of aerogel precursor, i.e. of “wet”
241 polysaccharide network with non-solvent in the pores (Figure 1). Shaping of bio-aerogels is thus fully
242 governed by shaping of polysaccharide solution before solvent exchange, either via gelation or phase

243 separation route. Both approaches are well known and depend on the type of polysaccharide used
244 and processing conditions such as polymer concentration and molecular weight, solution viscosity,
245 potentially surface and/or interfacial tension (for example, in the case of making beads),
246 temperature, pH and presence of ions or co-solutes. It is thus possible to make bio-aerogels in the
247 shape of monoliths of different forms, beads, fibers and films. This opens a lot of prospects in using
248 3D printing technique for making bio-aerogels of various and complex shapes which can be very
249 attractive for bio-medical applications such as scaffolds and wound dressings.

250 Till now the majority of bio-aerogels are made in the form of monoliths and beads (particles); to
251 form fibers and films is possible but is a bit challenging from the point of view of aerogel mechanical
252 properties. Making monoliths is easy and this is what is done in most of laboratory trials: monolithic
253 bio-aerogel takes the shape of the container in which solution was gelled or coagulated. Monoliths
254 allow easy determination of density and testing mechanical properties (usually uniaxial compression
255 of cylindrical samples). In some cases bio-aerogel disks are made to study the release of active
256 substances.

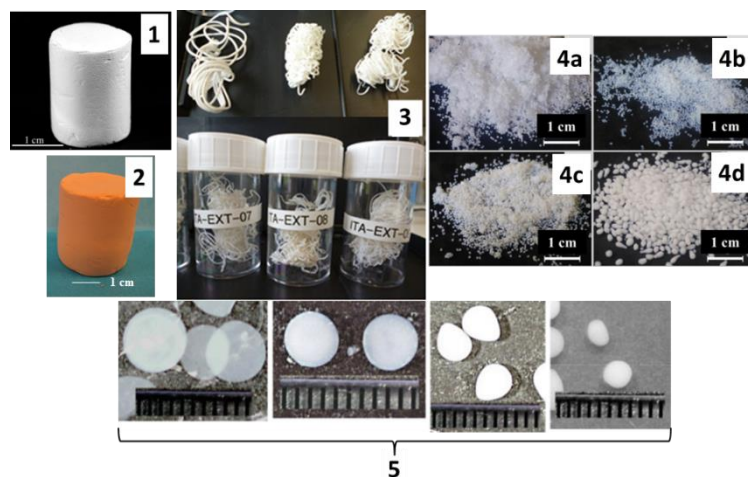
257 Two main ways of making bio-aerogel beads have been used till now: by dropping a solution in a
258 gelation or coagulation bath and using emulsion technique (Ganesan et al. 2018). As well as “wet”
259 polysaccharide gel particles, bio-aerogels in the form of beads can find applications in various fields
260 such as food, cosmetics, medical, pharma, sorption and separation. Particle size may vary from few
261 microns (usually in the case of emulsion technique) to few millimeters (dropping) and depends on
262 the shaping method used and solution parameters. As compared to monoliths, the whole process
263 efficiency is strongly increased in the case of beads because each processing step (solvent exchange,
264 drying) is diffusion controlled.

265 Bio-aerogel beads were made by dropping solution either in a very simple way, i.e. using a syringe
266 or pipette (Quignard et al. 2008; Veronovski et al. 2014) or by breaking solution jet (prilling, as shown
267 by De Cicco et al. 2016). For “easy-gelling” polysaccharides, their solutions are dropped in a bath in
268 which a droplet would gel. This is the case when pectin or κ -carrageenan or alginate solution is

269 dropped in a bath containing polyvalent metal salt which induces quick formation of a gelled layer on
270 the droplet surface, stabilizing droplet shape.

271 Emulsion technique can also be applied to the same “easy gelling” polysaccharides. The classical
272 approach is to disperse aqueous polymer solution in oil phase containing a surfactant. The system is
273 emulsified and polysaccharide droplet is gelled due to an external input (addition of metal salts in the
274 case of pectin or κ -carrageenan or alginate solution (Quignard et al. 2008; Veronovski et al. 2014), or
275 temperature decrease for starch solutions (García-González et al. 2012).

276 All said above can be partly applied to cellulose aerogels keeping in mind that cellulose solutions
277 are not “easy-gelling”, except the case of cellulose-(7-9)%NaOH/water. The shape of cellulose II
278 aerogel precursor is thus usually stabilized during solvent→non-solvent exchange. Some examples of
279 cellulose aerogels in the shape of monoliths, beads and fibers are shown in Figure 3. Monoliths are
280 obtained either from gelled solutions (here, from cellulose/8%NaOH/water) or from direct
281 solvent→non-solvent exchange when cellulose solvents are ionic liquids (Figure 3) or alkali/water
282 (NaOH or LiOH, with urea and/or ZnO added). A special case, different from other bio-aerogels, is
283 when the shape is given during solution solidification (not to be confused with gelation) due to
284 temperature decrease down to room conditions. This happens when cellulose solvents are N-
285 methylmorpholine-N-oxide monohydrate (NMMO), zinc chloride hydrate ($\text{ZnCl}_2 \cdot 6\text{H}_2\text{O}$) and calcium
286 thiocyanate ($\text{Ca}(\text{SCN})_2 \cdot 6\text{H}_2\text{O}$). Sometimes these solutions are called “melts” as they have to be
287 prepared and processed at elevated temperatures; they are of rather high viscosity and thus
288 resemble polymer melts. Some ionic liquids, such as 1-butyl-3-methylimidazolium chloride
289 ([Bmim][Cl]), and their cellulose solutions are also solid at room temperature. Cellulose aerogels in
290 the form of fibers were made by extruding hot cellulose/calcium thiocyanate solution into ethanol
291 (Figure 3) (Karadagli et al. 2015).



5

292

293

Figure 3

294

Examples of bio-aerogel monoliths, fibers and beads made from:

295 (1) gelled cellulose/8%NaOH/water. Reprinted with permission from (Gavillon R, Budtova T (2008)

296 *Aerocellulose: New Highly Porous Cellulose Prepared from Cellulose-NaOH Aqueous Solutions.*

297 *Biomacromolecules* 9:269–277). Copyright (2007) American Chemical Society;

298 (2) gelled cellulose/organosolv lignin/8%NaOH/water. Reprinted by permission from [Springer],

299 [Cellulose], [Sescousse R, Smacchia A, Budtova T (2010b) Influence of lignin on cellulose-NaOH-

300 water mixtures properties and on Aerocellulose morphology. *Cellulose* 17:1137–1146],[2010];

301 (3) extruded hot cellulose/calcium thiocyanate fibers. Reprinted from Karadagli I, Schulz B,

302 Schestakow M, Milow B, Gries T, Ratke L (2015) Production of porous cellulose aerogel fibers by an

303 extrusion process. *J. of Supercritical Fluids* 106:105–114, Copyright 2015, with permission from

304 Elsevier;

305 (4a, b, c, d) beads made with JetCutting technique from 2 % (a, b, c) and 3 % (d) cellulose/5-

306 diazabicyclo[4.3.0]non-5-enium propionate solution. Reproduced from Druel L, NiemeyerP, Milow B,

307 Budtova T (2018) Rheology of cellulose-[DBNH][CO₂Et] solutions and shaping into aerogel beads,

308 *Green Chemistry* 20:3993-4002 with permission from The Royal Society of Chemistry;

309 (5) particles of various shapes made by syringe-dropping of non-gelled cellulose/8%NaOH/water

310 solutions. Reprinted by permission from: [Springer] [*J Mater Sci*] [Sescousse R, Gavillon R, Budtova T

311 (2011b) Wet and dry highly porous cellulose beads from cellulose–NaOH–water solutions: influence

312 of the preparation conditions on beads shape and encapsulation of inorganic particles. J. Mater. Sci.
313 46:759–765], [2010]

314
315 Cellulose in the shape of beads is known since long time for using in various applications
316 (immobilization, purification, separation and filtration purposes). In most cases cellulose beads are
317 either never dried, with water in the pores, or, if dried, it is done at ambient pressure which results in
318 a non-porous material. The techniques used to make beads, when cellulose is dissolved either in a
319 direct solvent or via derivatization/regeneration route, are by dropping solution with a syringe
320 (Sescousse et al. 2011b; Trygg et al. 2013, 2014; Mohamed et al. 2015; Voon et al 2016), atomizers
321 (De Oliveira and Glasser 1996; Rosenberg et al. 2007) and using emulsion method (Luo and Zhang
322 2010; Lin et al 2009a; Zhang et al. 2018). Various ways of production of cellulose beads are
323 summarized in a recent review (Gericke et al. 2013).

324 Only few publications report on cellulose aerogel beads, and the majority is made with syringe-
325 dropping method from cellulose dissolved in alkali solvents. Using 7%NaOH/12%urea/water solvent,
326 beads were produced via dropping in aqueous non-solvent, and their size and shape were varied by
327 modifying coagulation conditions (bath temperature, from 5 to 50 °C, and concentration of HNO₃,
328 from 0.5 to 10 M): particles' volume varied from 8 to 20 mm³, and circularity was mainly influenced
329 by bath temperature with more deformed particles obtained at lower temperature (Trygg et al.
330 2013). ZnO of different concentration (from 0 to 2%) was added to the same solvent and beads were
331 formed in 2M HCl; their diameter was from 2 to 2.5 mm which increased with the increase of ZnO
332 concentration (Mohamed et al. 2015). Authors suggest that higher ZnO concentration better
333 preserves beads from shrinking. 8%NaOH/water without additives was also used to make aerogel
334 beads via dropping method (Sescousse et al. 2011b). It was shown that by varying solution viscosity,
335 distance between the syringe tip and coagulation bath and bath temperature, different shapes, from
336 very flat plates to spheres, can be obtained (Figure 3).

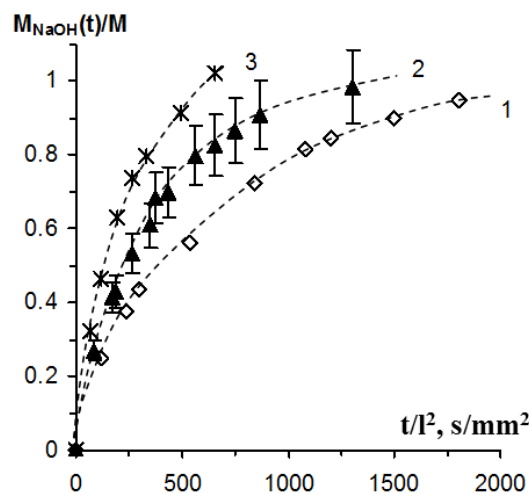
337 Ionic liquids, being powerful cellulose solvents, were also used for making cellulose aerogel
338 beads. Contrary to NaOH/water based solvents, ionic liquids allow dissolution of cellulose in a large
339 range of concentrations and molecular weights. Solution viscosity can additionally be varied by so-
340 called co-solvents such as dimethyl sulfoxide (DMSO) or dimethyl formamide (DMF). Voon et al
341 report on making cellulose aerogel beads from cellulose/1-allyl-3-methylimidazolium chloride
342 ([Amim][Cl]) solution by dropping it into water with a syringe (Voon et al. 2016). Particles' diameter
343 was from 0.4 to 2.2 mm and, as expected, the size increased with the increase of needle nozzle
344 diameter. Surprisingly, specific surface area decreased, from 500 to 100 m²/g, with the increase of
345 particle size. An opposite influence of cellulose aerogel geometrical dimensions was reported by
346 Karadagli et al. 2015, where Ca(SCN)₂·6H₂O was used to make aerogels in the shape of monoliths and
347 fibers. While the density of aerogels did not depend on sample shape and size, specific surface area
348 was lower in fibers as compared to monoliths.

349 Recently, jet-cutting technology, that can be easily scaled up, was used to make cellulose
350 aerogel beads (Druel et al. 2018). Contrary to “water jet-cutter machine” which is cutting the
351 material, it is the jet of liquid (here, polymer solution) which is cut with high speed rotating wires.
352 Liquid spheres are formed in the air due to surface tension; they are then collected into a bath. This
353 method is developed by GeniaLab (Germany) and used to make “easy-gelling” polysaccharide gel
354 beads. Cellulose beads from cellulose dissolved in ionic liquid 5-diazabicyclo[4.3.0]non-5-enium
355 propionate ([DBNH][CO₂Et]) were made with this technology and collected in water, ethanol and
356 isopropanol baths. Cellulose aerogel beads were with mean diameter from 0.5 to 1.8 mm (Figure 3),
357 density around 0.04 – 0.07 cm³/g and specific surface area around 240 – 300 m²/g. They had the
358 same density and specific surface area as the majority of their monolithic counterparts obtained
359 from ionic liquids and other solvents. The rheological properties of “cut” solutions were
360 demonstrated to be crucial for making cellulose aerogel beads with JetCutting method (Druel et al.
361 2018).

362

363 2.2.2. Kinetics of solvent exchange

364 Whatever the mechanisms of structure formation, gelation or phase separation, and the
365 method of shaping into a “wet” network, the next processing steps are the same for all bio-aerogels:
366 replacing solvent by a fluid miscible with CO₂ and drying (see Figure 1). Solvent in cellulose solutions
367 and gels is usually washed out by water or ethanol or acetone, rarely by isopropanol. If water is used,
368 it is then replaced by ethanol or acetone that are miscible with CO₂. All exchanges are diffusion
369 controlled processes and are thus rather slow. Time needed for cellulose solvent to diffuse out and
370 non-solvent to diffuse in depends on cellulose concentration, sample shape and bath temperature
371 (Figure 4). Higher is bath temperature and lower cellulose concentration, higher is diffusion
372 coefficient, as expected. Roughly, diffusion coefficient is proportional to sample thickness in power 2;
373 to wash out cellulose solvent from a thick monolithic sample takes several days. In order to calculate
374 solvent diffusion coefficient, size changes due to “wet” network shrinkage during solvent exchange
375 should also be taken into account (Sescousse and Budtova 2009).



376

377

Figure 4

378 Diffusion of NaOH from 5 wt%cellulose/7.6% NaOH/water gels into water bath (t is time, l is
379 sample half-thickness) at (1) 25, (2) 50 and (3) 80 °C. The lines are shown to guide the eye. Reprinted
380 with permission from Gavillon R, Budtova T (2007) Kinetics of Cellulose Regeneration from Cellulose-

381 NaOH-Water Gels and Comparison with Cellulose-N-Methylmorpholine-N-Oxide-Water Solutions.

382 Biomacromolecules 8:424-432. Copyright 2007 American Chemical Society

383

384 For the systems used to make cellulose aerogels, the kinetics of solvent→non-solvent exchange
385 (or of cellulose coagulation) was studied for cellulose/NMMO solutions (solid solutions) (Laity et al.
386 2002; Biganska and Navard 2005), cellulose/8%NaOH/water solutions and gels (Gavillon and Budtova
387 2007; Sescousse and Budtova 2009) and cellulose/imidazolium ionic liquid solutions (Sescousse et al.
388 2011a; Hedlund et al. 2017). In all cases cellulose solvent was replaced by water. Overall, it was
389 shown that the process is governed by Fick diffusion. When the release of NaOH from cellulose
390 solution and from gel of the same cellulose concentration was compared, it turned out that diffusion
391 is faster from a gel (Sescousse and Budtova 2009). The reason is that the structure in cellulose gels is
392 rather heterogeneous (they are opaque due to micro-phase separation), with pores being much
393 larger than the size of the diffusing solvent molecule. Local cellulose concentration in “gel pores” is
394 thus lower as compared to a homogeneous solution, making diffusion from the gel faster.

395 The interactions between cellulose solvent and non-solvent may influence the kinetics of solvent
396 exchange and should also be taken into account. This is the case of cellulose/ionic liquid solutions
397 when placed in water. For example, it was shown that 1-ethyl-3-methylimidazolium acetate
398 ([Emim][OAc]) and water are interacting, with reaction being exothermal and mixture temperature
399 exceeding room temperature by several tens of °C (Hall et al. 2012). Viscosity and diffusion
400 coefficients (measured by NMR) in [Emim][OAc]/water mixtures are several hundred per cent higher
401 than those predicted by the mixing rule (Hall et al. 2012). This can change the overall duration of
402 solvent exchange and, potentially, the morphology of the corresponding aerogels.

403

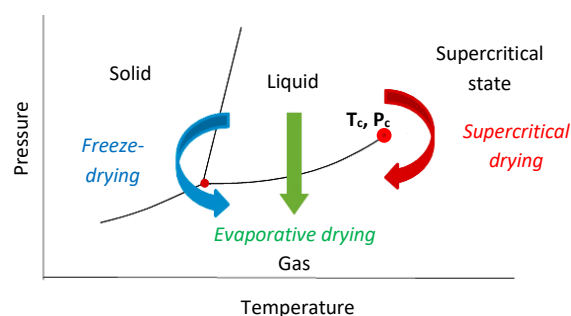
404 2.2.3. Drying

405 The final step in making aerogels is drying (Figure 1). While network morphology is stabilized
406 either during gelation or non-solvent induced phase separation, drying is critical to keep the

407 morphology as much intact as possible. The main goal is to avoid pores' collapse due to capillary
408 pressure. If willing to keep mesoporosity and avoid pores' chemical treatment to increase the contact
409 angle, drying should be done when the liquid in the pores is in supercritical state in which no
410 meniscus is formed (Figure 5).

411 Fluid in the supercritical state has diffusivity comparable to that of gases, density in-between gas
412 and liquid and high solvation power. Being discovered in the first half of the 19th century,
413 supercritical fluids are now used in various applications such as separation and extraction, in polymer
414 processing due to plasticizing effect and for foaming, in chemical and biochemical reactions,
415 "cleaning" in microelectronics and also for drying when making aerogels and samples for scanning
416 electron microscopy (Knez et al. 2014). Using supercritical fluids involves high-pressure technology
417 (see critical point pressure in Table 1) which has some drawbacks; however, low viscosity, high
418 diffusivity and solvation properties can counterbalance high-pressure disadvantage. For aerogels, CO₂
419 is the easiest solution to be used for drying as it has mild critical point temperature and pressure
420 (Table 1), is chemically inert, non-flammable, non-toxic and cheap. As far as bio-aerogels are
421 concerned, obviously neither water nor acetone or ethanol can be used because of their high critical
422 point temperature; water in supercritical state has, in addition, oxidizing properties.

423



424

425

Figure 5

426 Phase diagram with various ways of drying. Courtesy of Cyrielle Rudaz (Rudaz 2013)

427

428 Table 1. Critical point properties of some fluids

Fluid	Critical temperature, T_c , °C	Critical pressure, P_c , MPa	Density, g/cm ³
CO ₂	31	7.38	0.469
acetone	236	4.7	0.278
ethanol	241	6.14	0.276
water	374	22.1	0.322

429

430 Other ways of making 3D porous polysaccharide-based materials are also possible, but most of
431 drying methods do not lead to a mesoporous matter, i.e. with high specific surface area. Figure 1
432 shows the options of drying via lyophilisation (or freeze-drying) and via ambient pressure or low
433 vacuum drying. The terms “cryogel” and “xerogel” are used here for simplicity: strictly speaking,
434 “cryogels” correspond to a matter that is gelling under freezing or storage in the frozen state or
435 under thawing (Lozinsky et al. 2003). This is the case of some polysaccharides such as agarose
436 (Lozinsky et al. 2008). However, the term “cryogels” is often used when water is sublimated from a
437 frozen aqueous system which is also known as ice-templating. However, if no special precautions are
438 taken to decrease the growth of ice crystals, “bio-cryogels” are usually open-pores networks with
439 very low density, very large pores of the size of microns up to several hundreds of microns, rather
440 thick and often non-porous walls and low specific surface area. In the case of cellulose II, water is
441 frozen and sublimated from so-called cellulose “hydrogel” (3D network of coagulated cellulose with
442 water in the pores) (Buchtova and Budtova 2016), and in the case of cellulose I water is sublimated
443 from nanocellulose suspension.

444 To tune the morphology of “bio-cryogels” the control of the kinetics of ice crystal growth is
445 crucial. This can be done either by spray-freeze-drying which allows fast freezing in sub-micron size
446 pores, or by using mixed solvents (Guizard et al. 2014). Spray-freeze-drying was applied to make
447 “cellulose aerogels” (using the terminology of authors) (Cai et al. 2014; Jiménez-Saelices et al. 2017)
448 from nanofibrillated cellulose resulting in material with specific surface area 80-100 m²/g (Jiménez-

449 Saelices et al. 2017) and 390 m²/g (Cai et al. 2014). It is supposed that this method is not easy to
450 apply for making cellulose II “cryogels” as far as the network is already formed during cellulose
451 coagulation in water and spraying, even if done on mechanically weak wet precursors, will lead only
452 to the macroscopic breakage of the sample. As for using mixed solvents, the most popular way to
453 make “bio-cryogels” with certain mesoporosity is freeze-drying from tert-butanol(TBA)/water
454 (Borisova et al. 2015): for example, pectin “cryogels” of density from 0.044 to 0.144 g/cm³ and
455 specific surface area from 128 to 280 m²/g were made via freeze-drying from TBA/water of various
456 compositions. The lowest density was obtained for samples freeze dried from pure water and the
457 highest when TBA/water was at the composition corresponding to the first eutectic point of this
458 mixture. Freeze-drying from TBA resulted in high specific area of cellulose II, 260 – 330 m²/g (Hwang
459 et al. 2018). The same mixed solvent was used to make nanofibrillated cellulose “nanopaper”
460 (terminology of authors) with specific surface area from 45 to 117 m²/g (Sehaqui et al. 2011) and
461 esterified nanocellulose “aerogel” (terminology of authors) with specific surface area from 100 m²/g
462 to 180 m²/g (Fumagalli et al. 2013, 2015). Other solvents used for freeze-dried, such as 1,1,2,2,3,3,4-
463 heptafluorocyclopentane, also result in rather high specific surface area 190 – 210 m²/g (Wang et al.
464 2012).

465 The term “xerogel” strictly means “a dry gel”, but it is traditionally employed for meso- and
466 microporous systems, with porosity up to 50%, dried at ambient pressure or low vacuum. An
467 example of xerogels is silylated silica gel dried at ambient pressure and around 130-150 °C; it has the
468 internal structure similar to silica aerogels dried with supercritical CO₂. Such silica xerogels are with
469 high specific surface area (500 – 1000 m²/g) and low density (around 0.1 – 0.2 g/cm³) and are
470 sometimes called “ambient pressure dried aerogels”.

471 Very few works report on low density cellulose “xerogels” and most of them are with rather low
472 specific surface are; capillary pressure developing during evaporative drying coupled with hydrogen
473 bonding between polysaccharide chains usually lead to network collapse resulting in a non-porous
474 material. One way to decrease pore closing during drying is to use fluids with surface tension lower

475 than that of water (0.073 N/m): ethanol (0.022 N/m), acetone (0.0237 N/m), hexane (0.0184 N/m),
476 methanol (0.0226 N/m) or pentane (0.0158 N/m). This approach was applied to obtain open-pores
477 cellulose sheets: water was replaced first by methanol, then acetone and finally pentane, and then
478 samples were dried overnight by evaporation under forced convection of argon (Svensson et al.
479 2013). The specific surface area varied from 75 to 130 m²/g. Solvent exchange resulted in high
480 specific surface area of cellulose II as compared to conventional freeze-drying, 150 – 190 m²/g vs 70 –
481 100 m²/g, respectively (Jin et al. 2004).

482 Another way is to perform cellulose surface hydrophobisation which can be applied to cellulose
483 pulp (Tejado et al. 2010; Köhnke et al. 2010) and nanofibrilated cellulose (Sehaqui et al. 2014).
484 Hydrophobic cellulose nanopaper was with density 0.4-0.6 g/cm³ and specific surface area 40-60
485 m²/g (Sehaqui et al. 2014). Highly porous nanocellulose foams were obtained via high-pressure
486 homogenisation technique, cellulose caboxymethylation and drying at 60 °C in an oven without
487 convection; pore size was between 300 and 600 µm and density around 0.03 g/cm³ (Cervin et al.
488 2013). With such size of pores these foams cannot have high specific surface area. Inspired by the
489 approach used for making low density and high specific surface area silica xerogels, trityl cellulose
490 was synthesised via homogeneous reaction and then xerogels were prepared via dissolution-solvent
491 exchange-ambient drying route (Pour et al. 2015). Low density (0.1 and 0.2 g/cm³) hydrophobic
492 xerogels showing contact angle with water 140 ° were obtained when the degree of substitution was
493 0.72. Specific surface area was not high, from 13 to 27 m²/g. While bulky trityl groups on cellulose
494 chain prevent, to a certain extent, the formation of intra- and inter-molecular hydrogen bonds during
495 drying and thus lead to xerogels of low density, still chains aggregation occurs during solvent
496 exchange and drying which may explain the absence of mesoporosity.

497 The analysis and examples of various drying ways presented above show that if having the goal
498 to obtain light-weight and mesoporous cellulose II materials, drying with supercritical CO₂ is, till now,
499 the most successful option.

500

501 2.3. Characterisation of bio-aerogels

502 The methods used to characterize bio-aerogels are the same as for classical aerogels. However,
503 some features, specific for bio-aerogels, should be taken into account in order not to obtain
504 artefacts. One is high sensitivity of native polysaccharides to humidity and thus capability to adsorb
505 water vapours. For example, the weight of bio-aerogel may increase in room conditions by 10 - 20
506 wt% in the case of cellulose aerogels to several tens of wt% for aerogels based on water-soluble
507 polysaccharides. Higher humidity leads to even higher weight increase. As a result, characteristics
508 such as density and thermal conductivity of aged bio-aerogels should increase. An example of three
509 to five fold increase of thermal conductivity with relative humidity increase from 0 to 60% was
510 demonstrated for cellulose II cryogels (Shi et al. 2013a); no data is reported on cellulose II aerogels.
511 Subsequent drying should lead to pores' irreversible closing which is known for cellulose as
512 "hornification". This, in turn, may lead to aerogel shrinkage, change of density, morphology and
513 decrease of specific surface area. Bio-aerogel mechanical properties should also depend on aging
514 time. Till now, there is no quantitative analysis of bio-aerogel aging except some simple kinetics of
515 mass and volume uptake by cellulose aerogels as a function of relative humidity (Demilecamps
516 2015a). Samples' storage and characterisation should, ideally, be performed in controlled
517 temperature and humidity environment and sample "age" (time from drying to analysis) reported.

518 Bulk density ρ_{bulk} is the first obvious parameter to report for 3D porous materials; it is usually
519 determined by measuring sample mass and dimensions. Powder densitometer, such as Geopyc from
520 Micromeritics with DryFlo powder, is a useful option for samples with geometrically complex shapes
521 (Rudaz et al. 2014). Powder densitometer measures sample volume by using different chamber
522 volumes and tapping forces. Because bio-aerogels are deformable and compressible, the conditions
523 should be very carefully selected in order to avoid volume decrease during measurement. Skeletal
524 density ρ_{skeletal} of polysaccharides is known to be 1.5 – 1.7 g/cm³.

525 Scanning electron microscopy (SEM) is a very useful tool to visualize aerogel morphology,
526 however SEM cannot be used to quantify it. Specific surface area S_{BET} and pore size distribution are

527 the main parameters characterizing aerogel texture. As for classical aerogels, specific surface area of
528 bio-aerogels is determined using nitrogen adsorption technique and Brunauer–Emmett–Teller (BET)
529 theory. It should be noted that standard methods for measuring pore volume and size distribution
530 using Barrett-Joyner-Halenda (BJH) approach (via nitrogen adsorption) or mercury porosimetry
531 cannot be applied to bio-aerogels. Bio-aerogels possess macro- and mesopores, and are often with
532 large macropores (several hundreds of nanometers up to several microns). BJH method mainly
533 considers mesopores and small macropores (below 200 nm), which takes in account only 10–20% of
534 the total pore volume in bio-aerogels (Robitzer et al. 2011; Rudaz et al. 2014; Jiménez-Saelices et al
535 2017; Groult and Budtova 2018a). For example, mesopore volume in bio-aerogels is usually around
536 0.5 – 2.5 cm³/g while total pore volume V_{pores} calculated from bulk ρ_{bulk} and skeletal densities ρ_{sk} (eq.
537 2) can reach several tens of cm³/g due to macroporosity (Robitzer et al. 2011; Rudaz et al. 2014;
538 Groult and Budtova 2018a):

$$539 \quad V_{pores} = \frac{1}{\rho_{bulk}} - \frac{1}{\rho_{skeletal}} \quad (2)$$

540 Pore size distributions in bio-aerogels are clearly not limited to mesopores region. It may also be
541 possible that bio-aerogel is compressed at higher nitrogen pressure. If not keeping in mind the
542 limitations of BJH method applied to bio-aerogels, the values provided by equipment with inserted
543 programs may lead to a wrong understanding of bio-aerogel morphology. When mercury
544 porosimetry is used, bio-aerogels are often compressed without mercury penetration in the pores,
545 and thus the “value” given by the machine is an artefact (Rudaz 2013; Rudaz et al. 2014). Imaging,
546 such as SEM or 3D tomography, provide only qualitative ways to estimate pore sizes: in the former,
547 no automatic image analysis is available yet to analyse complex bio-aerogel morphology and the
548 latter does not allow the analysis of mesopores.

549 Thermoporosimetry was suggested to determine pore size distribution; this method was applied
550 to cellulose II aerogels (Pircher et al. 2015, 2016). The approach is based on the measurement of the
551 experimental shift of the melting point of an interstitial liquid caused by its confinement in small
552 pores (Gibbs–Thomson equation). Cellulose aerogels were soaked in o-xylene and crystallization

553 temperatures were recorded using differential scanning calorimeter. Till now, there are only two
554 examples of using thermoporosimetry for the characterization of pore size distribution in bio-
555 aerogels. It provides a reasonable correlation with cellulose aerogel morphology seen by SEM and
556 shows a significant difference with pore sizes predicted by BJH method.

557

558 **3. CELLULOSE II AEROGELS: CASE STUDIES**

559 For making cellulose II aerogels, two main ways of cellulose dissolution should be considered,
560 either via cellulose derivatization followed by regeneration or in direct solvents. In the latter case no
561 “regeneration” *per se* occurs, and thus the process of cellulose “recovery” from solution will be called
562 “coagulation” (or precipitation).

563 When dissolved in direct solvents, cellulose solutions can be “liquid” at room temperature,
564 gelled or solidified. In the next sections cellulose II aerogels will be discussed from the point of view
565 of the solvent used to dissolve cellulose; a special attention will be paid on the state of the matter
566 before solvent→non-solvent exchange. The mechanisms of cellulose dissolution in a particular
567 solvent and solution properties will not be discussed as far as this would make the article infinite; the
568 reader is advised to address an excellent review of Liebert 2010 and other review articles devoted to
569 cellulose dissolved in a specific solvent (for example, Fink et al. 2001 for cellulose/NMMO, Budtova
570 and Navard 2016 for cellulose/NaOH, Pinkert et al. 2009 and Mäki-Arvela et al. 2010 for cellulose-
571 ionic liquids). Table S1 of the Supporting Information summarises the properties of cellulose II
572 aerogels divided by the type of solvent, with the chronological order of publications within each
573 solvent family. Some special cases of porous cellulose with high specific surface area obtained via
574 freeze-drying are also presented at the end of this table.

575

576 **3.1 Aerogels from cellulose dissolved via derivatization**

577 Because the research on aerogels and on cellulose was not intersecting in the past except being
578 just briefly mentioned by Kistler 1931, it seems there is only one publication reporting on cellulose

579 aerogels obtained from viscose process (Ookuna et al. 1993). Aerogel beads of the diameter of
580 several hundreds of microns were produced and specific surface area varied from 15 to 400 m²/g
581 (Table S1). These materials, called “porous cellulose”, were suggested to be used as ion-exchangers
582 (Ookuna et al. 1993). Another example which can be placed in the category of dissolution via
583 derivatization is cellulose carbamate: it was synthesized by kneading cellulose in the excess of urea at
584 130 °C and dissolving in NaOH/water (Pinnow et al. 2008). Monoliths and beads were made, cellulose
585 regenerated, followed by drying in supercritical CO₂; some samples were pyrolysed. Neat cellulose
586 aerogels density varied from 0.06 to 0.22 g/cm³ and specific surface area from 360 to 430 m²/g;
587 pyrolysed counterparts’ density and specific surface area were higher, 0.21 – 0.27 g/cm³ and 490 -
588 660 m²/g, respectively (Table S1).

589 Surprisingly, no other examples of cellulose aerogels synthesized via derivatization route have
590 been reported. Viscose process is known to be not very eco-friendly and complicated to be done on
591 laboratory scale; however, other ways of making cellulose aerogels via derivatization-regeneration
592 route could be interesting to test. One example is making cellulose aerogels by saponification of
593 cellulose acetate gels. The synthesis of cellulose acetate and cellulose acetate butyrate gels and
594 aerogels via chemical cross-linking with isocyanates had already been described (Tan et al. 2001;
595 Fischer et al. 2006), thus cellulose regeneration before drying could, theoretically, be possible.
596 Cellulose acetate butyrate aerogels were reported to possess high impact strength for this type of
597 porous materials, 0.85 Nm (density 0.15 g/cm³, specific surface area 389 m²/g) versus ten times
598 lower value for resorcinol-formaldehyde aerogel of the same density, 0.08 Nm (density 0.15 g/cm³,
599 specific surface area 526 m²/g) (Tan et al. 2001). The synthesis of many other cellulose esters and
600 ethers is well known but was never used to obtain regenerated cellulose aerogels.

601

602 **3.2. Aerogels from cellulose dissolved in direct aqueous solvents**

603 Despite the difficulties in cellulose dissolution, many direct solvents are known (Liebert 2010).
604 Some, but not many, were used to dissolve cellulose for making aerogels. The classical examples are

605 aqueous alkali-based solvents, NaOH and LiOH, which turned out to be the most popular in making
606 cellulose II aerogels. The great majority of work was performed using additives, such as urea,
607 thiourea or ZnO, which improve cellulose dissolution and delay solution gelation. In these cases the
608 state of the matter before solvent→non-solvent exchange was solution.

609 4.6%LiOH/15%urea/water was used to fabricate cellulose aerogels mainly as a “support” matrix
610 (Table S1): of metal nanoparticles (Cai et al. 2009; Cui et al. 2018), to make interpenetrated
611 cellulose/poly(methyl methacrylate/butyl methacrylate) and cellulose/poly(methyl
612 methacrylate/butyl acrylate) networks (Shi et al. 2015) and composite aerogels with silica (Cai et al.
613 2012; Liu et al. 2013). In the latter case the specific surface area of composite aerogels was 270 – 340
614 m²/g, similar to that of neat cellulose counterpart (320 m²/g). Cai et al. 2008 performed a systematic
615 study of the influence of cellulose concentration, coagulation bath temperature and cellulose
616 solvent, LiOH/urea vs NaOH/urea, on cellulose aerogel properties. It seems that if keeping all
617 processing parameters the same (origin and concentration of cellulose, coagulation bath type and
618 temperature), there is no influence of solvent type on aerogel properties (density around 0.26 g/cm³
619 and specific surface area 364 – 381 m²/g) (Cai et al. 2008). Overall, except the increase in density
620 with the increase of polymer concentration, which is expected, other trends are not very clear most
621 probably because of “too many” processing conditions which are not always easy to consider.

622 (7-9)%NaOH/water was used as cellulose solvent in two ways, either as is (Gavillon and Budtova
623 2008; Sescousse and Budtova 2009; Sescousse et al. 2010b, 2011a, 2011b; Demilecamps et al. 2016),
624 or with additives: urea (Cai et al. 2008; Trygg et al. 2013), thiourea (Chin et al. 2014) or urea/ZnO
625 (Mohamed et al. 2015) (Table S1). It is well known that cellulose/NaOH based solutions are gelling
626 with time and temperature increase (Roy et al. 2003) causing problems for processing (fiber spinning
627 and film casting), and thus additives are used to delay gelation. However, gelation property can be
628 useful for making aerogels of various and easily controlled shapes as far as sample shape remains the
629 same during all processing steps (only volume decreases). Gelation was used, for example, for
630 making cylindrical and disk carbon aerogels for electro-chemical applications (Rooke et al. 2012). It is

631 also known that in NaOH-based solvents it is not possible to dissolve cellulose of high DP and at
632 concentrations above 7-8 wt% (Egal et al. 2007). To make a self-standing aerogel precursor, polymer
633 concentration should be at least two-three times above the overlap concentration which is around 1
634 wt% for microcrystalline cellulose in this solvent. These constraints on the minimal and maximal
635 cellulose concentrations make the processing interval in NaOH-based solvents rather narrow,
636 decreasing the possibility of varying aerogel structure and properties.

637 When NaOH/water solvent was used without additives, solutions gelled. Gelation occurs due to
638 cellulose-cellulose preferential interactions via hydrogen bonding resulting in packing of cellulose
639 chains and formation of cellulose-rich domains; gels become opaque indicating entities that are
640 scattering visible light. This heterogeneous morphology with rather large pores and thick pore walls
641 might be the reason of lower specific surface area of aerogels made from gelled solutions, around
642 200 – 250 m²/g (Gavillon and Budtova 2008; Sescousse et al. 2010b; Demilecamps et al 2014), as
643 compared to their non-gelled counterparts of similar density but with surface area of 300 – 400 m²/g
644 when made from NaOH/water solvent with additives (Cai et al. 2008; Trygg et al. 2013; Mohamed et
645 al. 2015) or from LiOH/urea/water (see Table S1). Similar trend was reported for pectin aerogels:
646 specific surface area for aerogels based on non-gelled solutions was more than twice higher than
647 that of their gelled counterparts (Groult and Budtova 2018b).

648 As well as urea, ZnO also delays gelation, but its low solubility (around 0.5 - 0.7 wt% at pH 14
649 which is pH of 8 wt%NaOH/water) and presence of non-dissolved particles if above the solubility limit
650 should be taken into account (Liu et al. 2011). Mohamed et al studied the influence of ZnO
651 concentration on the properties of cellulose aerogels (Mohamed et al. 2015). A non-monotonous
652 behaviour of bulk density and specific surface area as a function ZnO concentration was found. The
653 authors speculate that the increase of specific surface area with the increase of ZnO concentration is
654 correlated with the increase of the number of zincate molecules which are swelling cellulose and
655 thus creating small pores (Mohamed et al. 2015). After the maximum solubility of ZnO is reached
656 (around 0.5 wt% ZnO, according to the authors), the presence of undissolved ZnO leads to the

657 decrease of the amount of zincate, which in turn decreases specific surface area. Bulk density of
658 aerogels shows a maximum at 0.4 wt% ZnO (Mohamed et al. 2015).

659

660 **3.3. Aerogels from cellulose dissolved in direct non-aqueous solvents**

661 Non-aqueous cellulose solvents used to make aerogels are NMMO, ionic liquids and molten salt
662 hydrates such as zinc chloride and calcium thiocyanate.

663 *Aerogels from cellulose/NMMO solutions.* Lenzing, Austria, was the first to report on cellulose
664 aerogels using NMMO (Firgo et al. 2004; Innerlohinger et al. 2006a, b). The work was performed
665 within EC 6th framework program, “AeroCell” project, which boosted the research on cellulose
666 aerogels and, probably, on bio-aerogels in general. Within AeroCell project aerogels were also made
667 from cellulose dissolved in 8%NaOH/water (Center for Materials Forming, MINES ParisTech, France),
668 cellulose carbamate dissolved in NaOH/water (Fraunhofer IAP, Germany) and cellulose acetate
669 dissolved in acetone and chemically cross-linked (Centre for processes, renewable energies and
670 energy systems, MINES ParisTech, France). For aerogels based on cellulose dissolved in NMMO,
671 bleached, unbleached and cotton linter pulps were used (Innerlohinger et al. 2006a, b). Samples of
672 various shapes were prepared either by solidifying cellulose/NMMO solution in moulds of different
673 forms or by dropping hot solution in water. Because of large amount of different starting parameters
674 (cellulose DP and concentration, type of pulp, way of structure formation (from solid or liquid
675 solution), type of non-solvent) it was difficult to build correlations except few evident ones such as
676 the increase in aerogel density with the increase of cellulose concentration, as already mentioned for
677 aerogels made from cellulose/alkali solutions. Interestingly, specific surface area of aerogels made
678 via dropping of hot solutions in water bath was the highest (300 – 350 m²/g) as compared to aerogels
679 prepared from solidified solutions (below 250 m²/g) (Innerlohinger et al. 2006a, b). For
680 cellulose/NMMO solutions it is known that it is free solvent which is crystallising at room
681 temperature leading to “pre-forming” of the morphology of future aerogel, as in the case of cellulose

682 solution gelation. This confirms the hypothesis that aerogels with higher mesoporosity are formed
683 via direct non-solvent induced phase separation.

684 Further work on cellulose aerogels from NMMO solutions was continued in the group of Falk
685 Liebner (BOKU, Austria) (Liebner et al. 2008, 2009, 2012; Pircher et al. 2016). The majority of the
686 initial solutions were of 3 wt% cellulose (cotton linters, various pulps) resulting in aerogels of density
687 $0.05 - 0.06 \text{ g/cm}^3$ and specific surface area $200 - 300 \text{ m}^2/\text{g}$ (Table S1); pulp type and cellulose
688 molecular weight (from 80 to 665 kg/mol) did not seem to influence either density or specific surface
689 area (Liebner et al. 2009). It was reported that solvent exchange directly with ethanol
690 (NMMO→ethanol), as compared with two-step exchange to water and then to ethanol
691 (NMMO→water→ethanol), leads to lower aerogel density, 0.06 vs 0.09 g/cm^3 , respectively (Liebner
692 et al. 2008).

693 *Aerogels from cellulose/ionic liquid solutions.* Since ionic liquids became in the focus of cellulose
694 research as the medium for cellulose derivatization and processing at the beginning of the 21st
695 century, they were also used to make cellulose aerogels. Ionic liquids allow cellulose easy dissolution
696 in a wide range of molecular weights and concentrations, and also the dissolution of lignocellulose
697 and even wood. This opens many ways to perform systematic experiments in order to test and
698 understand processing-structure-properties relationships in cellulose aerogels, and also make
699 aerogels with desired characteristics. Still the research is at the beginning of the long way and a lot of
700 questions remain. For example, the highest value of specific surface area ever obtained for cellulose
701 aerogels, $539 \text{ m}^2/\text{g}$, was for aerogel prepared from bleached softwood Kraft pulp dissolved at 1.5
702 wt% in [Bmim][Cl] (Aaltonen and Jauhiainen 2009). Other high surface area values for aerogels from
703 cellulose solutions in imidazolium-based ionic liquids are for aerogels from waste paper, $478 \text{ m}^2/\text{g}$
704 (Voon et al. 2017) and from eucalyptus pulp with maximum specific surface area $350 \text{ m}^2/\text{g}$ (Wang et
705 al. 2013) (Table S1). The addition to cellulose (from bleached softwood Kraft pulp) of lignin and xylan,
706 or their presence in spruce wood, strongly decreased specific surface area from $539 \text{ m}^2/\text{g}$ to $210-220$
707 m^2/g and $122 \text{ m}^2/\text{g}$, respectively (Aaltonen and Jauhiainen 2009). Other works report aerogels

708 obtained from cellulose/ionic liquids with densities and specific surface areas similar to those from
709 other solvents: 0.05 – 0.2 g/cm³ and 130 – 300 m²/g (Table S1) (Tsiptsias et al. 2008; Sescousse et al.
710 2011a; Pircher et al. 2015, 2016; Demilecamps et al. 2015b; Buchtova and Budtova 2016).

711 *Aerogels from molten salt hydrates.* Zinc chloride (ZnCl₂·6H₂O) and two options of calcium
712 thiocyanate, Ca(SCN)₂·6H₂O and Ca(SCN)₂·8H₂O/LiCl, were used to dissolve cellulose and make
713 aerogels (Table S1). Rege et al. 2016 report that within the same interval of cellulose concentrations
714 in solution, from 1 to 5 wt%, the density of cellulose aerogels made from zinc chloride solutions are
715 several times higher than that from Ca(SCN)₂·6H₂O solutions (Table S1). As a consequence of higher
716 density, Young's moduli of aerogels from zinc chloride route are much higher than those from
717 Ca(SCN)₂·6H₂O, in the same range of initial cellulose concentrations, 2 – 10 MPa vs 5 – 95 MPa,
718 respectively (Table S1). Cellulose/ZnCl₂·6H₂O solutions were coagulated in isopropanol and
719 cellulose/Ca(SCN)₂·6H₂O in ethanol (Rege et al. 2016) which may influence aerogel properties.
720 Indeed, in another work the same team reported that aerogels of the same density obtained from
721 cellulose/ZnCl₂·6H₂O and coagulated in isopropanol possess Young's modulus almost twice higher
722 than that when coagulated in ethanol (Schestakow et al. 2016a).

723 Ca(SCN)₂·6H₂O and Ca(SCN)₂·8H₂O/LiCl were used to make cellulose aerogels of dual porosity
724 using porogens, either oil or polymethylmethacrylate solid spheres (Pircher et al. 2015; Ganesan et
725 al. 2016). As expected, the presence of large pores remaining after leached out porogens led to
726 density and Young's modulus decrease as compared to reference (without porogens) aerogels.

727

728 **4. OVERVIEW ON CELLULOSE II AEROGELS STRUCTURE AND PROPERTIES**

729 In this section the analysis of general trends of processing-structure-properties correlations for
730 cellulose II aerogel is performed. Because of a huge number of parameters used to prepare cellulose
731 aerogels an adequate comparison is rather challenging. The main parameters, corresponding to each
732 preparation step, are as follows (see Figure 1): cellulose origin and presence of other components
733 (hemicellulose, lignin), molecular weight and concentration in solution; type of solvent and presence

734 of additive(s) or co-solvent(s); mechanism of structure formation (via gelation or solidification or
735 non-solvent induced phase separation); type of non-solvent, bath temperature, solvent/non-solvent
736 interactions and way of solvent exchange (gradual or not); parameters of supercritical drying
737 (temperature, pressure, pressurization and depressurisation rate) and, finally, samples' aging.
738 Considering, in addition, that not all publications provide comprehensive information on aerogel
739 preparation, the understanding and prediction of cellulose II aerogel structure and properties is not
740 an easy task.

741

742 **3.1. Volume change during processing and cellulose II aerogel density**

743 Those who are involved in making bio-aerogels noticed that sample volume decreases from the
744 initial solution to final aerogel, and this is also the case for cellulose II aerogels. Volume shrinkage
745 seems to depend on the type of polysaccharide: for example, for 2 – 2.5 wt% solutions it is 90 – 95
746 vol% for κ -carrageenan while it is 40 – 50 vol% for chitosan and around 20 vol% for calcium alginate
747 (Quignard et al. 2008). This difference was interpreted by different chain flexibility; low shrinkage of
748 calcium alginate was suggested to be due to the formation of “egg-box” structure during calcium-
749 induced gelation. Rather low shrinkage occurs in nanocellulose based aerogels (Lavoine and
750 Bergstrom 2017). Volume decrease during solvent exchange and drying may look a “too simple”
751 phenomenon to be studied, however, it reflects the fundamental property of polymer chain to
752 change its conformation as a function of external conditions, in particular, in the presence of a non-
753 solvent. Here the mechanism of network structure formation, via gelation or non-solvent induced
754 phase separation, plays a very important role (for example, around 75 % volume shrinkage for non-
755 cross-linked vs around 35 % for calcium cross-linked pectin aerogels made from 3 wt% low-
756 methylated pectin solutions (Groult and Budtova 2018b)). A comparison with synthetic polymers of
757 different flexibility would be very interesting.

758 As far as cellulose II aerogels are concerned, volume shrinkage was reported to depend on
759 cellulose concentration in solution and type of non-solvent (Innerlohinger et al. 2006a; Sescousse

760 and Budtova 2009; Schestakow et al. 2016a; Buchtova and Budtova 2016). Shrinkage occurs at both
761 solvent exchange and drying steps. The reason for the first one is clear: from being in solution,
762 macromolecules tend to decrease their volume in a non-solvent. The extent of this decrease may
763 depend on if the polymer is “stabilized” in a network or not (see the case of pectin mentioned
764 above), but this was never systematically studied for cellulose. Volume decrease during drying with
765 supercritical CO₂ is, somehow, “against” the theoretical prediction which states that shrinkage should
766 be zero as far as capillary pressure is zero. However, CO₂ is cellulose non-solvent with very low
767 polarity and very different solubility parameter: 5 – 8 MPa^{0.5} for CO₂ in supercritical state (Zhang et
768 al. 2017) vs 39 MPa^{0.5} for cellulose (Hansen 2007). This and certain pressure needed to reach
769 supercritical conditions (around 8 – 10 MPa) may together be the reasons of volume decrease during
770 drying.

771 An example of the dependence of volume shrinkage during solvent exchange and drying on
772 cellulose initial concentration in solution is shown in Figure 6, aerogels were made from
773 cellulose/[Emim][OAc]/DMSO solutions coagulated in ethanol (Buchtova and Budtova 2016). Here
774 major shrinkage occurred at drying step; total volume is better preserved at higher cellulose
775 concentration: shrinkage is around 70 vol% for 3 wt% cellulose in solution vs around 20 vol% for 11
776 wt% cellulose. Higher cellulose concentration helps mechanically “resisting” solvent exchange and
777 drying. The same trend was reported by other authors (Schestakow et al. 2016; Innerlohinger et al.
778 2006a): for example, for aerogels made from cellulose/NMMO solutions coagulated in water
779 shrinkage was from around 80 - 85 vol% for 0.5 wt% cellulose solutions to around 40 – 50 vol% for 9
780 wt% solutions (Innerlohinger et al. 2006a).

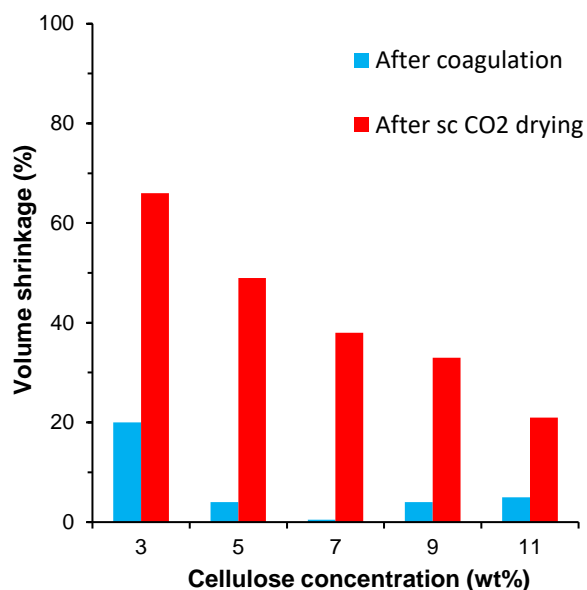
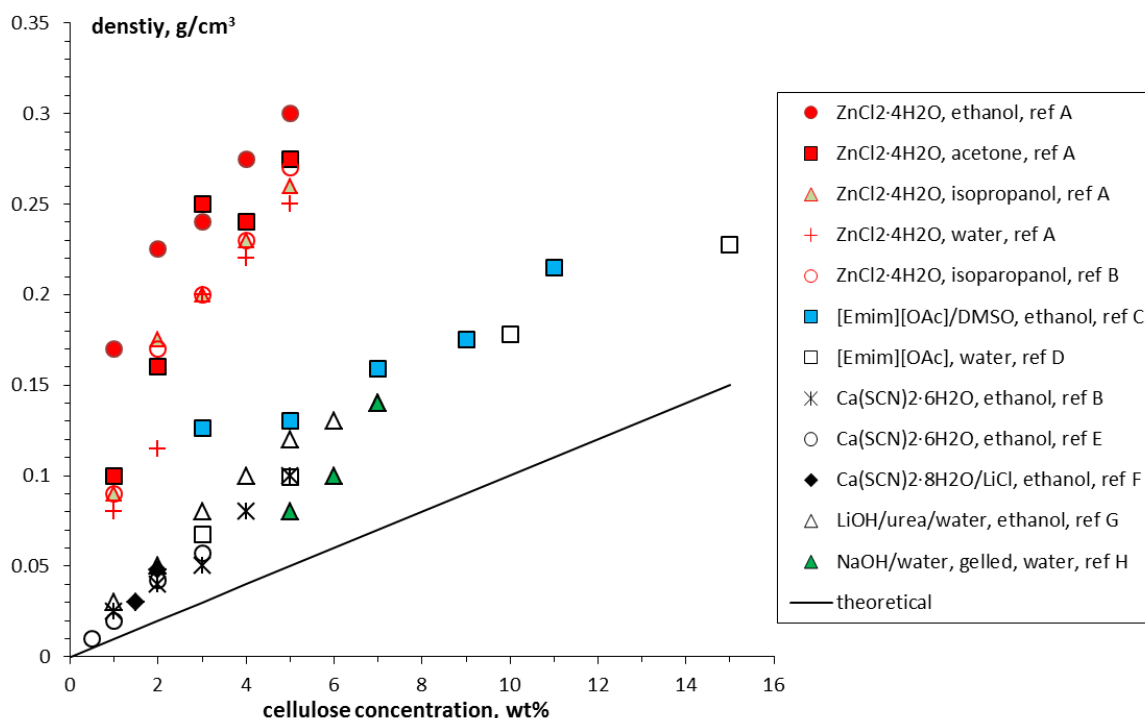


Figure 6

Volume shrinkage during solvent exchange and total shrinkage after drying for cellulose aerogels as a function of cellulose concentration. Cellulose was dissolved in [Emim][OAc]/DMSO, data taken from Buchtova and Budtova 2016

The influence of non-solvent type on cellulose shrinkage was demonstrated in by Schestakow et al. 2016a. The comparison was made for all processing conditions being the same, except non-solvent type. Higher volume loss was reported for cellulose coagulated in acetone (60 – 70 vol%) followed by ethanol and isopropanol (40 – 60 vol%) and then by water (30 – 40 vol%). This was interpreted by different solubility of cellulose solvent, zinc chloride tetrahydrate, in the corresponding non-solvent; the highest was in water and the lowest in acetone. Similar trend, i.e. higher shrinkage of cellulose II aerogels made from cellulose/[DBNH][CO₂Et] solution was reported when non-solvent was ethanol as compared to water (density 0.04 vs 0.05 g/cm³, respectively) (Druel et al. 2018). However, when cellulose solvent was NMMO, higher shrinkage occurred when non-solvent was water as compared to ethanol (density 0.09 vs 0.06 g/cm³, respectively) (Liebner et al. 2008).

798 Aerogel bulk density is inversely proportional to sample shrinkage if no volume and/or mass loss
 799 occurs. The latter may happen when pulp is used as far as hemicelluloses can be washed out during
 800 coagulation and washing in water. Bulk density can be compared to the ideal case of no volume
 801 change during the preparation steps, from solution to aerogel. The density of “no-shrinkage case”
 802 can be taken “equal” to cellulose concentration, in a very rough approximation, as far as the majority
 803 of solutions are rather dilute, below 10 wt%. A summary of cellulose II aerogel density as a function
 804 of cellulose concentration for different solvents and non-solvents is presented in Figure 7.
 805



806
 807
 808
 809
 810
 811
 812
 813

Figure 7

Density of cellulose II aerogels as a function of cellulose concentration in solution, for different solvents and non-solvents; solid line corresponds to the case of no shrinkage and no mass loss. Experimental data are from the following references: ref A: Schestakow et al. 2016a; ref B: Rege et al. 2016; ref C: Buchtova and Budtova 2016; ref D: Sescousse et al. 2011a; ref E: Hoepfner et al. 2008; ref F: Pircher et al. 2016; ref G: Cai et al. 2008 and ref H: Gavillon and Budtova 2008

814 As already mentioned in the previous section, the first and obvious trend is that aerogel bulk
815 density increases with the increase of cellulose concentration in solution. More matter is in a given
816 volume, higher is material density. The second trend is that all experimental densities are higher than
817 that calculated for the case of no volume shrinkage. As mentioned above, whatever experimental
818 conditions are, shrinkage occurs during solvent exchange and drying. Except $\text{ZnCl}_2 \cdot 4\text{H}_2\text{O}$, there is no
819 significant influence of solvent or non-solvent type on cellulose II aerogel density. It should be kept in
820 mind that different research groups use experimental conditions (for example, the way of solvent
821 exchange (gradual or not) and drying parameters) that differ one from another; the exact match of
822 experimental values is thus not expected. Finally, density does not seem to linearly increase with
823 cellulose concentration; the most probable reason is the decrease of shrinkage with the increase of
824 concentration.

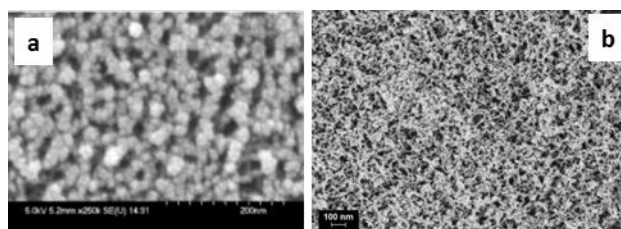
825 Much higher bulk density was reported for cellulose aerogels from $\text{ZnCl}_2 \cdot 4\text{H}_2\text{O}$ solvent whatever
826 is non-solvent type (Figure 7). This solvent was used only in two publications and more work is
827 needed to understand this trend. Was cellulose well dissolved? The values of specific surface area,
828 which could indicate the presence of non-dissolved fibers not participating to mesoporosity, are
829 similar to those reported for aerogels made from other solvents. The argument of bad solubility of
830 $\text{ZnCl}_2 \cdot 4\text{H}_2\text{O}$ in non-solvent (acetone, as reported in Schestakow et al. 2016a) cannot work here as far
831 as density is high even when water was used as coagulation bath, in which $\text{ZnCl}_2 \cdot 4\text{H}_2\text{O}$ is highly
832 soluble.

833

834 **4.2. Morphology and specific surface area**

835 Before discussing the morphology of cellulose II aerogels, a brief overview of the representative
836 morphologies of some classical aerogels based on silica, synthetic polymers and bio-aerogels is
837 presented. The microstructure of silica aerogels is shown in Figure 8a and 8b. The difference
838 between two is that Figure 8a shows the morphology of a classical silica aerogel, with “pearl-
839 necklace” structure (Leventis et al. 2002; Katti et al. 2006), and Figure 8b corresponds to the

840 morphology of prepolymerised silica sol (Markevicius et al. 2017). Classical silica aerogels consist of a
841 “pearl-necklace” mesoporous network of particles of around 5 – 10 nm in diameter, connected by
842 “necks” and formed by dissolution and reprecipitation of silica during aging (Leventis et al. 2002).
843 Thin “necks” are the main reason of extremely fragile mechanical properties of silica aerogels.
844 Prepolymerised tetraethyl orthosilicate (TEOS) (Figure 8b) show more fibrous-like structure
845 (Markevicius et al. 2017); by varying silica concentration and, as a consequence, aerogel density, it
846 was possible to obtain aerogels with various mechanical behaviour (from ductile compaction to
847 elastic deformation and to brittle fracture) (Wong et al. 2014).



848
849 **Figure 8**

850 Silica aerogels based on:

851 (a) classical base-catalysed silica (Reprinted with permission from Katti A, Shimpi N, Roy S, Lu H,

852 Fabrizio EF, Dass A, Capadona LA, Leventis N (2006) Chemical, Physical, and Mechanical

853 Characterization of Isocyanate Cross-linked Amine-Modified Silica Aerogels. Chem. Mater. 18:85-296.

854 Copyright 2006 American Chemical Society) and

855 (b) prepolymerised oligomers of TEOS (Reprinted by permission from: [Springer] [J Mater Sci]

856 [Markevicius G, Ladj R, Niemeyer P, Budtova T, Rigacci A (2017) Ambient-dried thermal

857 superinsulating monolithic silica-based aerogels with short cellulosic fibers. J Mater Sci 52:2210–222],

858 [2017])

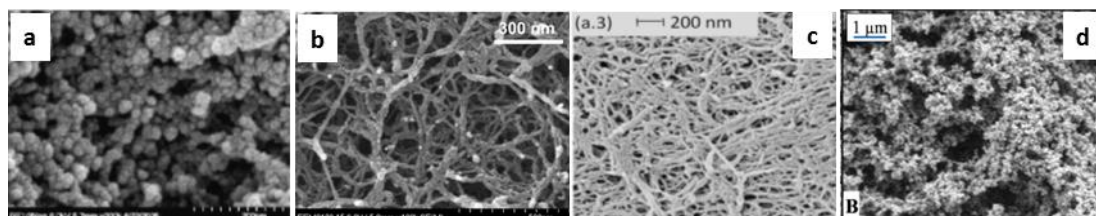
859

860 The morphology of various synthetic polymer aerogels based on resorcinol-formaldehyde,

861 polyimide, polyurea and polyurethane is shown in Figure 9. While some show bead-like structure

862 (resorcinol-formaldehyde and polyurethane, Figure 9a and 9d, respectively), polyimide and polyurea
863 are represented by a fibrous network (Figure 9b and 9c, respectively).

864



865

866

Figure 9

867

SEM images of morphology of aerogels based on:

868

(a) acid-catalysed resorcinol-formaldehyde (Reprinted with permission from Mulik S, Sotiriou-

869

Leventis C, Leventis N (2007) Time-Efficient Acid-Catalyzed Synthesis of Resorcinol-Formaldehyde

870

Aerogels. *Chem. Mater.* 19:6138–6144. Copyright 2007 American Chemical Society),

871

(b) polyimide (Reprinted with permission from Meador MAB, Agnello M, McCorkle L, Vivod SL,

872

Wilmoth N (2016) Moisture-Resistant Polyimide Aerogels Containing Propylene Oxide Links in the

873

Backbone. *ACS Appl. Mater. Interfaces* 8:29073–29079. Copyright 2016 American Chemical Society),

874

(c) polyurea (Weigold L, Reichenauer G (2014) Correlation between mechanical stiffness and

875

thermal transport along the solid framework of a uniaxially compressed polyurea aerogel. *Journal of*

876

Non-Crystalline Solids 406:73–78, Copyright 2014, with permission from Elsevier) and

877

(d) polyurethane (Reprinted from Diascorn N, Calas S, Sallée H, Achard P, Rigacci A (2015)

878

Polyurethane aerogels synthesis for thermal insulation – textural, thermal and mechanical properties.

879

J. of Supercritical Fluids 106:76–84, Copyright 2015, with permission from Elsevier)

880

881

Bio-aerogels made by dissolution-solvent exchange route possess net-like morphology, see

882

examples for pectin, alginate and starch aerogels in Figure 10. They are all “easy-gelling”

883

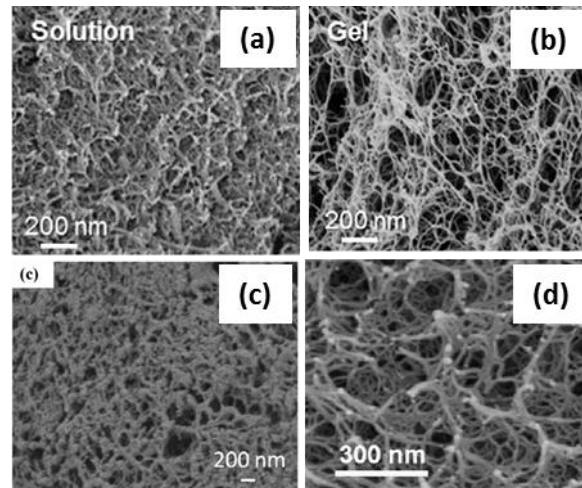
polysaccharides. One exception of aerogel made from non-gelled low-methylated pectin solution is

884

shown in Figure 10a: it is much denser (bulk density 0.12 vs 0.045 g/cm³ for its cross-linked

885 counterpart, Figure 10b) and with higher specific surface area (550 vs 400 m²/g, respectively) (Groult
886 and Budtova 2018b).

887



888

889

Figure 10

890

Morphology of bio-aerogels based on:

891

(a) pectin non-gelled solution and (b) pectin gelled with calcium (Reprinted from Groult S,

892

Budtova T (2018b) Tuning structure and properties of pectin aerogels. *European Polymer Journal*

893

108:250–261, Copyright 2018, with permission from Elsevier,

894

(c) corn starch (Reprinted from García-González CA, Uy JJ, Alnaief M, Smirnova I (2012)

895

Preparation of tailor-made starch-based aerogel microspheres by the emulsion-gelation method,

896

Carbohydrate Polymers 88:1378–138, Copyright 2012, with permission from Elsevier and

897

(d) alginate gelled with calcium (Reprinted from Escudero RR, Robitzer M, Di Renzo F, Quignard F

898

(2009) Alginate aerogels as adsorbents of polar molecules from liquid hydrocarbons: Hexanol as

899

probe molecule. *Carbohydrate Polymers* 75:52–57, Copyright 2009, with permission from Elsevier)

900

901

The morphology of cellulose II aerogels shows, for the majority of cellulose solvents, a net-like

902

texture. This is the case of aerogels made from cellulose/alkali, cellulose/ZnCl₂·4H₂O,

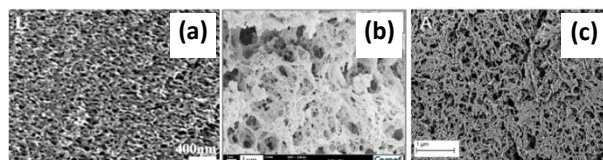
903

cellulose/TBAF/DMSO, cellulose/calcium thiocyanate and solid cellulose/NMMO. The examples are

904

shown in Figure 11-15. There are some exceptions which correspond to the cases when aerogels

905 were made from hot cellulose/NMMO and from cellulose/[Emim][OAc] solutions (Figures 12b,c, 13a
906 and 14b). These solutions are liquid before solvent exchange, and it was suggested that when such
907 solution is placed in a non-solvent, network structure is formed due to spinodal decomposition
908 mechanism leading to periodic bead-like morphology with beads of the same size (Sesousse et al.
909 2011a). This is not that evident for aerogels made from other cellulose/ionic liquids solutions (Figure
910 13b,c): when cellulose/[Bmim][Cl] was used (solvent is solid in room conditions but authors specified
911 that solutions were not solidified before being placed in non-solvent) (Aaltonen and Jauhiainen
912 2009), beads, if formed, are of much smaller size as compared to cellulose/[Emim][OAc] or
913 cellulose/NMMO case, and aerogels from cellulose/1-hexyl-3-methyl-1H-imidazolium chloride
914 ([Hmim][Cl]) solutions do not show bead-like morphology (Wang et al. 2013). Most of cellulose/alkali
915 solutions were not gelled before solvent exchange but aerogels do not show bead-like morphology
916 either. The difference in the morphology of aerogels from gelled and not cellulose/NaOH/water
917 solutions was demonstrated (Demilecamps et al. 2014): gelled solutions resulted in net-like aerogel
918 structure and bead-like morphology was recorded when cellulose was mixed with sodium silicate,
919 both dissolved in 8%NaOH/water. Sodium silicate was inducing cellulose coagulation by competing
920 with common solvent. It should be noted that in NaOH/water based solvents cellulose is not
921 dissolved on the molecular level, aggregates are formed (Lu et al. 2011). Overall, the state of the
922 matter (solution or gel), the kinetics of phase separation and the interactions between cellulose and
923 non-solvent have to be taken into account when interpreting the morphology of cellulose II aerogels.
924



925
926 **Figure 11**

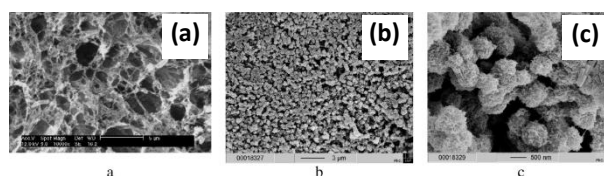
927 Morphology of cellulose II aerogels from cellulose/alkali solutions:

928 (a) 4 wt% cellulose/LiOH/urea/water, non-solvent ethanol (With permission from Wiley: Cai J,
929 Kimura S, Wada M, Kuga S, Zhang L (2008) Cellulose Aerogels from Aqueous Alkali Hydroxide–Urea
930 Solution. ChemSusChem 1:149 – 154),

931 (b) 5 wt% cellulose/NaOH/ZnO, non-solvent 0.3 M HCl (Reprinted by permission from: [Springer]
932 [Cellulose] [Demilecamps A, Reichenauer G, Rigacci A, Budtova T (2014) Cellulose–silica composite
933 aerogels from “one-pot” synthesis. Cellulose 21:2625–2636], [2014]) and

934 (c) 5 wt% cellulose/NaOH/urea, non-solvent 2 M HCl (Republished with permission of [Royal
935 Society of Chemistry], from [Mohamed SMK, Ganesan K, Milow B, Ratke L (2015) The effect of zinc
936 oxide (ZnO) addition on the physical and morphological properties of cellulose aerogel beads. RSC
937 Adv. 5:90193-90201]; permission conveyed through Copyright Clearance Center, Inc)

938



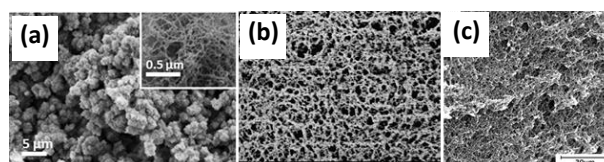
939

940

Figure 12

941 Morphology of cellulose II aerogels from solid (a) and molten (b, c) 5 wt% cellulose/NMMO
942 solutions, non-solvent was water. Image (b) is courtesy of R. Gavillon (Gavillon 2007) and images (a)
943 and (c) are reprinted from Sescousse R, Gavillon R, Budtova T (2011) Aerocellulose from cellulose–
944 ionic liquid solutions: Preparation, properties and comparison with cellulose–NaOH and cellulose–
945 NMMO routes. Carbohydrate Polymers 83:1766–1774, Copyright 2011, with permission from Elsevier

946



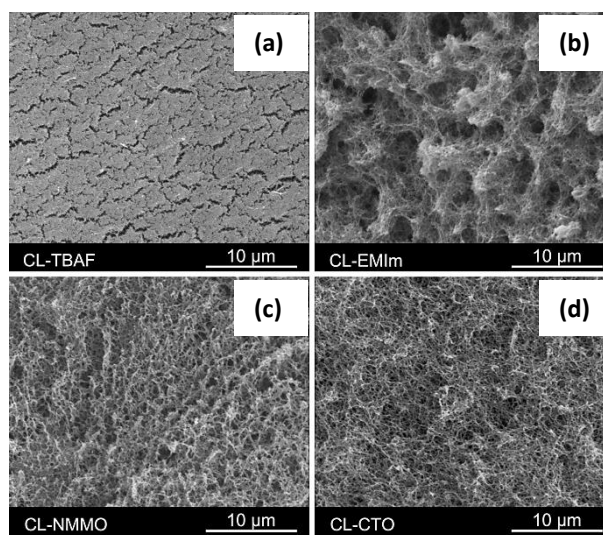
947

948

Figure 13

949 Morphology of cellulose II aerogels from cellulose/ionic liquid solutions:

950 (a) 5 wt% cellulose/[Emim][OAc]/DMSO, non-solvent ethanol (Buchtova and Budtova 2016)
951 (Reprinted by permission from: [Springer] [Cellulose] [Buchtova N, Budtova T (2016) Cellulose aero-,
952 cryo- and xerogels: towards understanding of morphology control, Cellulose 23:2585–2595], [2016]);
953 (b) 1.5 wt% bleached pulp/[Bmim][Cl], non-solvent ethanol (Reprinted from Aaltonen O, Jauhiainen
954 O (2009) The preparation of lignocellulosic aerogels from ionic liquid solutions, Carbohydrate
955 Polymers 75:125–129, Copyright 2009, with permission from Elsevier) and
956 (c) 1.5 wt% cellulose/[Hmim][Cl], non-solvent ethanol (Wang et al. 2013)
957



958
959 **Figure 14**
960 Morphology of cellulose II aerogels from 3 wt% cotton linters (CL) in (a) TBAF/DMSO, (b)
961 [Emim][OAc]/DMSO, (c) NMMO and (d) 1.5 w% cotton linters in $\text{Ca}(\text{SCN})_2 \cdot 8\text{H}_2\text{O}/\text{LiCl}$, non-solvent was
962 ethanol (Pircher et al. 2016)
963

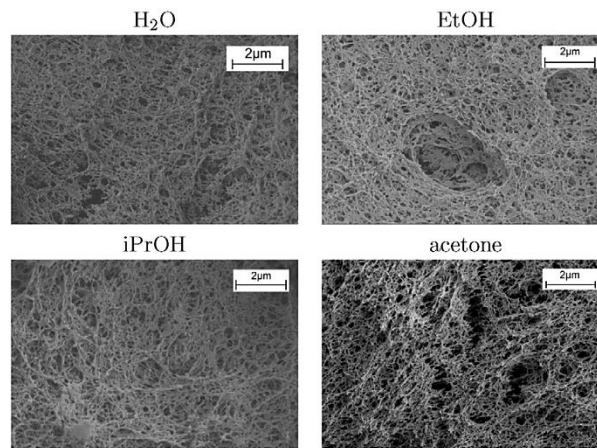
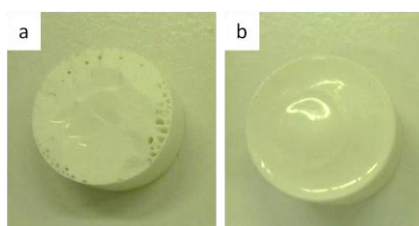


Figure 15

Morphology of cellulose II aerogels from 5 wt% cellulose/ $\text{ZnCl}_2 \cdot 4\text{H}_2\text{O}$ solutions coagulated in water, ethanol, isopropanol and acetone (Reprinted from Schestakow M, Karadagli I, Ratke L (2016a) Cellulose aerogels prepared from an aqueous zinc chloride salt hydrate melt. Carbohydrate Polymers 137:642–649, Copyright 2016, with permission from Elsevier)

It should be noted that the interactions between cellulose solvent and non-solvent should also be taken into account when investigating aerogel morphology and properties. For example, it was shown that exothermal reaction occurs when mixing [Emim][OAc] and water (Hall et al. 2012). At the moment of mixing, the temperature of [Emim][OAc]/water can increase as much as by 30 – 40 °C (Hall et al. 2012). It was hypothesised that this may create air bubbles in coagulating cellulose/[Emim][OAc] solution leading the “traces” as channels in cellulose aerogel, as shown in Figure 16. These large “holes” decrease density and increase porosity; potentially they can modify aerogel mechanical properties. Depending on the application, this phenomenon could be an interesting way to vary cellulose II aerogel morphology making hierarchical structure with pores of very different sizes, however, the control of structure formation is not easy.



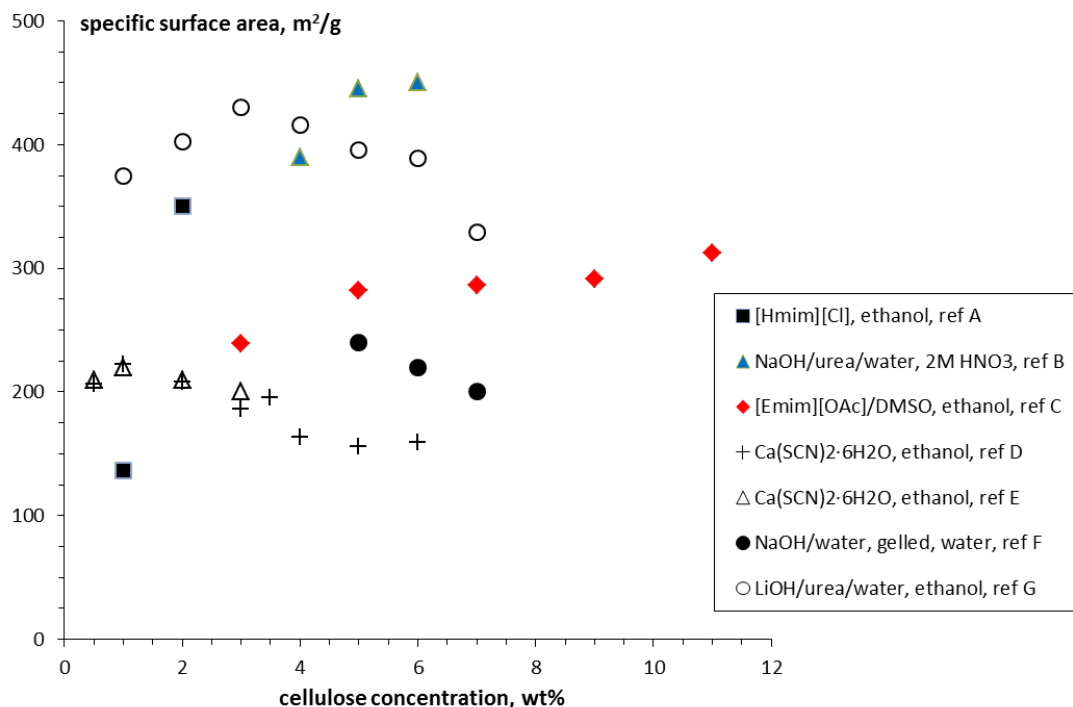
982

Figure 16

983 Cellulose II aerogels prepared from 15% cellulose/[Emim][OAc]/DMSO solutions coagulated in (a)
984 water and (b) ethanol (Rudaz 2013). Courtesy of C. Rudaz

985

986 Specific surface area of cellulose II aerogels is shown in Figure 17 as a function of cellulose
987 concentration which is the obvious parameter to vary when making aerogels, keeping all the others
988 the same. While density is easy to measure and many data are available, much less systematic results
989 are reported for specific surface which requires special and rather expensive equipment. Aging of
990 cellulose aerogels should be considered: it drastically influences mesoporosity with pores closing due
991 to humidity adsorption and not re-opening during degassing because of hornification effect. The type
992 of aerogel morphology, net-like or bead-like (see Figures 11-15), does not seem to influence specific
993 surface area (Figure 17), but here again more systematic experiments are needed to make convincing
994 conclusions.



995

996

Figure 17

997 Specific surface area of cellulose II aerogels as a function of cellulose concentration in solution for
998 cellulose dissolved in different solvents and coagulated in different non-solvents. Ref A: Wang et al.
999 2013; ref B: Trygg et al. 2013; ref C: Buchtova and Budtova 2016; ref D: Karadagli et al. 2015; ref E:
1000 Hoepfner et al. 2008; ref F: Gavillon and Budtova 2008; ref G: Cai et al. 2008

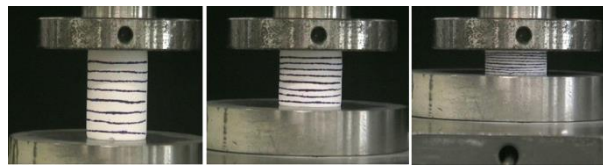
1001
1002 The increase of cellulose concentration leads to three types of trends for specific surface area,
1003 all contradicting each other (Figure 17): surface area i) increases (case of cellulose dissolved in
1004 NaOH/urea/water and in ionic liquids [Emim][OAc] and [Hmim][Cl], all coagulated in ethanol), ii)
1005 decreases (cellulose dissolved and gelled in NaOH/water and in $\text{Ca}(\text{SCN})_2 \cdot 6\text{H}_2\text{O}$) and iii) without any
1006 clear trend (cellulose dissolved in $\text{Ca}(\text{SCN})_2 \cdot 6\text{H}_2\text{O}$ and in LiOH/urea/water). The increase in specific
1007 surface area with the increase of aerogel density (which is proportional to cellulose concentration as
1008 shown in Figure 7) was also reported for four cases when cellulose was dissolved in $\text{ZnCl}_2 \cdot 4\text{H}_2\text{O}$ and
1009 coagulated in non-solvents such as water, ethanol, acetone and isopropanol (Schestakow et al.
1010 2016). The increase of specific surface area with the increase of cellulose concentration was
1011 suggested to be the result of pores “division” into smaller ones and not due to the increase of pore
1012 walls thickness (Buchtova and Budtova 2016). More careful and systematic experiments are needed
1013 to confirm or not this hypothesis.

1014

1015 **4.3. Mechanical properties of cellulose II aerogels and their composites**

1016 The majority of bio-aerogel’s mechanical properties are tested in the uniaxial compression mode
1017 which is due to the easiness of the preparation of cylindrical samples. While theoretical approaches
1018 interpreting the mechanical response of silica aerogels have been developed (see, for example,
1019 Alaoui et al. 2008), the understanding of the mechanical properties of bio-aerogels and of the
1020 influence of various parameters (type of polysaccharide, polymer molecular weight, type of solvent
1021 and non-solvent, morphology, etc) still remain to be unveiled.

1022 Under the uniaxial compression cellulose II aerogel does not buckle, it uniformly decreases its
1023 height keeping diameter constant within experimental errors (Figure 18); it was thus deduced that
1024 Poisson ratio is zero (Sescousse et al. 2011a; Schestakow et al. 2016a; Rege et al. 2016). Aerogel can
1025 be compressed without breakage till 80% strain (after that the experiments are stopped). Similar
1026 properties were reported for other bio-aerogels, for example, based on nanocellulose (Plappert et al.
1027 2017) and pectin (Rudaz et al. 2014). Being highly compressed, bio-aerogels do not recover their
1028 shape, strong densification occurs.



1029

1030

Figure 18

1031 Images of cellulose II aerogel under the uniaxial compression (Gavillon 2007), courtesy of R.

1032

Gavillon

1033

1034 Compression stress-strain curves of cellulose II aerogels look as classical ones obtained for
1035 porous materials such as foams (Gibson and Ashby 1997) and inorganic and synthetic polymer
1036 aerogels (Figure 19). At low strains (up to few per cent strain units), stress is linearly proportional to
1037 strain; this region is characterized by compressive modulus which is also often called Young's
1038 modulus. Further increase of strain leads to progressive buckling of cell walls followed by their
1039 collapse; it corresponds to stress plateau the beginning of which is characterized by yield stress.
1040 Finally, at high strains cell walls touch each other, broken fragments pack and, theoretically, wall
1041 material itself is compressed (densification region). This type of compression behaviour was reported
1042 for cellulose II aerogels made from various solvents with different non-solvents.

1043

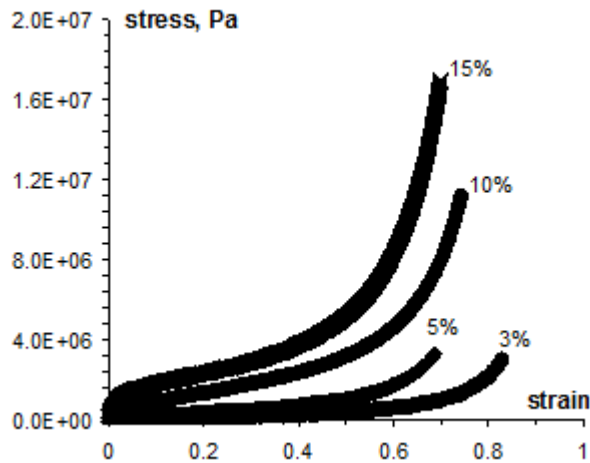


Figure 19

Stress-strain curves of aerogels made from cellulose/[Emim][OAc] solution of various cellulose concentrations, non-solvent was water (Reprinted from Sescousse R, Gavillon R, Budtova T (2011) Aerocellulose from cellulose–ionic liquid solutions: Preparation, properties and comparison with cellulose–NaOH and cellulose–NMMO routes. Carbohydrate Polymers 83:1766–1774, Copyright 2011, with permission from Elsevier)

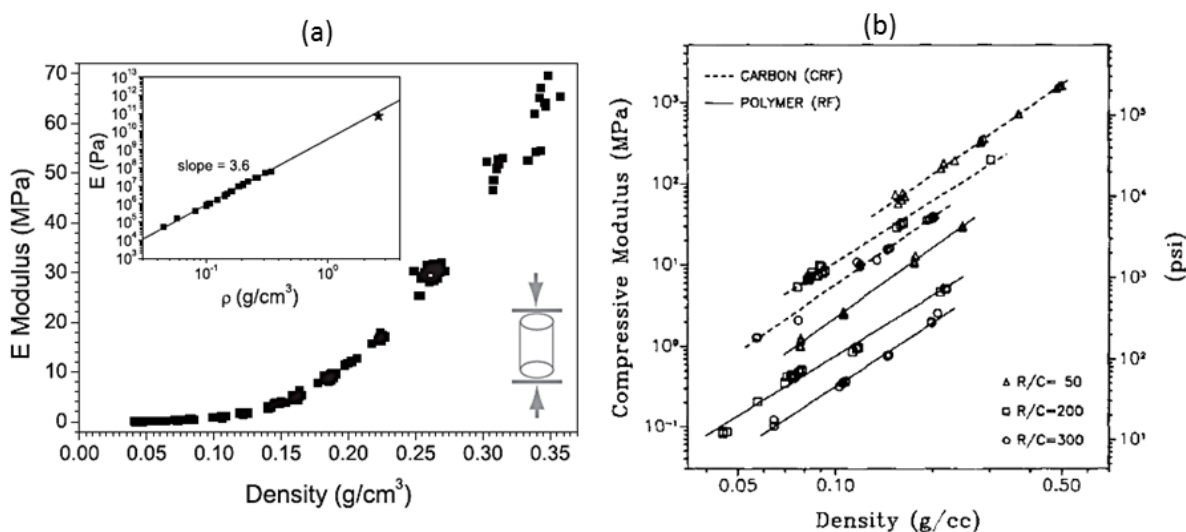
To better understand the mechanical properties of materials, loading-unloading tests should be performed and strain recovery should be followed as a function of strain (see, for example, amine-modified silica aerogels (Katti et al. 2006) or polyurea aerogels (Weigold and Reichenauer 2014)). For classical aerogels in the linear regime the deformation is recovered, and at higher strains a hysteresis occurs with strain recovery becoming lower and lower with strain increase and finally being irreversible (Alaoui et al. 2008). This type of experiments was not performed on cellulose II aerogels. Strain recovery coupled with density and morphology analysis at each compression step would help the understanding of structure-properties relationships in cellulose aerogels. In particular, a comparison of strain recovery of aerogels based on cellulose I (Martoia et al. 2016) and cellulose II would be very interesting.

1062 A usual way to analyse the mechanical properties of aerogels is to plot compressive modulus E
 1063 as a function of bulk density. For porous materials E is power-law dependent on aerogel bulk density
 1064 (Gibson and Ashby 1997):

$$1065 \quad E \sim \rho_{bulk}^n \quad (3)$$

1066 For regular open-cell foams the exponent $n = 2$, for silica aerogels it is usually around 3 – 4 (Cross et
 1067 al. 1989; Alaoui et al. 2008; Wong et al. 2014) and for synthetic polymer aerogels it is, in general,
 1068 around 2 - 3 ($n = 2$ was reported for polyurea aerogels (Weigold and Reichenauer 2014), $n = 2.7$ for
 1069 resorsinol-formaldehyde (Pekala et al. 1990) but $n = 3.7$ for polyurethane aerogels (Diascorn et al.
 1070 2015)). The examples of compressive modulus vs bulk density for silica ($n = 3.6$) and resorcinol-
 1071 formaldehyde ($n = 2.7$) aerogels are shown in Figure 20a and 20b, respectively.

1072



1073

1074

Figure 20

1075

Compressive modulus as a function of aerogel density for:

1076

(a) polyethoxydisiloxane aerogels (Reprinted from Wong JCH, Kaymak H, Brunner S, Koebel MM

1077

(2014) Mechanical properties of monolithic silica aerogels made from Polyethoxydisiloxanes.

1078

Microporous and Mesoporous Materials 183:23–29, Copyright 2014, with permission from Elsevier)

1079

and

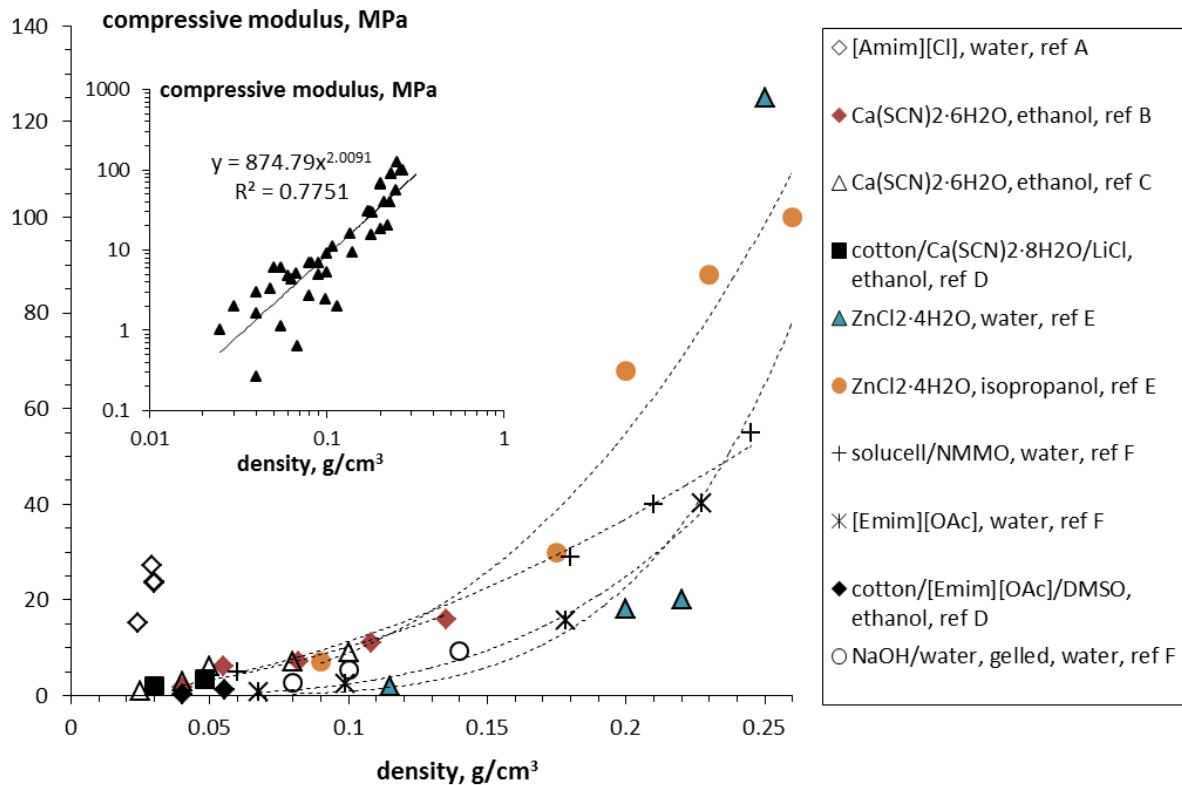
1080 (b) resorcinol-formaldehyde aerogels and their carbons (Reprinted from Pekala RW, Alviso CT, LeMay
1081 JD (1990) Organic aerogels: microstructural dependence of mechanical properties in compression.
1082 Journal of Non-Crystalline Solids 125:67-75, Copyright 1990, with permission from Elsevier)

1083

1084 Uniaxial compression tests have been performed on cellulose I aerogels and foams. For
1085 nanofibrillated freeze-dried cellulose, the exponent 2.29 was obtained for TEMPO-oxidised foams
1086 and 3.11 for foams from enzymatically pre-treated cellulose (Martoia et al. 2016). A linear
1087 relationship between compressive modulus and aerogel density was reported by Kobayashi et al.
1088 2014 and Plappert et al. 2017. For pectin aerogels n was 2.8 (Rudaz et al. 2014).

1089 The compression modulus of cellulose II aerogels made from various celluloses dissolved in
1090 different solvents is demonstrated in Figure 21; power law trends are shown by dashed lines. In a
1091 narrow density interval modulus can be seen as linearly dependent on aerogel density. However, this
1092 is only part of the trend, the straight line is a tangent to modulus vs density curve which clearly
1093 follows the power law in a wide range of densities (eq. 3). The exponent for cellulose aerogels made
1094 from cellulose/ $\text{ZnCl}_2 \cdot 4\text{H}_2\text{O}$ solutions and coagulated in isopropanol is $n = 2.6$, from
1095 cellulose/ $\text{ZnCl}_2 \cdot 6\text{H}_2\text{O}$ solutions and coagulated in water $n = 4.6$, from cellulose (DP 1175)/NMMO
1096 coagulated in water and from cellulose/calcium thiocyanate coagulated in ethanol $n = 1.7$ and for
1097 cellulose (DP 180)/[Emim][OAc] coagulated in water $n = 3.4$.

1098



1099

1100

Figure 21

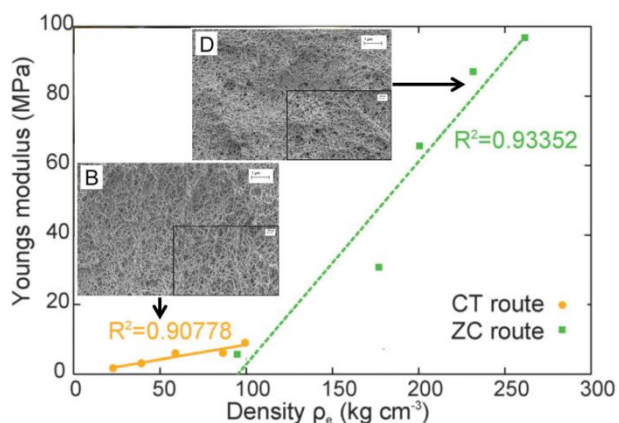
1101 Compressive modulus vs cellulose II aerogel density for various cellulose origins dissolved in
 1102 different solvents and coagulated in different non-solvents. Dashed lines are power-law fits (see
 1103 more details in the text). Data are taken from ref A: Mi et al. 2016; ref B: Karadaglia et al. 2015; ref C:
 1104 Rege et al. 2016; ref D: Pircher et al. 2016; ref E: Schestakow et al. 2016a; ref F: Sescousse et al.
 1105 2011a.

1106

1107 Linear approximation was used by Rege et al. 2016 to analyse modulus vs density of aerogels
 1108 made from cellulose/ $\text{Ca}(\text{SCN})_2 \cdot 6\text{H}_2\text{O}$ and cellulose/ $\text{ZnCl}_2 \cdot 4\text{H}_2\text{O}$ solutions (Figure 22). Each shows a
 1109 linear dependence being within a narrow interval of densities. Authors interpret high moduli values
 1110 of aerogels from cellulose/ $\text{ZnCl}_2 \cdot 4\text{H}_2\text{O}$ by the fact that “considerable amount of cellulose type I found
 1111 in ZC-derived cellulose aerogels leads to the formation of a stronger backbone” (Rege et al. 2016). To
 1112 find cellulose I after dissolution is surprising; SEM images of aerogel morphology from
 1113 cellulose/ $\text{ZnCl}_2 \cdot 4\text{H}_2\text{O}$ do not show any undissolved cellulose and the texture is similar to that from

1114 cellulose/ $\text{Ca}(\text{SCN})_2 \cdot 6\text{H}_2\text{O}$ route (Figure 22). As mentioned in Section 3.3 and shown in Section 4.1, all
1115 aerogels from cellulose/ $\text{ZnCl}_2 \cdot 4\text{H}_2\text{O}$ route have much higher density than that of aerogels made from
1116 cellulose dissolved in any other solvent which results in very high moduli.

1117



1118

1119

Figure 22

1120 Compressive modulus vs density for aerogels made from cellulose/ $\text{Ca}(\text{SCN})_2 \cdot 6\text{H}_2\text{O}$ coagulated in
1121 ethanol ("CT route") and from cellulose/ $\text{ZnCl}_2 \cdot 4\text{H}_2\text{O}$ coagulated in isopropanol ("ZC route") together
1122 with the corresponding SEM images. For more details see (Rege et al. 2016). Adapted with
1123 permission of [Royal Society of Chemistry], from [Rege A, Schestakow M, Karadagli I, Ratke L, Itskov
1124 M (2016) Micro-mechanical modelling of cellulose aerogels from molten salt hydrates. Soft Matter
1125 12:7079-7088, copyright 2016]; permission conveyed through Copyright Clearance Center, Inc

1126

1127 The trend for compressive modulus vs density for all data plotted together (inset in Figure 21)
1128 gives $n = 2$ but with low correlation coefficient, $R^2 = 0.77$. The exponent $n = 2$ was not expected
1129 because cellulose II aerogels are far from being regular foams, however, the same exponent was
1130 obtained for polyurea aerogels (Weigold and Reichenauer 2014) which shows morphology similar to
1131 some of cellulose II aerogels (see Section 4.2 and Figure 9). To put all data for cellulose II aerogels
1132 without distinguishing (at least) by cellulose molecular weight is, certainly, a too rough
1133 approximation, however, even if keeping data for low-molecular weight cellulose only, the trend
1134 remains with the same exponent. On one hand, Sescousse et al. 2011a showed that compressive

1135 modulus of aerogels from cellulose (Solucell, DP 950) dissolved in NMMO is higher than that made
1136 from cellulose (microcrystalline, DP 180) dissolved in 8%NaOH/water. On the other hand, modulus is
1137 the same for aerogels made from pulps, hardwood of DP 665 and softwood of DP 148 (Liebner et al.
1138 2009); however, a huge decrease in cellulose DP from 665 to 129 was reported after the dissolution
1139 in NMMO which may be the reason of comparable moduli values of aerogels.

1140 One of the problems in the understanding of of the trends in the properties of bio-aerogels is
1141 their sensitivity to moisture, as mentioned in Section 2.3. "Characterisation of bio-aerogels". While
1142 mechanical testing of classical polymers and their composites is usually performed on conditioned
1143 samples and at fixed and controlled humidity and temperature according to the norms,
1144 unfortunately this is rare for the case for bio-aerogels. The norms should be applied to bio-aerogels
1145 for the adequate comparison of data from different publications.

1146 The mechanical properties of cellulose aerogels vary if another component is added resulting in
1147 composite aerogel material. To make composite cellulose aerogels, usually a "wet" cellulose
1148 precursor is impregnated by a second component which is polymerized inside cellulose network, the
1149 whole is then dried with supercritical CO₂. The values obtained for such composite aerogels must be
1150 analysed with care as far as aerogel density and morphology are modified as compared to neat
1151 cellulose counterpart, and the interactions between the components and the morphology of the
1152 second network should be considered. For example, a strong increase in the mechanical properties
1153 of cellulose/polymethylmethacrylate interpenetrated network aerogels as compared to neat
1154 cellulose aerogels was reported (Pircher et al. 2015). When cellulose/silica aerogel composites were
1155 prepared, Cai et al reported a "softening effect" (decrease of the modulus) due to the presence of
1156 silica (Cai et al. 2012), while Demilecamps et al. 2015b and Liu et al. 2013 demonstrated a strong
1157 increase in compressive modulus of cellulose/silica aerogel composites. The influence of the
1158 conditions in which the second component is polymerised on composite aerogel properties should
1159 also be considered: for example, cellulose degradation occurred during acid catalysis of alkoxylane, in
1160 the view of making interpenetrated cellulose/silica aerogels (Litschauer et al. 2011). The formation of

1161 silica aerogel was not confirmed in this case as far as specific surface area of the composite, 220 –
1162 290 m²/g, was the same as of neat cellulose aerogel, 255 m²/g, while it is known that TEOS-based
1163 silica aerogels possess very high specific surface area, around 700 – 1000 m²/g. The case of silica
1164 particles (dispersed in cellulose aerogel matrix), and not silica aerogel, was reported for cellulose
1165 mixed with sodium silicate, both dissolved in 8% NaOH/water, however, the mechanical properties of
1166 composite aerogels were slightly improved (Demilecamps et al. 2014).

1167

1168 **3.4. Thermal conductivity of cellulose II aerogels.**

1169 Thermal conductivity is the most peculiar and exciting property of aerogels. Because of low
1170 density and mesoporosity, some classical aerogels (silica, resorcinol-formaldehyde and polyurethane
1171 based) are thermal super-insulating materials, i.e. with thermal conductivity below that of air in
1172 ambient conditions, 0.013 – 0.015 vs 0.025 W/m.K. In the first approximation, thermal conductivity λ
1173 of a porous material is an additive sum of gaseous (λ_{gas}) and solid (λ_{solid}) phase conduction and of the
1174 radiative heat transfer (λ_{rad}):

$$1175 \lambda = \lambda_{\text{gas}} + \lambda_{\text{solid}} + \lambda_{\text{rad}} \quad (4)$$

1176 Solid phase conduction increases with density increase; it is power-law dependent on aerogel
1177 density (Lu et al. 1992). To minimize the conduction of the gaseous phase two options are possible:
1178 either evacuation of the gas (air), or decrease of pores' size down to mesoporous region. According
1179 to Knudsen effect, when pore size is below the mean free path of air molecule, which is around 70
1180 nm at 25 °C and 1 atm, λ_{gas} is lower than that of ambient air. λ_{rad} is not significant at room
1181 temperatures and optically thick materials (Figure 23). Intuitively it is thus clear that the lowest
1182 thermal conductivity can be reached for low-density mesoporous materials. For silica and resorcinol-
1183 formaldehyde aerogels it was demonstrated that the dependence of thermal conductivity on density
1184 has a U-shape, as shown in Figure 23 (Lu et al. 1992): higher density leads to conductivity increase
1185 because of λ_{solid} input, and lower density leads to λ_{gas} increase because of the presence of large pores
1186 which do not contribute to Knudsen effect.

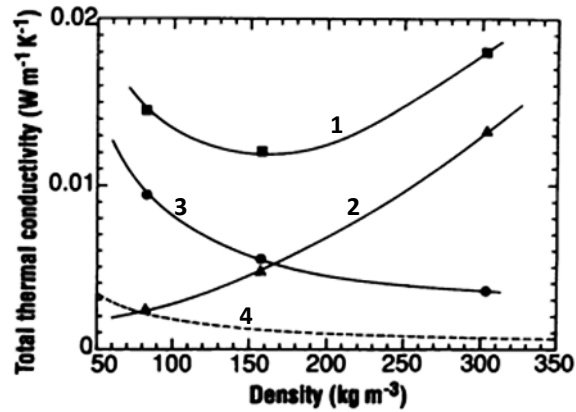


Figure 23

Total thermal conductivity (1), solid phase conductivity (2), gaseous conductivity (3) and calculated radiative conductivity (4) of resorcinol-formaldehyde aerogels as a function of density at ambient conditions (From [Lu X, Arduini-Schuster MC, Kuhn J, Njilsson O, Fricke J, Pekala RW (1992) Thermal Conductivity of Monolithic Organic Aerogels. *Science* 255:971-972]. Reprinted with permission from AAAS)

Not much is known about the thermal conductivity of bio-aerogels. Low thermal conductivity, around 0.015–0.022 W/m.K, was reported for aerogels based on pectin (Rudaz et al. 2014; Groult and Budtova 2018a), nanofibrillated cellulose (Jiménez-Saelices et al. 2017; Kobayashi et al. 2014; Seantier et al. 2016), alginate (Raman et al. 2015) and starch (Druel et al. 2017). Recently, U-shape conductivity-density dependence was obtained for low-methylated pectin aerogels, see Figure 24 (Groult and Budtova 2018a), showing that bio-aerogels obey classical trends.

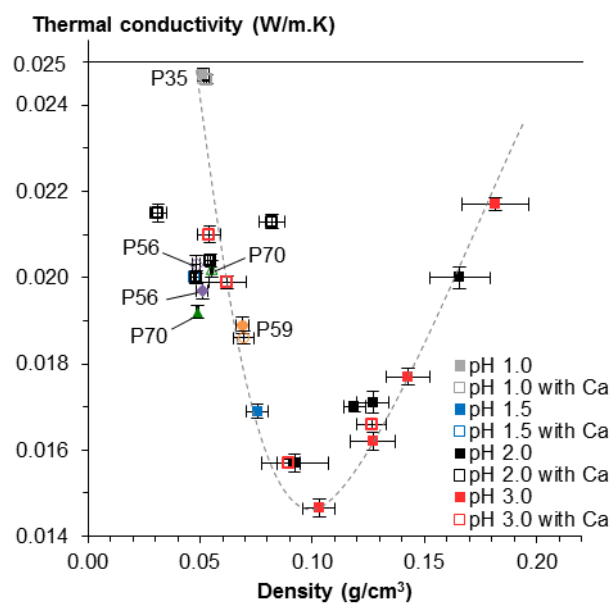


Figure 24

1201

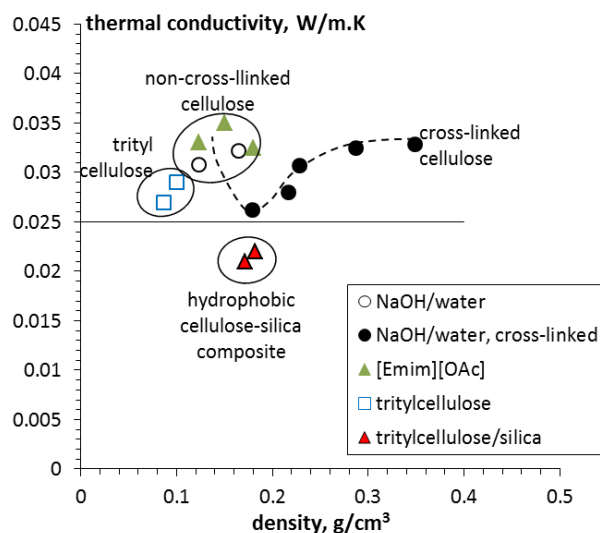
1202

1203 Thermal conductivity vs density for low methylated pectin aerogels, made at various pH and
 1204 cross-linked with calcium and not. For more details see Groult and Budtova 2018a. Reprinted from
 1205 Groult S, Budtova T (2018a) Thermal conductivity/structure correlations in thermal super-insulating
 1206 pectin aerogels. Carbohydrate Polymers 196:73–81, Copyright 2018, with permission from Elsevier
 1207

1207

1208 Thermal conductivity of cellulose II aerogels was also studied in details and many efforts were
 1209 made to find the conditions in which these aerogels should become a thermal superinsulating
 1210 material. None resulted in conductivity lower than that of air, 0.025 W/m.K (Figure 25). When
 1211 cellulose was dissolved in $\text{Ca}(\text{SCN})_2 \cdot 4\text{H}_2\text{O}$, aerogel conductivity was either 0.044 – 0.55 W/m.K
 1212 (Laskowski et al. 2015) or even higher, 0.04 – 0.075 W/m.K (Karadagli et al. 2015). The conductivity
 1213 of aerogels from cellulose/LiOH/urea/water was 0.025 W/m.K (Cai et al. 2012) and from
 1214 cellulose/NaOH/water and cellulose/[Emim][OAc] around 0.03 – 0.032 W/m.K (Rudaz 2013) (Table
 1215 S1). Freeze-dried cellulose aerogels possessed similar conductivity of around 0.029 – 0.032 (Nguyen
 1216 et al. 2014). Cellulose cross-linking with epichlorohydrin (ECH) in NaOH/water was performed in the
 1217 view of decreasing pore size and thus decreasing gaseous phase conduction, see eq. 4 (Rudaz 2013).

1218 This allowed decreasing the conductivity to 0.026 W/m.K (Figure 25), however, the “barrier” of air
1219 conductivity was not overcome.
1220



1221

1222

Figure 25

1223 Thermal conductivity vs bulk density of cellulose II aerogels (solvents: NaOH/water and
1224 [Emim][OAc]), tritylcellulose and tritylcellulose/hydrophobised silica aerogels. Solid line corresponds
1225 to the conductivity of air, dashed line is given to guide the eye. Data are taken from (Rudaz 2013;
1226 Demilecamps 2015a, 2016)

1227

1228 Cellulose is hydrophilic and adsorbs humidity from air which results in densification and increase
1229 of conductivity. Tritylcellulose was synthesized and aerogels prepared; their conductivity was lower
1230 than that of non-modified cellulose (0.027 – 0.029 W/m.K, see Figure 25) but again it was higher than
1231 the one of air (Demilecamps et al. 2016). Thermal conductivity of freeze-dried cellulose aerogels
1232 hydrophobised with plasma treatment was 0.03 – 0.033 W/m.K (Shi et al. 2013a).

1233 In the view of decreasing the conductivity of cellulose aerogels, composite aerogels based on
1234 cellulose/silica were prepared. When cellulose/Ca(SCN)₂·4H₂O solutions were mixed with granular
1235 superinsulating silica aerogel, the conductivity of composite aerogels slightly decreased as compared
1236 to neat cellulose aerogel counterpart but was still high, 0.04 – 0.05 W/m.K (Laskowski et al. 2015).

1237 When “wet” cellulose was impregnated with silica sol (TEOS) in order to fill the pores of cellulose
1238 matrix and thus decrease the conduction of the gas (air) phase, surprisingly the conductivity of
1239 composite aerogels increased from 0.025 to 0.04 – 0.05 W/m.K (Cai et al. 2012). The reason could be
1240 a strong increase in the density of composite aerogel (0.14 g/cm³ for neat cellulose aerogel, 0.19 for
1241 neat silica aerogel and 0.3 – 0.6 g/cm³ for composite aerogels) which means that the formation of
1242 silica aerogel inside the pores of cellulose matrix was perturbed and did not lead to a formation of a
1243 superinsulating material. Similar impregnation approach was used by Demilecamps et al. 2015b:
1244 cellulose was dissolved in [Emim][OAc]/DMSO, coagulated in ethanol and impregnated with
1245 polyethoxydisiloxane. Thermal conductivity decreased from 0.033 W/m.K for neat cellulose aerogel
1246 to 0.026 W/m.K for composite cellulose-silica (Demilecamps et al. 2015b). A similar decrease in
1247 conductivity was reported for cellulose matrix filled with TEOS, freeze-dried and hydrophobised via
1248 plasma treatment: from 0.03 W/m.K for the neat cellulose to 0.026 W/m.K for cellulose-silica
1249 composite (Shi et al. 2013b).

1250 The only way which resulted in cellulose-based thermal superinsulating aerogels was making
1251 fully hydrophobic cellulose/silica interpenetrated network. “Wet” (coagulated) tritylcellulose was
1252 impregnated with polyethoxydisiloxane which was gelled inside cellulose matrix, silica was
1253 hydrophobised and all was dried with supercritical CO₂. As a result, tritylcellulose matrix was filled
1254 with superinsulating hydrophobic silica aerogel which led to conductivities of 0.021 – 0.022 W/m.K
1255 (Demilecamps et al. 2016). The evolution of morphology from macroporous tritylcellulose to
1256 mesoporous tritylcellulose/silica composite aerogel is shown in Figure 26 which demonstrates that
1257 pores of cellulosic matrix were homogeneously filled with silica aerogel. A strong increase in the
1258 fraction of mesopores was confirmed by specific surface area: from 250 – 330 m²/g for tritylcellulose
1259 to 610 – 750 m²/g for composite aerogels (Demilecamps et al. 2016).

1260

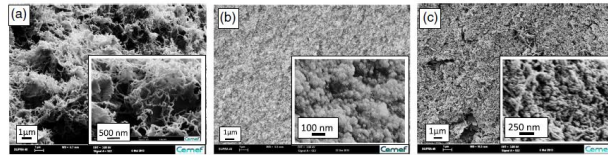


Figure 26

SEM images of aerogels based on (a) tritylcellulose, (b) polyethoxydisiloxane and (c) tritylcellulose/polyethoxydisiloxane interpenetrated network (Reprinted from Demilecamps A, Alves M, Rigacci A, Reichenauer G, Budtova T (2016) Nanostructured interpenetrated organic-inorganic aerogels with thermal superinsulating properties. *Journal of Non-Crystalline Solids* 452:259–265, Copyright 2016, with permission from Elsevier)

Why it is not possible to make thermal superinsulating cellulose II aerogels while this is feasible with nanocellulose and several other polysaccharides such as pectin, starch and alginate? The reason is, probably, in “unfavourable” cellulose II aerogel morphology (see Section 4.2), with too thick pore walls and too many large macropores. Molecular modelling could be very helpful to answer how cellulose chains are packing during non-solvent exchange and why this is different from other polysaccharides that form finely nanostructured thermal superinsulating aerogels.

4. POTENTIAL APPLICATIONS OF CELLULOSE II AEROGELS

Cellulose aerogels are said to be versatile materials suitable for numerous applications, and indeed they are, especially if considering additional properties coming from different options in cellulose functionalization and making composite and hybrid materials. Some applications of cellulose II aerogels are already tested and they will be overviewed below. Each section will start with a very brief description of the application area focusing on cellulose materials (other than aerogels) and on aerogels (other than cellulose-based). Cellulose I aerogels and freeze-dried cellulose II will also be considered as there are not many publications devoted to cellulose II aerogels’ applications. The reader will see that still there is a lot of room for improvements and applications to explore.

1285 **5.1. Bio-medical applications**

1286 Until now, the largest potential pharma- and/or bio-medical applications of bio-aerogels is
1287 suggested to be a carrier for the release of active substances, mainly drugs. There are different ways
1288 of drug incorporation in a bio-aerogel: either mixing with polysaccharide solution, or impregnating
1289 into “wet” aerogel precursor, or during drying (recall Figure 1). The choice of the route mainly
1290 depends on drug solubility in the corresponding fluid. In order to have high drug loading, it should be
1291 obviously not washed out during subsequent processing steps. Aerogels based on alginate, pectin,
1292 starch and chitosan have been reported as drug carriers (García-González et al. 2011), and the
1293 majority of literature describes drug loading in bio-aerogels using adsorption in supercritical carbon
1294 dioxide. The kinetics of drug release depends on several parameters such as the state of the drug
1295 (crystalline or amorphous) and matrix behaviour (swelling or contraction, dissolution) during mass
1296 transport in/from the matrix. Potentially, the release can be tuned by functionalization of the matrix
1297 and by making a composite or hybrid matrix, for example, organic-inorganic or organic-organic
1298 (based on different polymers). It was also demonstrated that bio-aerogels (based on alginate,
1299 alginate/lignin, pectin/xanthan, starch and starch/caprolactone) are non-cytotoxic, feature good cell
1300 adhesion and some can be used for bone regeneration (Martins et al. 2015; Quraishi et al. 2015;
1301 Horvat et al. 2017; Goimil et al. 2017).

1302 Cellulose I aerogels and foams (based on bacterial and nanofibrillated cellulose) have been
1303 widely studied in the view of their use in bio-medical applications as they are biocompatible, non-
1304 toxic and support growth and proliferation of cells (for more details, see Liebner et al. 2016). They
1305 can be used as matrices for drug delivery as release kinetics can be controlled by pore size and
1306 functionalization. The addition of silver or zinc oxide particles makes cellulose I aerogels antibacterial
1307 materials.

1308 Surprisingly, only few publications demonstrate the potential use of cellulose II aerogels in bio-
1309 medical applications, despite that many suggest it. Biocompatibility was demonstrated for cellulose II
1310 aerogels with dual porosity, with large pores made by porogens that are leached out and smaller

1311 pores coming from supercritical drying of coagulated cellulose matrix (Pircher et al. 2015). Aerogels
1312 made from phosphorylated cellulose, with low degree of substitution, showed good
1313 hemocompatibility (Liebner et al. 2012).

1314

1315 **5.2. Absorption and adsorption**

1316 Absorption of oils and organic solvents is an important environmental problem to solve with one
1317 example being spilled hydrocarbons in seawater. Various “sorption” (in the large sense of the term)
1318 approaches exist involving physical, chemical, biological treatments and their combinations. Porous
1319 materials with high efficiency, selectivity and allowing multiple reuse (many cycles) and easy
1320 degradation (better biodegradation) are in the focus of research with low cost also being an
1321 important criterion. Non-modified natural materials such as sugar cane bagasse, rice and coconut
1322 husk, natural fiber mats and fabrics have traditionally been used for absorption purposes, however
1323 their absorption capacity is not high (below 10 g/g) and selectivity (capability to absorb only oil) is
1324 rather poor as they are hydrophilic.

1325 Aerogels are discussed in literature for their potential applicability in oil and organic fluids
1326 absorption as they are highly porous and with high specific surface area which can be chemically
1327 tuned to increase the selectivity. An overview of the advantages (performance) and disadvantages
1328 (price) of using aerogels for environmental applications is given by Maleki 2016. Carbon and
1329 graphene aerogels seem to have the highest absorption capacity of oils and organic solvents, up to
1330 200 times their own weight (Maleki 2016).

1331 Cellulose aerogels, both from cellulose I and cellulose II, are good candidates to be used for
1332 absorption provided they are chemically modified to increase the selectivity. Here only non-
1333 pyrolysed freeze-dried and supercritically dried cellulose will be discussed as absorption and
1334 adsorption applications of the corresponding carbons are presented in Section 5.4. Only few studies
1335 report the use of cellulose II aerogels for absorption of organic fluids: for example, cellulose was
1336 coated with TiO₂ and showed five times higher absorption capacity of oil, up to 28 g/g, as compared

1337 to non-coated counterpart (Chin et al. 2014, see details on aerogel preparation in Table S1 of the
1338 Supporting Information). Most of the studies on absorption of oils and organic solvents are
1339 performed on freeze-dried cellulose II and all use silylation (with trimethylchlorosilane,
1340 octadecyltrimethoxysilane, etc.) or plasma treatment (Lin et al. 2015) or chemical vapour deposition
1341 (Zhang et al. 2016; Liao et al. 2016). The absorption capacity of oils is usually within 20 – 25 g/g (Lin
1342 et al. 2015; Zhang et al. 2016) with the best result, up to 59 g/g, obtained for cellulose dissolved in
1343 NaOH/urea/water, cross-linked with N,N'-methylenebisacrylamide, freeze-dried and functionalized
1344 with trimethylchlorosilane (Liao et al. 2016). The absorption of organic solvents is around 40 – 50 g/g
1345 (Zhang et al. 2016). As expected, the absorption capacity decreases with the increase of fluid
1346 viscosity. Most of the publications cited above report good cellulose hydrophobicity and recyclability
1347 with up to 10-15 cycles tested. Similar absorption capacities were reported for nanofibrillated freeze-
1348 dried cellulose either TiO₂ functionalised (Korhonen et al. 2011) or silylated (Cervin et al. 2012) or
1349 surface-grafted and cross-linked (Mulyadi et al. 2016). Higher values were obtained for
1350 nanofibrillated cellulose treated with methyltrimethoxysilane and freeze-dried: the absorption
1351 capacity of oil was up to 50 – 60 g/g and of organic solvents up to 100 g/g (Zhang et al. 2014). Finally,
1352 very high absorption values were reported for surface-modified bacterial cellulose with
1353 trimethylchlorosilane in liquid phase and freeze-dried: absorption of oils was up to 100 – 120 g/g and
1354 of organics up to 185 g/g (Sai et al. 2015). Interestingly, high absorption of oils (up to 95 g/g), even
1355 better than by many of cellulose I and cellulose II cryo- and aerogels, was obtained for “simple”
1356 recycled cellulose fibers, cross-linked with Kymene, freeze-dried and coated with
1357 methyltrimethoxysilane (Feng et al. 2015).

1358 The analysis of the absorption capacity obtained for various cellulose I and cellulose II porous
1359 materials and of the reasons of different results reported can be a topic of another review article.
1360 What are the main driving forces of high absorption by cellulose-based materials: porosity, way and
1361 type of functionalization, surface area, type of cellulose? Should cellulose be dissolved or
1362 “delaminated” to obtain aero- or cryogels with fine structure for having high absorption capacity?

1363 These questions need answers if willing to use cellulose I and/or cellulose II aero- and cryogels in
1364 absorption applications.

1365 Another important environmental problem to solve is water pollution with heavy metal ions.
1366 Adsorption is considered to be one of the efficient methods among others such as membrane
1367 filtration and separation, precipitation, ion exchange, etc. The price, re-use, metal recovery and
1368 adsorbent regeneration (if possible) and degradation are playing an important role as in the case of
1369 absorption. Cellulose, when chemically modified (etherification, esterification, oxydation, grafting of
1370 various ligands) is considered as an alternative to synthetic adsorbents, with adsorption capacity
1371 being as high as 45 mg/g for Cr (VI), 105 mg/g for Pb (II), 169 mg/g for Cd (II), 188 mg/g for Ni (II) and
1372 246 mg/g for Cu (II) (O'Connel et al. 2008). Similar and even better values are reported for chitosan
1373 and its composites (Wan Ngah et al. 2011). It should be noted that adsorption capacity significantly
1374 depends on solution pH and initial concentration of metal ions.

1375 For the same reasons as for the absorption of organic pollutants, aerogels are considered to be
1376 promising materials due to their high adsorption performance, with carbon aerogels being the
1377 leaders: for example, 68 mg/g for Cr (VI) and 240 mg/g for Pb (II) (Maleki, 2016). As far as cellulose I
1378 and cellulose II cryo- and aerogel are concerned, cellulose modification is needed to make them
1379 efficient adsorbents. Cellulose II aerogels were prepared via the dissolution of microcrystalline
1380 cellulose in NaOH/urea/water, immersed in FeCl₃ and MnCl₂ solutions to obtain MnFe₂O₄ cellulose
1381 aerogel which adsorbed Cu (II) up to 90 mg/g (Cui et al. 2018). Another way to get high adsorption is
1382 to make composites: cellulose was dissolved in NaOH/urea/water, mixed with graphene oxide, cross-
1383 linked with N,N'-methylene bisacrylamide and freeze-dried; the adsorption of methylene blue was
1384 138 mg/g and of Cu (II) 85 mg/g (Geng, 2018). Nanocellulose is often chemically modified and tested
1385 for the adsorption of heavy metals. For example, freeze-dried nanofibrillated cellulose was grafted
1386 with poly(methacrylic acid-co-maleic acid) and Pb was adsorbed at around 95 mg/g and Cd at around
1387 90 mg/g (Maatar and Boufi 2015). However, high adsorption of metal ions can also be obtained on
1388 never-dried nanocellulose: for example, cellulose nanocrystals and nanofibers were enzymatically

1389 phosphorylated and the adsorption of Cu (II) was 117 mg/g and 114 mg/g, respectively (Liu et al.
1390 2015).

1391 High specific surface area of cellulose I and cellulose II aerogels should, theoretically, promote
1392 high adsorption capacity of heavy metal ions. Is the drying of coagulated cellulose or of nanocellulose
1393 needed to get high adsorption? Is there any advantage of nanocellulose vs cellulose II or it is cellulose
1394 modification which counts the most? Depending on the answers to these questions the price of
1395 cellulose adsorbent will be very different. A detailed analysis of results reported in literature taking
1396 into account the “state” of cellulose (polymorph type, wet or dry, way of drying, surface area and
1397 chemical modification) would be helpful to provide the best recipe in terms of performance.

1398

1399 **5.3. Composite aerogels with metal (nano)particles and quantum dots**

1400 Polymer/metal nanoparticles composites is a quickly developing area due to their various
1401 applications in optics, electronics, medical, catalysis and sensors. One of the challenges is to prevent
1402 nanoparticle self-aggregation and this is the reason why they are often immobilized or loaded in/on
1403 polymers, graphene or carbons. Another challenge is not to modify particles’ activity and selectivity
1404 due to their immobilization. Cellulose (in various forms: fibers, fabric and nanocellulose) is often used
1405 as metal nanoparticle support as cellulose is biodegradable and biocompatible and also binds metal
1406 nanoparticles minimizing the risk of contamination. The latter is possible if the surface of cellulose
1407 material is modified in the adequate way to immobilize the nanoparticle, usually by electrostatic
1408 interactions. Many publications report on making antimicrobial cellulose fibers and fabrics with Ag,
1409 Cu and Zn nanoparticles. Different forms of nanocellulose were shown to be very promising in
1410 catalysis applications: nanocellulose can be metal nanoparticle support, stabilizer and also a reducing
1411 agent in the *in situ* synthesis of metal nanoparticles (Kaushik and Moores, 2016).

1412 Whatever is the matter of nanoparticles’ support, porosity is one of the pre-requisites for having
1413 an efficient incorporation of metal nanoparticles. Aerogels are thus excellent candidates for metal
1414 nanoparticles’ support. Aerogels based on β -lactoglobulin amyloid fibrils loaded with gold

1415 nanoparticles were demonstrated to be a promising catalyst (Nystrom et al. 2016). Often carbon-
1416 based aerogels are employed as metal nanoparticles support. For example, carbons from pyrolysed
1417 resorcinol-formaldehyde aerogels and loaded with Pt or Ru nanoparticles can be used as electrode
1418 materials and catalyst support in proton-exchange membrane fuel cells (Biener et al. 2011). Fe₃O₄
1419 nanoparticles supported by freeze-dried nitrogen-doped graphene was demonstrated to be efficient
1420 cathode catalysts for oxygen reduction reaction (Wu et al. 2012).

1421 Cellulose II aerogels were used as support of metal (nano)particles (Cai et al. 2009; Chin et al.
1422 2014; Schestakow et al. 2016b; Cui et al. 2018). Schestakow et al. 2016b and Cai et al. 2009 report
1423 the deposition of noble metal (silver, gold and platinum) nanoparticles into cellulose aerogel
1424 network. Metals were impregnated into “wet” aerogel precursor, and nanoparticles were attached
1425 to cellulose via reduction reaction. In these cases composite aerogel density slightly increased and
1426 specific surface area remained the same as in the corresponding neat cellulose II aerogels (Table S1).
1427 The potential in using Ag-doped cellulose II aerogel as catalyst was demonstrated (Schestakow et al.
1428 2016b).

1429 Magnetic cellulose II aerogels were synthesized by adding either Fe₂O₃ nanoparticles (Chin et al.
1430 2014) or MnFe₂O₄ (Cui et al. 2018). In the first case aerogel was coated with TiO₂ and used for the
1431 absorption of oil which was up to 25 g/g. The magnetic property of aerogel was used to extract the
1432 sample with absorbed oil from the container. When magnetic cellulose/MnFe₂O₄ aerogels were
1433 synthesised, composite aerogel density increased and specific surface area increased slightly (Cui et
1434 al. 2018). These composites showed the adsorption of copper ions up to 63 mg/g, and magnetic
1435 property was used, as in the previous case, for the separation of the sample from water.

1436 Freeze-dried bacterial cellulose (density 0.015 g/cm³, specific surface area 103 m²/g) was used
1437 as a support of ferrite crystal nanoparticles (size from 40 to 60 nm and up to 120 nm at high
1438 FeSO₄/CoCl₂ concentrations) (Olsson et al. 2010). Nanoparticles were deposited on freeze-dried
1439 bacterial cellulose from solution followed by heating at 90 °C, immersing in NaOH/KNO₃ at 90 °C and

1440 then freeze-dried again. Flexible magnetic samples (density 0.3 g/cm^3) were obtained; they were
1441 suggested to be used as electronic actuators (Olsson et al. 2010).

1442 Quantum dots are semiconductor nanocrystals of a size of few nanometers, with a new
1443 generation of quantum dots based on carbon and graphene. Due to their unique electro-optical
1444 properties, so-called “quantum confinement”, they have superior brightness and photostability
1445 compared to conventional fluorescent dyes, well suited for multicolour applications, for biological
1446 imaging (bioassays, bioprobes and biosensors) and various energy related devices (LED,
1447 photodetectors, solar cells, etc.).

1448 Organic and inorganic aerogels were used as a support of quantum dots. Pyrolysed resorcinol-
1449 formaldehyde aerogels were used as carriers of carbon quantum dots and this composite
1450 supercapacitor showed excellent stability over 1000 charge-discharge cycles and 20 times higher
1451 specific capacitance as compared to its neat counterpart (Lv et al. 2014). Silica aerogels were
1452 functionalized with polyethylenimine-capped quantum dots and new NO_2 gas sensor was obtained
1453 (Wang et al. 2013). CdSe–ZnS quantum dots were covalently immobilized on tetramethylorthosilicate
1454 and luminescent aerogels were obtained (Sorensen et al. 2006).

1455 It seems there is only one publication reporting on cellulose/quantum dots aerogels. Cellulose
1456 was dissolved in [Hmim][Cl] and mixed with 3-(trimethoxysilyl)-propyl-functionalized $(\text{ZnS})_x(\text{CuInS}_2)_{1-x}$
1457 core/ZnS shell suspended in toluene (Wang et al. 2013). 1-mercapto-3-(trimethoxysilyl)-propyl
1458 ligands allowed the migration of quantum dots from toluene to cellulose/ionic liquid solutions which
1459 resulted in quantum dots covalently bonded to cellulose. Fluorescent aerogels were obtained.

1460 Depending on the thickness of quantum dot shell, specific surface area of aerogels increased almost
1461 twice and mechanical properties of composite aerogels were also improved as compared to their
1462 neat cellulose counterpart (Wang et al. 2013).

1463

1464 **5.4. Carbon cellulose aerogels**

1465 Carbon aerogels are mesoporous and microporous materials with high electrical conductivity.
1466 They are made by pyrolysis of organic aerogels in an inert atmosphere. Since resorcinol-
1467 formaldehyde aerogels were synthesized in the 90s of the last century (Pekala et al. 1995), their
1468 carbon counterparts (Pekala et al. 1998), including those made from xerogels, remain the most
1469 popular and studied. Other systems, such as phenolic–furfural, melamine–formaldehyde,
1470 polyacrylonitrile, and polyurethane were also used for making carbon aerogels. Carbon aerogels
1471 usually have high specific surface area, around 500-1000 m²/g; density can be higher than that of
1472 non-pyrolysed counterparts, around 0.1 - 0.5 g/cm³. Pyrolysis is usually performed during 8 – 10
1473 hours at temperature rising up to 1000 °C which leads to volume shrinkage and mass loss (for
1474 resorcinol-formaldehyde aerogels, linear shrinkage is around 30 % and mass loss around 50 %) (Shen
1475 et al. 2011). Carbon aerogels are proposed to be used in electrochemical and energy applications: in
1476 double layer capacitors (supercapacitors), lithium-ion batteries, for hydrogen storage, adsorption, as
1477 catalyst supports when metal-doped and for thermal insulation at high temperatures.

1478 The information on carbon aerogels from bio-aerogels is scarce with very few systematic studies
1479 correlating the morphology and properties of neat aerogels with processing parameters and resulting
1480 structure and properties of carbons. A significant input was made by the team from the university of
1481 York, UK. Starch-based mesoporous carbons, so-called Starbons, were obtained from pyrolysed
1482 dissolved-retrograded high amylose corn starch, doped with acid and dried at ambient pressure
1483 (Budarin et al. 2006). The increase of temperature from 150 °C to 700 °C led to the increase of
1484 specific surface area, from 200 to 500 m²/g, respectively. These carbons were suggested to be used
1485 as an alternative to acid catalysts (White et al. 2009). Similar approach was applied to other types of
1486 starches, and carbons with specific surface area around 170 – 370 m²/g were synthesised (Bakierska
1487 et al 2014). Carbons were obtained by pyrolysis of alginate aerogels: specific surface area of the
1488 starting aerogel was 320 m²/g and it first increased with the increase of temperature (up to 388 m²/g
1489 at 500 °C) and then decreased to 300 m²/g at 1000 °C (White et al. 2010a). These carbon aerogels
1490 were suggested to be used for the separation of some low molecular weight carbohydrates (White et

1491 al. 2010a). Carbons from pectin aerogels were also prepared by the same team (White et al. 2010b).
1492 As for alginate carbon aerogels, specific surface area of pectin-based carbons increased with the
1493 increase of temperature, from 200 m²/g for pectin aerogel to 377 m²/g for carbon aerogel made at
1494 450 °C, and then decreased to 298 m²/g at 700 °C (White et al. 2010b). The mass loss at 700 °C was
1495 around 70 %.

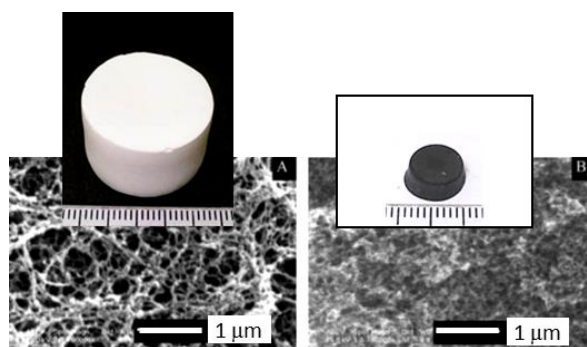
1496 As far as carbons from cellulose aerogels are concerned, the majority are made from pyrolysed
1497 freeze-dried either “nanocellulose” or dissolved-coagulated cellulose aerogels. Most of the work is
1498 focused not on cellulose matrix and its transformations, but on testing the properties of new porous
1499 biomass-based carbons for various applications. For example, bacterial cellulose was freeze-dried,
1500 pyrolysed and nitrogen-doped (specific surface area 916 m²/g) for making metal-free oxygen
1501 reduction electrocatalyst, for fuel cells and metal-air batteries (Liang et al. 2015). The same group
1502 used pyrolysed freeze-dried bacterial cellulose for the absorption of organic fluids (100–300 times its
1503 weight) (Wu et al. 2013). Interestingly, this carbon showed a high shape recovery under compression.
1504 The absorption of oils was also tested on carbonised freeze-dried cross-linked microfibrillated
1505 cellulose; from 40 to 60 g/g of oil was absorbed within few minutes (Meng et al. 2015). As mentioned
1506 in Section 5.2, efficient oil absorption can be obtained for functionalised, but not pyrolysed, freeze-
1507 dried nanofibrillated cellulose (for example, 20 – 40 g/g when coated with TiO₂ (Korhonen et al.
1508 2011) or up to 45 g/g when hydrophobised with octyltrichlorosilanes (Cervin et al. 2012)). Pyrolysed
1509 freeze-dried bacterial cellulose was also explored as anode material in lithium ion batteries (Wang et
1510 al. 2014b).

1511 Similar approaches were applied to pyrolysed freeze-dried dissolved-coagulated cellulose. For
1512 example, cellulose was dissolved in LiOH/urea/water, freeze-dried from TBA and pyrolysed; specific
1513 surface area of neat cellulose was 149 m²/g, of pyrolysed counterpart 500 m²/g and absorption
1514 capacity of hydrocarbons and oil was up to 25 g/g (Wang et al. 2014a). Similar absorption was
1515 reported for pyrolysed freeze-dried cellulose from cellulose/NaOH/urea/water (Lei et al. 2018).
1516 Carbons from freeze-dried cellulose dissolved in NaOH/water based solvent were reported as

1517 supercapacitor electrodes when nitrogen-doped (Hu et al. 2016), KOH activated (Yang et al. 2018)
1518 and CO₂ activated (Zhuo et al. 2016, Zu et al. 2016). These carbons were also shown to possess high
1519 CO₂ adsorption capacity (Zhuo et al. 2016; Hu et al. 2016) and be suitable as monolithic catalysts
1520 when MnO_x/N doped (Zhou et al. 2018).

1521 Very few is reported on carbons from cellulose II supercritically dried aerogels. They were made
1522 by pyrolysis of cellulose aerogels prepared by cellulose dissolution in [Emim][OAc] (Sescousse 2010a)
1523 and in NaOH/water (Gavillon 2007; Guilminot et al. 2008; Sescousse 2010a; Rooke et al. 2011, 2012).
1524 Mass and volume loss after pyrolysis was around 80% and 90%, respectively (Gavillon 2007). The
1525 interesting point is that despite a severe shrinkage, the samples kept their initial shape (Figure 27).
1526 This means that the volume and shape of carbon aerogel can be predicted and controlled from the
1527 very first steps of preparation (here, gelation of cellulose/NaOH/water solutions).

1528



1529

1530

Figure 27

1531 Representative photos of cellulose aerogels and its carbon counterpart and the corresponding
1532 SEM images. Aerogel was made from 7 wt% cellulose/NaOH/water solution, gelled and coagulated in
1533 ethanol. Photos are courtesy of R. Sescousse (Sescousse 2010a), SEM images are adapted with
1534 permission of [Electrochemical Society], from [Rooke J, de Matos Passos C, Chatenet M, Sescousse R,
1535 Budtova T, Berthon-Fabry S, Mosdale R, Maillard F (2011) Synthesis and Properties of Platinum
1536 Nanocatalyst Supported on Cellulose-Based Carbon Aerogel for Applications in PEMFCs. Journal of
1537 The Electrochemical Society 158:B779-B789]; permission conveyed through Copyright Clearance

1538

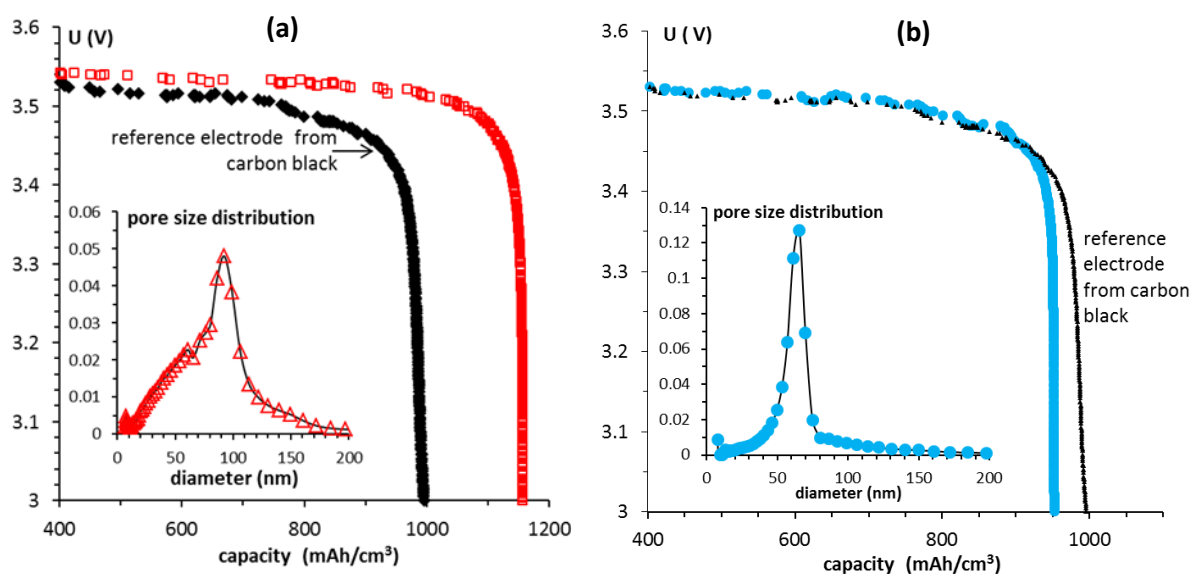
Center, Inc

1539
1540
1541
1542
1543
1544
1545
1546
1547
1548
1549
1550
1551
1552
1553
1554
1555
1556
1557
1558
1559
1560
1561
1562
1563
1564

SEM images in Figure 27 show densification of carbon aerogel as compared to its non-pyrolised counterpart; bulk density of carbons is usually higher by 50 to 100% reaching the values of 0.25 – 0.35 g/cm³ (Gavillon 2007; Sescousse 2010a). As well as for carbons from other organic aerogels, the number of macropores in carbons from porous cellulose seems to be reduced as compared to their counterparts before pyrolysis, possibly due to shrinkage. This can be deduced from the increasing specific surface area: 299 m²/g in aerogel vs 892 m²/g in CO₂ activated carbon (Zu et al. 2016); 149 m²/g in freeze-dried from TBA vs 500 m²/g in carbon (Wang et al. 2014), 130 m²/g in TBA vacuum dried cellulose tunicate nanocrystals vs 667 m²/g (pyrolysis under nitrogen) and 549 m²/g (pyrolysis under HCl) in carbons (Ishida et al. 2004) and 145 m²/g in aerogel vs 244 m²/g in carbon (Sescousse 2010a). It should be noted that activation step may strongly increase specific surface area.

The microstructure of carbon cellulose aerogels determines the application to be selected. For example, carbons from aerogels based on cellulose dissolved in NaOH/water turned out to be very promising as cathodes in Li/SOCl₂ primary batteries. Typical electrodes for this type of batteries are made from carbon black powders with polytetrafluoroethylene binder. While classical batteries have solid cathode and anode and the discharge is limited by the amount of oxidant or reductant, in liquid cathode cells it is limited by the porosity of carbon current collector. The optimal collector should have the highest possible pores volume with pore size in the range of mesopores up to small macropores (< 100 nm). The discharge properties of carbon aerogels from cellulose/8 wt%NaOH/water gelled solutions are presented in Figure 28 and compared with the reference material used by French company SAFT. “Green” carbon aerogels are excellent current collectors and in some cases their capacity is higher than that of the reference material (Rooke et al. 2012). The difference in the performance (Figure 28, case (a) vs case (b)) is related to the size of the pores in the carbon aerogel: while the volume of mesopores is practically the same, 2.9 and 3.2 cm³/g, it is the mean size of the pores which is different, 92 nm (a) vs 61 nm (b) (Rooke et al. 2012). Pore size distributions are shown in the insets of Figure 28a and 28b.

1565



1566

1567

Figure 28

1568

Discharge at 0.4 mA of Li/SOCl₂ button-type battery with a thin carbon aerogels collector disk.

1569

Carbons are made from pyrolysed aerogels prepared from (a) 5 wt% cellulose/NaOH/water gelled

1570

solution and (b) 7 wt% cellulose/NaOH/water gelled solution. The discharge time was in the range of

1571

300-400 hours. Data are taken from (Sescousse 2010a) and (Rooke et al. 2012). Insets correspond to

1572

pore size distributions.

1573

1574

The same carbon aerogels, doped with platinum, were shown to have suitable properties to be

1575

used in proton exchange membrane fuel cell (PEMFC) (Guilminot et al. 2008; Rooke et al. 2012).

1576

Platinum nanoparticles can be homogeneously deposited on carbon aerogel matrix and this “green”

1577

electrocatalyst compares well with standard Pt/carbon black materials.

1578

The evolution of cellulose mass and composition during pyrolysis is known to be a complex

1579

process: briefly, after the loss of water cellulose depolymerisation occurs, levoglucosan is formed

1580

which is then decomposed into various anhydrosugars, which in turn can react and form unstable

1581

intermediates (furanes, volatile substances) and char (Li et al. 2001; Lin et al. 2009b). While pyrolysis

1582

of cellulose has been extensively studied, practically nothing is known on the evolution of porous

1583

cellulose (aerogel or freeze-dried) mass, volume, porosity, density and pore size during pyrolysis as a

1584 function of temperature profile. How does the structure of carbon aerogel correlate with that of the
1585 corresponding porous cellulose? How all parameters, which control structure formation in cellulose II
1586 aerogels, influence the structure and properties of their carbons? These questions need to be
1587 answered if willing to make carbons with added value from cellulose II aerogels. It is a huge area
1588 worth exploring as the properties these carbons are very promising for various applications.

1589

1590 **6. CONCLUSIONS AND PROSPECTS**

1591 This review presented the main results obtained, till now, on cellulose II aerogels made via
1592 dissolution-solvent exchange-drying with supercritical CO₂. The main trends, not always well
1593 established, are analysed and discussed. The properties and morphology of cellulose II aerogels are
1594 compared, when possible, when those of classical (inorganic, synthetic polymer) aerogels and bio-
1595 aerogels.

1596 As mentioned in the Introduction, there are numerous open questions that remain to be
1597 answered, and this is the leitmotif of practically each topic discussed, on the trends in cellulose II
1598 aerogels structure and properties, and on aerogels' applications. Cellulose aerogels, and bio-aerogels
1599 in general, are very "young" materials and are at the interface of different disciplines that were
1600 previously non crossing: polymer/cellulose physics and chemistry and aerogels/porous materials. If
1601 adding all other various disciplines related to applications (controlled release, electro-chemistry,
1602 sorption, pharma, bio-medical), it is clear that cellulose aerogels need a multidisciplinary approach
1603 and common efforts of the experts from different scientific fields.

1604 The understanding of the formation of cellulose II aerogel structure during coagulation is one of
1605 fundamental questions to be looked at. How cellulose chains are packing? What is the influence of
1606 non-solvent? Does the state of the matter before coagulation, solution or gel, influence aerogel
1607 structure? How cellulose derivatization may influence structure formation and properties of
1608 aerogels? The advantage of supercritical drying is that it preserves, to a large extent, the morphology
1609 of coagulated cellulose and thus allows answering these questions in future. As a consequence, this

1610 may help the understanding why, for example, cellulose II aerogels are not thermal superinsulating
1611 materials while cellulose I and some other bio-aerogels are.

1612 Cellulose II aerogels are materials with high added value. At least two application domains seem
1613 to be very promising now, but the list is certainly far incomplete: in pharma/bio-medical and as
1614 carbons. In the first case biocompatible materials with controlled and hierarchical porosity can be
1615 made. Controlled release and scaffolds are thus the potential areas. The first results on pyrolysed
1616 cellulose aerogels turned out to show excellent discharge properties. The possibility of making
1617 cellulose II “wet” (coagulated) and “dry” (aerogel, cryogel) objects of complex shapes using “direct
1618 ink writing” (or 3D printing) technique is not well explored yet. This approach can be very attractive
1619 in making, for example, cellulose II aerogels of individualized shape and controlled porosity for both
1620 application areas mentioned above. Finally, numerous options of cellulose derivatization and/or
1621 functionalization may definitely open new cellulose aerogel applications which remain unexplored.

1622

1623

1624 **REFERENCES**

- 1625 Aaltonen O, Jauhiainen O (2009) The preparation of lignocellulosic aerogels from ionic liquid
1626 solutions, *Carbohydrate Polymers* 75:125–129
- 1627 Aegerter MA, Leventis N, Koebel MM, *Aerogels Handbook*, Springer, New York, 2011
- 1628 Alaoui AH, Woignier T, Scherer GW, Phalippou J (2008) Comparison between flexural and uniaxial
1629 compression tests to measure the elastic modulus of silica aerogel. *Journal of Non-Crystalline Solids*
1630 354:4556–4561
- 1631 Bakierska M, Molenda M, Majda D, Dziembaj R (2014) Functional starch based carbon aerogels for
1632 energy applications. *Procedia Engineering* 98:14 – 19
- 1633 Biener J, Stadermann M, Suss M, Worsley MA, Biener MM, Rose KA, Baumann TF (2011) Advanced
1634 carbon aerogels for energy applications. *Energy Environ. Sci.* 4:656-667
- 1635 Biesmans G, Randall D, Francais E, Perrut M (1998) Polyurethane-based organic aerogels' thermal
1636 performance. *J. Non-Cryst. Solids* 225:36 – 40
- 1637 Biganska O, Navard P (2005) Kinetics of Precipitation of Cellulose from Cellulose-NMMO-Water
1638 Solutions. *Biomacromolecules* 6:1948-1953
- 1639 Borisova A, De Bruyn M, Budarin V L, Shuttleworth PS, Dodson Mateus JR, Segatto L, Clark JH (2015)
1640 A sustainable freeze-drying route to porous polysaccharides with tailored hierarchical meso- and
1641 macroporosity. *Macromolecular Rapid Communications* 36:774-779
- 1642 Buchtova N, Budtova T (2016) Cellulose aero-, cryo- and xerogels: towards understanding of
1643 morphology control. *Cellulose* 23:2585–2595
- 1644 Budarin V, Clark JH, Hardy JJA, Luque R, Milkowski K, Tavener SJ, Wilson AJ (2006) Starbons: new
1645 starch-derived mesoporous carbonaceous materials with tunable properties. *Angew. Chem., Int. Ed.*,
1646 45:3782–3786
- 1647 Budtova T, Navard P (2016) Cellulose in NaOH–water based solvents: a review. *Cellulose* 23:5–55
- 1648 Cai H, Sharma S, Liu W, Mu W, Liu W, Zhang X, Deng Y (2014) Aerogel Microspheres from Natural
1649 Cellulose Nanofibrils and Their Application as Cell Culture Scaffold. *Biomacromolecules* 15:2540-2547
- 1650 Cai J, Kimura S, Wada M, Kuga S (2009) Nanoporous Cellulose as Metal Nanoparticles Support.
1651 *Biomacromolecules* 10:87-94
- 1652 Cai J, Kimura S, Wada M, Kuga S, Zhang L (2008) Cellulose Aerogels from Aqueous Alkali Hydroxide–
1653 Urea Solution. *ChemSusChem* 1:149 – 154
- 1654 Cai J, Liu S, Feng J, Kimura S, Wada M, Kuga S, Zhang L (2012) Cellulose–Silica Nanocomposite
1655 Aerogels by In Situ Formation of Silica in Cellulose Gel. *Angew. Chem. Int. Ed.* 51:2076 – 2079
- 1656 Cervin NT, Andersson L, Ng JBS, Olin P, Bergström L, Wågberg L (2013) Lightweight and Strong
1657 Cellulose Materials Made from Aqueous Foams Stabilized by Nanofibrillated Cellulose.
1658 *Biomacromolecules* 14:503-511

- 1659 Cervin NT, Aulin C, Larsson PT, Wagberg L (2012) Ultra porous nanocellulose aerogels as separation
1660 medium for mixtures of oil/water liquids. *Cellulose* 19:401–410
- 1661 Chin SF, Romainor ANB, Pang SC (2014) Fabrication of hydrophobic and magnetic cellulose aerogel
1662 with high oil absorption capacity. *Materials Letters* 115:241–243
- 1663 Chtchigrovsky M, Primo A, Gonzalez P, Molvinger K, Robitzer M, Quignard F, et al. (2009)
1664 Functionalized chitosan as a green, recyclable, biopolymer-supported catalyst for the [3+2] Huisgen
1665 cycloaddition. *Angewandte Chemie International Ed.* 48(32):5916–5920
- 1666 O’Connell DW, Birkinshaw C, O’Dwyer TF (2008) Heavy metal adsorbents prepared from the
1667 modification of cellulose: A review. *Bioresource Technology* 99:6709–6724
- 1668 Cross J, Goswin R, Gerlach R, Fricke J (1989) Mechanical properties of SiO₂ – aerogels. *Revue de*
1669 *physique appliquée, Colloque c4, Supplement au n° 4, tome 24, c4-184-c4-195*
- 1670 Cui S, Wang X, Zhang X, Xia W, Tang X, Lin B, Qi W, Zhang X, Shen X (2018) Preparation of magnetic
1671 MnFe₂O₄-Cellulose aerogel composite and its kinetics and thermodynamics of Cu(II) adsorption.
1672 *Cellulose* 25:735–751
- 1673 De Cicco F, P. Russo P, Reverchon E, García-González CA, Aquino RP, Del Gaudio P (2016) Prilling and
1674 supercritical drying: A successful duo to produce core-shell polysaccharide aerogel beads for wound
1675 healing, *Carbohydrate Polymers* 147:482–489
- 1676 De France KJ, Hoare T, Cranston ED (2017) Review of Hydrogels and Aerogels Containing
1677 Nanocellulose. *Chem. Mater.* 29:4609–4631
- 1678 De Oliveira W, Glasser WG (1996) Hydrogels from Polysaccharides. 1. Cellulose Beads for
1679 Chromatographic Support *J. Appl. Polym. Sci.* 60:63–73
- 1680 Demilecamps A (2015a) Synthesis and characterization of polysaccharide-silica composite aerogels
1681 for thermal superinsulation. PhD thesis, Mines ParisTech, France
- 1682 Demilecamps A, Alves M, Rigacci A, Reichenauer G, Budtova T (2016) Nanostructured
1683 interpenetrated organic-inorganic aerogels with thermal superinsulating properties. *Journal of Non-*
1684 *Crystalline Solids* 452:259–265
- 1685 Demilecamps A, Beauger C, Hildenbrand C, Rigacci A, Budtova T (2015b) Cellulose–silica aerogel.
1686 *Carbohydrate Polymers* 122:293–300
- 1687 Demilecamps A, Reichenauer G, Rigacci A, Budtova T (2014) Cellulose–silica composite aerogels from
1688 “one-pot” synthesis. *Cellulose* 21:2625–2636
- 1689 Diascorn N, Calas S, Sallée H, Achard P, Rigacci A (2015) Polyurethane aerogels synthesis for thermal
1690 insulation – textural, thermal and mechanical properties. *J. of Supercritical Fluids* 106:76–84
- 1691 Druel L, Bardl R, Vorweg W, Budtova T (2017) Starch Aerogels: A Member of the Family of Thermal
1692 Superinsulating Materials. *Biomacromolecules* 18:4232–4239
- 1693 Druel L, Niemeyer P, Milow B, Budtova T (2018) Rheology of cellulose-[DBNH][CO₂Et] solutions and
1694 shaping into aerogel beads. *Green Chemistry* 20:3993-4002

- 1695 Egal M, Budtova T, Navard P (2007) Structure of aqueous solutions of microcrystalline cellulose-
1696 sodium hydroxide below 0°C and the limit of cellulose dissolution. *Biomacromolecules* 8:2282-2287
- 1697 Escudero RR, Robitzer M, Di Renzo F, Quignard F (2009) Alginate aerogels as adsorbents of polar
1698 molecules from liquid hydrocarbons: Hexanol as probe molecule. *Carbohydrate Polymers* 75:52–57
- 1699 Feng J, Nguyen ST, Fan Z, Duong HM (2015) Advanced fabrication and oil absorption properties of
1700 super-hydrophobic recycled cellulose aerogels. *Chemical Engineering Journal* 270:168–175
- 1701 Fink HP, Weigel P, Purz HJ, Ganster J (2001) Structure formation of regenerated cellulose materials
1702 from NMMO solutions. *Prog. Polym. Sci* 26:1473-1524
- 1703 Firgo H, Rűf H, Hainbucher KM, Weber H (2004) Method for the production of a porous cellulose
1704 body. WO/2004/065424
- 1705 Fischer F, Rigacci A, Pirard R, Berthon-Fabry S, Achard P (2006) Cellulose-based aerogels. *Polymer*
1706 47:7636-7645
- 1707 Fumagalli M, Ouhab D, Molina Boisseau S, Heux L (2013) Versatile Gas-Phase Reactions for Surface to
1708 Bulk Esterification of Cellulose Microfibrils Aerogels. *Biomacromolecules* 14:3246–3255
- 1709 Fumagalli M, Sanchez F, Molina-Boisseau S, Heux L (2015) Surface-restricted modification of
1710 nanocellulose aerogels in gas-phase esterification by di-functional fatty acid reagents. *Cellulose*
1711 22:1451–1457
- 1712 Ganesan K, Dennstedt A, Barowski A, Ratke L (2016) Design of aerogels, cryogels and xerogels of
1713 cellulose with hierarchical porous structures. *Materials and Design* 92:345–355
- 1714 Ganesan K, Budtova T, Ratke L, Gurikov P, Baudron V, Preibisch I, Niemeyer P, Smirnova I, Milow B
1715 (2018) Review on the Production of Polysaccharide Aerogel Particles. *Materials* 11:2144-2181
- 1716 Garcia-Gonzalez CA, Alnaief M, Smirnova I. (2011). Polysaccharide-based aerogels-promising
1717 biodegradable carriers for drug delivery systems. *Carbohydrate Polymers* 86: 1425–1438
- 1718 Garcia-Gonzalez CA, Uy JJ, Alnaief M, Smirnova I (2012) Preparation of tailor-made starch-based
1719 aerogel microspheres by the emulsion-gelation method. *Carbohydrate Polymers* 88:1378– 138
- 1720 Gavillon R (2007) Preparation et caracterisation de materiaux cellulosiques ultra poreux. PhD Thesis.
1721 Mines ParisTech, France
- 1722 Gavillon R, Budtova T (2007) Kinetics of Cellulose Regeneration from Cellulose-NaOH-Water Gels and
1723 Comparison with Cellulose-N-Methylmorpholine-N-Oxide-Water Solutions. *Biomacromolecules*
1724 8:424-432
- 1725 Gavillon R, Budtova T (2008) Aerocellulose: New Highly Porous Cellulose Prepared from Cellulose-
1726 NaOH Aqueous Solutions. *Biomacromolecules* 9:269–277
- 1727 Geng H (2018) Preparation and characterization of cellulose/N,N'-methylene bisacrylamide/graphene
1728 oxide hybrid hydrogels and aerogels. *Carbohydrate Polymers* 196:289–298
- 1729 Gericke M, Trygg J, Fardim P (2013) Functional Cellulose Beads: Preparation, Characterization, and
1730 Applications *Chem. Rev.* 113:4812–4836

- 1731 Gibson LJ, Ashby MF. (1997). Cellular solids. Structure and properties (2nd ed.). Cambridge University
1732 Press
- 1733 Glenn GM, Irving DW (1995) Starch-Based Microcellular Foams. *Cereal Chem.* 72: 155–161
- 1734 Goimil L, Braga MEM, Dias AMA, Gómez-Amoza JL, Concheiro A, Alvarez-Lorenzo C, de Sousa HC,
1735 García-González CA (2017) Supercritical processing of starch aerogels and aerogel-loaded poly(ϵ -
1736 caprolactone) scaffolds for sustained release of ketoprofen for bone regeneration. *Journal of CO₂*
1737 *Utilization* 18:237–249
- 1738 Groult S, Budtova T (2018a) Thermal conductivity/structure correlations in thermal super-insulating
1739 pectin aerogels. *Carbohydrate Polymers* 196:73–81
- 1740 Groult S, Budtova T (2018b) Tuning structure and properties of pectin aerogels. *European Polymer*
1741 *Journal* 108:250–261
- 1742 Guilminot E, Gavillon R, Chatenet M, Berthon-Fabry S, Rigacci A, Budtova T (2008) New
1743 nanostructured carbons based on porous cellulose: Elaboration, pyrolysis and use as platinum
1744 nanoparticles substrate for oxygen reduction electrocatalysis. *Journal of Power Sources* 185, 717–
1745 726
- 1746 Guizard C, Leloup J, Deville S (2014) Crystal Templating with Mutually Miscible Solvents: A Simple
1747 Path to Hierarchical Porosity. *J. Am. Ceram. Soc.* 97:2020–2023
- 1748 Hall CA, Le KA, Rudaz C, Radhi A, Lovell CS, Damion RA, Budtova T, Ries ME (2012) Macroscopic and
1749 Microscopic Study of 1-Ethyl-3-methyl-imidazolium Acetate–Water Mixtures. *J. Phys. Chem. B*
1750 116:12810–12818
- 1751 Hansen CM (2007) Hansen Solubility Parameters : A User’s Handbook, Second Edition, CRC Press
- 1752 Hedlund A, Kohnke T, Theliander H (2017) Diffusion in Ionic Liquid–Cellulose Solutions during
1753 Coagulation in Water: Mass Transport and Coagulation Rate Measurements. *Macromolecules*
1754 50:8707-8719
- 1755 Hoepfner S, Ratke L, Milow B (2008) Synthesis and characterisation of nanofibrillar cellulose aerogels.
1756 *Cellulose* 15:121–129
- 1757 Horvat G, Khanari K, Finsgar M, Gradisnik L, Maver U, Knez Z, Novak Z (2017) Novel ethanol-induced
1758 pectin–xanthan aerogel coatings for orthopedic applications. *Carbohydrate Polymers* 166:365–376
- 1759 Hu Y, Tong X, Zhuo H, Zhong L, Peng W, Wang S, Sun R (2016) 3D hierarchical porous N-doped carbon
1760 aerogel from renewable cellulose: an attractive carbon for high-performance supercapacitor
1761 electrodes and CO₂ adsorption. *RSC Adv.* 6:15788-15795
- 1762 Hwang K, Kwon G-J, Yang J, Kim M, Hwang WJ, Youe W, Kim D-Y (2018) *Chlamydomonas angulosa*
1763 (Green Alga) and *Nostoc commune* (Blue-Green Alga) Microalgae-Cellulose Composite Aerogel
1764 Beads: Manufacture, Physicochemical Characterization, and Cd (II) Adsorption. *Materials* 11:562-581
- 1765 Innerlohinger J, Weber HK, Kraft G (2006a) Aerocellulose: Aerogels and Aerogel-like Materials made
1766 from Cellulose Macromol. Symp. 244:126–135
- 1767 Innerlohinger J, Weber HK, Kraft G (2006b) Aerocell Aerogels from cellulosic materials. *Lenzinger*
1768 *Berichte*, 86:137-143

- 1769 Ishida O, Kim D-Y, Kuga S, Nishiyama Y, Brown RM (2004) Microfibrillar carbon from native cellulose.
1770 Cellulose 11:475–480
- 1771 Jiménez-Saelices C, Seantier B, Cathala B, Grohens Y (2017) Spray freeze-dried nanofibrillated
1772 cellulose aerogels with thermal superinsulating properties. Carbohydrate Polymers 157:105–113
- 1773 Jin H, Nishiyama T, Wada M, Kuga S (2004) Nanofibrillar cellulose aerogels. Colloids and Surfaces A:
1774 Physicochem. Eng. Aspects 240:63–67
- 1775 IUPAC. Compendium of Chemical Terminology, 2nd ed. (the "Gold Book"). Compiled by A. D.
1776 McNaught and A. Wilkinson. Blackwell Scientific Publications, Oxford (1997). XML on-line corrected
1777 version: <http://goldbook.iupac.org> (2006-) created by M. Nic, J. Jirat, B. Kosata; updates compiled by
1778 A. Jenkins. ISBN 0-9678550-9-8. <https://doi.org/10.1351/goldbook>. Last update: 2014-02-24; version:
1779 2.3.3
- 1780 Karadagli I, Schulz B, Schestakow M, Milow B, Gries T, Ratke L (2015) Production of porous cellulose
1781 aerogel fibers by an extrusion process. J. of Supercritical Fluids 106:105–114
- 1782 Katti A, Shimpi N, Roy S, Lu H, Fabrizio EF, Dass A, Capadona LA, Leventis N (2006) Chemical, Physical,
1783 and Mechanical Characterization of Isocyanate Cross-linked Amine-Modified Silica Aerogels. Chem.
1784 Mater. 18:85-296
- 1785 Kaushik M, Moores A (2016) Review: nanocelluloses as versatile supports for metal nanoparticles and
1786 their applications in catalysis. Green Chem. 18:622-637
- 1787 Kistler SS (1931) Coherent expanded aerogels and gellies. Nature 127 (3211):741
- 1788 Knez Z, Markocic E, Leitgeb M, Primozic M, Hrncic MK, Skerget M (2014) Industrial applications of
1789 supercritical fluids: A review. Energy 77:235-243
- 1790 Kobayashi Y, Saito T, Isogai A (2014) Aerogels with 3D Ordered Nanofiber Skeletons of Liquid-
1791 Crystalline Nanocellulose Derivatives as Tough and Transparent Insulators. Angew. Chem. Int. Ed.
1792 53:10394 –10397
- 1793 Köhnke T, Lund K, Brelid H, Westman G (2010) Kraft pulp hornification: A closer look at the
1794 preventive effect gained by glucuronoxylan adsorption. Carbohydr. Polym 81:226-233
- 1795 Korhonen JT, Kettunen M, Ras RHA, Ikkala O (2011) Hydrophobic Nanocellulose Aerogels as Floating,
1796 Sustainable, Reusable, and Recyclable Oil Absorbents. ACS Appl. Mater. Interfaces 3:1813–1816
- 1797 Laity PR, Glover PM, Hay JN (2002) Composition and phase changes observed by magnetic resonance
1798 imaging during non-solvent induced coagulation of cellulose. Polymer 43:5827-5837
- 1799 Laskowski J, Milow B, Ratke L (2015) The effect of embedding highly insulating granular aerogel
1800 in cellulosic aerogel. J. of Supercritical Fluids 106:93–99
- 1801 Lavoine N, Bergstrom L (2017) Nanocellulose-based foams and aerogels: processing, properties, and
1802 applications. J. Mater. Chem. A 5: 16105-16117
- 1803 Lei E, Li W, Ma C, Liu S (2018) An ultra-lightweight recyclable carbon aerogel from bleached softwood
1804 kraft pulp for efficient oil and organic absorption. Materials Chemistry and Physics 214:291-296

- 1805 Leventis N, Sotiriou-Leventis C, Zhang G, Rawashdeh A-M M (2002) Nanoengineering Strong Silica
1806 Aerogels. *Nano Letters* 2:957-960
- 1807 Li S, Lyons-Hart J, Banyasz J, Shafer K (2001) Real-time evolved gas analysis by FTIR method: an
1808 experimental study of cellulose pyrolysis. *Fuel* 80:1809–1817
- 1809 Liang H-W, Wu Z-Y, Chen L-F, Li C, Yu S-H (2015) Bacterial cellulose derived nitrogen-doped carbon
1810 nanofiber aerogel: An efficient metal-free oxygen reduction electrocatalyst for zinc-air battery. *Nano*
1811 *Energy* 11:366–376
- 1812 Liao Q, Su X, Zhu W, Hu W, Qian Z, Li L, Yao J (2016) Flexible and durable cellulose aerogels for highly
1813 effective oil/water separation. *RSC Adv.* 6:63773-63781
- 1814 Liebert T (2010) Cellulose Solvents – Remarkable History, Bright Future. In Liebert et al.; Cellulose
1815 Solvents: For Analysis, Shaping and Chemical Modification, ACS Symposium Series; American
1816 Chemical Society: Washington, DC
- 1817 Liebner F, Dunareanu R, Opietnik M, Haimer E, Wendland M, Werner C, Maitz M, Seib P, Neouze M-
1818 A, Potthast A, Rosenau T (2012) Shaped hemocompatible aerogels from cellulose phosphates:
1819 preparation and properties. *Holzforschung* 66:317–321
- 1820 Liebner F, Haimer E, Potthast A, Loidl D, Tschegg S, Neouze MA (2009) Cellulosic aerogels as ultra-
1821 lightweight materials. Part 2: Synthesis and properties. *Holzforschung* 63:3–11
- 1822 Liebner F, Pircher N, Schimper C, Haimer E, Rosenau T (2016) Aerogels: Cellulose-Based, In
1823 Encyclopedia of Biomedical Polymers and Polymeric Biomaterials. Taylor and Francis: New York, pp
1824 37-75
- 1825 Liebner F, Potthast A, Rosenau T, Haimer E, Wendland M (2008) Cellulose aerogels: Highly porous,
1826 ultra-lightweight materials. *Holzforschung* 62:129–135
- 1827 Lin C, Zhan H, Liu M, Fu S, Lucia LA (2009a) Novel Preparation and Characterization of Cellulose
1828 Microparticles Functionalized in Ionic Liquids. *Langmuir* 25:10116–10120
- 1829 Lin R, Li A, Zheng T, Lu L, Cao Y (2015) Hydrophobic and flexible cellulose aerogel as an efficient,
1830 green and reusable oil sorbent. *RSC Adv.* 5:82027-82033
- 1831 Lin Y-C, Cho J, Tompsett GA, Westmoreland PR, Huber GW (2009b) Kinetics and mechanism of
1832 cellulose pyrolysis. *J Phys Chem C* 113:20097–20107
- 1833 Litschauer M, Neouze M-A, Haimer E, Henniges U, Potthast A, Rosenau T, Liebner F (2011) Silica
1834 modified cellulosic aerogels. *Cellulose* 18:143–149
- 1835 Liu P, Borrell PF, Bozic M, Kokol V, Oksman K, Mathew AP (2015) Nanocelluloses and their
1836 phosphorylated derivatives for selective adsorption of Ag⁺, Cu²⁺ and Fe³⁺ from industrial effluents.
1837 *Journal of Hazardous Materials* 294:177–185
- 1838 Liu S, Yu T, Hu N, Liu R, Liu X (2013), High strength cellulose aerogels prepared by spatially confined
1839 synthesis of silica in bioscaffolds. *Colloids and Surfaces A: Physicochem. Eng. Aspects* 439:159– 166
- 1840 Liu W, Budtova T, Navard P (2011) Influence of ZnO on the properties of dilute and semi-dilute
1841 cellulose-NaOH-water solutions. *Cellulose* 18:911–920

- 1842 Lozinsky VI, Damshkaln LG, Bloch KO, Vardi P, Grinberg NV, Burova TV, Grinberg VY (2008),
 1843 Cryostructuring of Polymer Systems. XXIX. Preparation and Characterization of Supermacroporous
 1844 (Spongy) Agarose-Based Cryogels Used as Three-Dimensional Scaffolds for Culturing Insulin-
 1845 Producing Cell Aggregates. *Journal of Applied Polymer Science* 108:3046–3062
- 1846 Lozinsky VI, Galaev IYu , PlievaFM , Savina IN, Jungvid H, Mattiasson B (2003) Polymeric cryogels as
 1847 promising materials of biotechnological interest. *TRENDS in Biotechnology* 21:445-451
- 1848 Lu A, Liu Y, Zhang L, Potthast A (2011) Investigation on metastable solution of cellulose dissolved in
 1849 NaOH/urea aqueous system at low temperature. *J Phys Chem B* 115:12801–12808
- 1850 Lu X, Arduini-Schuster MC, Kuhn J, Njilsson O, Fricke J, Pekala RW (1992) Thermal Conductivity of
 1851 Monolithic Organic Aerogels. *Science* 255:971-972
- 1852 Luo X, Zhang L (2010) Creation of regenerated cellulose microspheres with diameter ranging from
 1853 micron to millimeter for chromatography applications. *J. Chromatogr. A* 1217:5922–5929
- 1854 Lv L, Fan Y, Chen Q, Zhao Y, Hu Y, Zhang Z, Chen N, Qu L (2014) Three-dimensional multichannel
 1855 aerogel of carbon quantum dots for high-performance supercapacitors. *Nanotechnology* 25:235401
 1856 (9pp)
- 1857 Maatar W, Boufi S (2015) Poly(methacrylic acid-co-maleic acid) grafted nanofibrillated cellulose as a
 1858 reusable novel heavy metal ions adsorbent. *Carbohydrate Polymers* 126:199–207
- 1859 Mäki-Arvelaa P, Anugwoma I, Virtanenena P, Sjöholma R, Mikkola JP (2010) Dissolution of
 1860 lignocellulosic materials and its constituents using ionic liquids—A review. *Industrial Crops and*
 1861 *Products* 32:175–201
- 1862 Maleki H (2016) Recent Advances in Aerogels for Environmental Remediation Applications: A review.
 1863 *Chemical Engineering Journal* 300:98–118
- 1864 Maleki H, Duraes L, Portugal A (2014) An overview on silica aerogels synthesis and different
 1865 mechanical reinforcing strategies. *J. Non-Cryst. Solids* 385:55-74
- 1866 Markevicius G, Ladj R, Niemeyer P, Budtova T, Rigacci A (2017) Ambient-dried thermal
 1867 superinsulating monolithic silica-based aerogels with short cellulosic fibers. *J Mater Sci* 52:2210–222
- 1868 Martins M, Barros AA, Quraishi S, Gurikov P, Raman SP, Smirnova I, Duarte ARC, Reis RL (2015)
 1869 Preparation of macroporous alginate-based aerogels for biomedical applications. *J. of Supercritical*
 1870 *Fluids* 106:152–159
- 1871 Martoia F, Cochereau T, Dumont PJJ, Orgéas L, Terrien M, Belgacem MN (2016) Cellulose nanofibril
 1872 foams: Links between ice-templating conditions, microstructures and mechanical properties.
 1873 *Materials and Design* 104:376–391
- 1874 Meador MAB, Agnello M, McCorkle L, Vivod SL, Wilmoth N (2016) Moisture-Resistant Polyimide
 1875 Aerogels Containing Propylene Oxide Links in the Backbone. *ACS Appl. Mater. Interfaces*
 1876 8:29073–29079
- 1877 Meador MAB, Alemn CR, Hanson K, Ramirez N, Vivod SL, Wilmoth N, McCorkle L (2015) Polyimide
 1878 Aerogels with Amide Cross-Links: A Low Cost Alternative for Mechanically Strong Polymer Aerogels.
 1879 *ACS Appl. Mater. Interfaces* 7:1240-1249

- 1880 Meng Y, Young TM, Liu P, Contescu CI, Huang B, Wang S (2015) Ultralight carbon aerogel from
1881 nanocellulose as a highly selective oil absorption material. *Cellulose* 22:435–447
- 1882 Mi Q-Y, Ma S-R, Yu J, He J-S, Zhang J (2016) Flexible and Transparent Cellulose Aerogels with Uniform
1883 Nanoporous Structure by a Controlled Regeneration Process. *ACS Sustainable Chem. Eng.* 4:656–660
- 1884 Mohamed SMK, Ganesan K, Milow B, Ratke L (2015) The effect of zinc oxide (ZnO) addition on the
1885 physical and morphological properties of cellulose aerogel beads. *RSC Adv.* 5:90193-90201
- 1886 Mulik S, Sotiriou-Leventis C, Leventis N (2007) Time-Efficient Acid-Catalyzed Synthesis of Resorcinol-
1887 Formaldehyde Aerogels. *Chem. Mater.* 19:6138–6144
- 1888 Mulyadi A, Zhang Z, Deng Y (2016) Fluorine-Free Oil Absorbents Made from Cellulose Nanofibril
1889 Aerogels. *ACS Appl. Mater. Interfaces* 8:2732–2740
- 1890 Nguyen ST, Feng J, Ng SK, Wong JPW, Tan VBC, Duong HM (2014) Advanced thermal insulation and
1891 absorption properties of recycled cellulose aerogels. *Colloids and Surfaces A: Physicochem. Eng.*
1892 *Aspects* 445:128–134
- 1893 Nyström G, Fernández-Ronco MP, Bolisetty S, Mazzotti M, Mezzenga R (2016) Amyloid Templated
1894 Gold Aerogels. *Adv. Mater.* 28:472–478
- 1895 Olsson RT, Samir MASA, Salazar-Alvarez G, Belova L, Strom V, Berglund LA, Ikkala O, Nogues J, Gedde
1896 UW (2010) Making flexible magnetic aerogels and stiff magnetic nanopaper using cellulose
1897 nanofibrils as templates. *Nature Nanotechnology* 5:584-588
- 1898 Ookuna S, Igarashi K, Hara M, Aso K, Yoshidone H, Nakayama H, Suzuki K, Nakajima K (1993) Porous
1899 ion-exchanged fine cellulose particles, method for production thereof, and affinity carrier.
1900 USOO5196527A
- 1901 Pekala R.W, Farmer JC, Alviso CT, Tran TD, Mayer CT, Miller JM, Dunn B (1998) Carbon aerogels for
1902 electrochemical applications. *Journal of Non-Crystalline Solids* 225:74–80
- 1903 Pekala R.W., Alviso CT, Lu X, Gross J, Fricke J (1995) New organic aerogels based upon a phenolic-
1904 furfural reaction. *Journal of Non-Crystalline Solids* 188:34-40
- 1905 Pekala RW (1989) Organic aerogels from the polycondensation of resorcinol with formaldehyde. *J*
1906 *Mater Sci* 24:3221–3227
- 1907 Pekala RW, Alviso CT, LeMay JD (1990) Organic aerogels: microstructural dependence of mechanical
1908 properties in compression. *Journal of Non-Crystalline Solids* 125:67-75
- 1909 Pierre AC (2011) History of Aerogels, In: M.A. Aegerter et al. (eds.), *Aerogels Handbook, Advances in*
1910 *Sol-Gel Derived Materials and Technologies*, Springer New York Dordrecht Heidelberg London,
1911 Springer Science+Business Media, pp 813-831
- 1912 Pinkert A, Marsh KN, Pang S, Staiger MP (2009) Ionic Liquids and Their Interaction with Cellulose.
1913 *Chem. Rev.* 109:6712–6728
- 1914 Pinnow M, Fink HP, Fanter C, Kunze J (2008) Characterization of Highly Porous Materials from
1915 Cellulose Carbamate. *Macromol. Symp.* 262:129–139

- 1916 Pircher N, Carbajal L, Schimper C, Bacher M, Rennhofer H, Nedelec J-M, Lichtenegger HC, Rosenau T,
 1917 Liebner F (2016) Impact of selected solvent systems on the pore and solid structure of cellulose
 1918 aerogels. *Cellulose* 23:1949–1966
- 1919 Pircher N, Fischhuber D, Carbajal L, Strau C, Nedelec J-M, Kasper C, Rosenau T, Liebner F (2015)
 1920 Preparation and Reinforcement of Dual-Porous Biocompatible Cellulose Scaffolds for Tissue
 1921 Engineering. *Macromol. Mater. Eng.* 300:911–924
- 1922 Plappert SF, Nedelec J-M, Rennhofer H, Lichtenegger HC, Liebner FW (2017) Strain Hardening and
 1923 Pore Size Harmonization by Uniaxial Densification: A Facile Approach toward Superinsulating
 1924 Aerogels from Nematic Nanofibrillated 2,3-Dicarboxyl Cellulose. *Chem. Mater.* 29:6630–6641
- 1925 Pour G, Beauger C, Rigacci A, Budtova T (2015) Xerocellulose: lightweight, porous and hydrophobic
 1926 cellulose prepared via ambient drying. *J Mater Sci* 50:4526–4535
- 1927 Quignard F, Valentin R, Di Renzo F. (2008). Aerogel materials from marine polysaccharides. *New*
 1928 *Journal of Chemistry* 32:1300–1310
- 1929 Quraishi S, Martins M, Barros AA, Gurikov P, Raman SP, Smirnova I, Duarte ARC, Reis RL (2015) Novel
 1930 non-cytotoxic alginate–lignin hybrid aerogels as scaffolds fortissue engineering. *J. of Supercritical*
 1931 *Fluids* 105:1–8
- 1932 Raman SP, Gurikov P, Smirnova I (2015) Hybrid alginate based aerogels by carbon dioxide induced
 1933 gelation:Novel technique for multiple applications. *J. of Supercritical Fluids* 106:23–33
- 1934 Rege A, Schestakow M, Karadagli I, Ratke L, Itskov M (2016) Micro-mechanical modelling of cellulose
 1935 aerogels from molten salt hydrates. *Soft Matter* 12:7079-7088
- 1936 Rein DM, Cohen Y (2011) Aeropolysaccharides, composites and preparation thereof. *EP 2 354 165 A1*
- 1937 Robitzer M, Di Renzo F, Quignard F (2011) Natural materials with high surface area. Physisorption
 1938 methods for the characterization of the texture and surface of polysaccharide aerogels. *Microporous*
 1939 *and Mesoporous Materials* 140:9–16
- 1940 Rooke J, de Matos Passos C, Chatenet M, Sescousse R, Budtova T, Berthon-Fabry S, Mosdale R,
 1941 Maillard F (2011) Synthesis and Properties of Platinum Nanocatalyst Supported on Cellulose-Based
 1942 Carbon Aerogel for Applications in PEMFCs. *Journal of The Electrochemical Society* 158:B779-B789
- 1943 Rooke J, Sescousse R, Budtova T, Berthon-fabry S, Simon B, Chatenet M (2012) Cellulose-based
 1944 nanostructured carbons for energy conversion and storage devices. In “Green Carbon Materials:
 1945 Advances and Applications”, T. Rufford, D. Hulicova-Jurcakova, J. Zhu Eds., Pan Stanford Publishing
 1946 Pte Ltd, Singapore pp. 89-111
- 1947 Rosenberg P, Suominen I, Rom M, Janicki J, Fardim P (2007) Tailored cellulose beads for novel
 1948 applications. *Cellul. Chem. Technol.* 41:243–254
- 1949 Roy C, Budtova T, Navard P (2003) Rheological properties and gelation of aqueous cellulose-NaOH
 1950 solutions. *Biomacromolecules* 4:259-264
- 1951 Rudaz C (2013) Cellulose and Pectin Aerogels: Towards their nano-structuration. PhD thesis, MINES
 1952 ParisTech

- 1953 Rudaz C, Courson R, Bonnet L, Calas-Etienne S, Sallée H, Budtova T (2014). Aeropectin: Fully Biomass-
1954 Based Mechanically Strong and Thermal Superinsulating Aerogel. *Biomacromolecules* 15: 2188-2195
- 1955 Sai H, Fu R, Xing L, Xiang J, Li Z, Li F, Zhang T (2015) Surface Modification of Bacterial Cellulose
1956 Aerogels' Web-like Skeleton for Oil/Water Separation. *ACS Appl. Mater. Interfaces* 7:7373–7381
- 1957 Schestakow M, Karadagli I, Ratke L (2016a) Cellulose aerogels prepared from an aqueous zinc
1958 chloride salt hydrate melt. *Carbohydrate Polymers* 137:642–649
- 1959 Schestakow M, Muench F, Reimuth C, Ratke L, Ensinger W (2016b) Electroless synthesis of cellulose-
1960 metal aerogel composites. *Appl. Phys. Lett.* 108:213108-213108-4
- 1961 Seantier B, Bendahou D, Bendahou A, Grohens Y, Kaddami H (2016) Multi-scale cellulose based new
1962 bio-aerogel composites with thermalsuper-insulating and tunable mechanical properties.
1963 *Carbohydrate Polymers* 138:335–348
- 1964 Sehaqui H, Zhou Q, Ikkala O, Berglund LA (2011) Strong and Tough Cellulose Nanopaper with High
1965 Specific Surface Area and Porosity. *Biomacromolecules* 12:3638–3644
- 1966 Sehaqui H, Zimmermann T, Tingaut P (2014) Hydrophobic cellulose nanopaper through a mild
1967 esterification procedure. *Cellulose* 21:367-382
- 1968 Sescousse R (2010a) Nouveaux matériaux cellulosiques ultra-poreux et leurs carbones à partir de
1969 solvants verts. PhD thesis, Mines ParisTech, France
- 1970 Sescousse R, Budtova T (2009) Influence of processing parameters on regeneration kinetics and
1971 morphology of porous cellulose from cellulose–NaOH–water solutions. *Cellulose* 16:417–426
- 1972 Sescousse R, Gavillon R, Budtova T (2011a) Aerocellulose from cellulose–ionic liquid solutions:
1973 Preparation, properties and comparison with cellulose–NaOH and cellulose–NMMO routes.
1974 *Carbohydrate Polymers* 83:1766–1774
- 1975 Sescousse R, Gavillon R, Budtova T (2011b) Wet and dry highly porous cellulose beads from
1976 cellulose–NaOH–water solutions: influence of the preparation conditions on beads shape and
1977 encapsulation of inorganic particles. *J. Mater. Sci.* 46:759–765
- 1978 Sescousse R, Smacchia A, Budtova T (2010b) Influence of lignin on cellulose-NaOH-water mixtures
1979 properties and on Aerocellulose morphology. *Cellulose* 17:1137–1146
- 1980 Shen J, Guan DY (2011) Preparation and Application of Carbon Aerogels. In: M.A. Aegerter et al.
1981 (eds.), *Aerogels Handbook, Advances in Sol-Gel Derived Materials and Technologies*, Springer New
1982 York Dordrecht Heidelberg London, Springer Science+Business Media, pp 813-831
- 1983 Shi J, Lu L, Guo W, Sun Y, Cao Y (2013a) An Environment-Friendly Thermal Insulation Material from
1984 Cellulose and Plasma Modification. *J Appl Polym Sci* 3652-3658
- 1985 Shi J, Lu L, Guo W, Zhang J, Cao Y (2013b) Heat insulation performance, mechanics and hydrophobic
1986 modification of cellulose–SiO₂ composite aerogels. *Carbohydrate Polymers* 98:282– 289
- 1987 Shi Z, Huang J, Liu C, Ding B, Kuga S, Cai J, Zhang L (2015) Three-Dimensional Nanoporous Cellulose
1988 Gels as a Flexible Reinforcement Matrix for Polymer Nanocomposites. *ACS Appl. Mater. Interfaces*
1989 7:22990–22998

- 1990 Sorensen L, Strouse GF, Stiegman AE (2006) Fabrication of Stable Low-Density Silica Aerogels
1991 Containing Luminescent ZnS Capped CdSe Quantum Dots. *Adv. Mater.* 18:1965–1967
- 1992 Svensson A, Larsson PT, Salazar-Alvarez G, Wågberg L (2013) Preparation of dry ultra-porous
1993 cellulosic fibres: Characterization and possible initial uses. *Carbohydr Polym* 92:775-783.
- 1994 Tan C, Fung B, Newman JK, Vu C (2001) Organic Aerogels with Very High Impact Strength. *Adv Mater*
1995 13:644-646
- 1996 Teichner SJ (1986) Aerogels of inorganic oxides. In: Frick J (ed) *Aerogels*, Springer Proceedings in
1997 Physics 6, Proceedings of the First International Symposium, Worzburg, Fed. Rep. of Germany,
1998 September 23-25, 1985 Springer-Verlag Heidelberg New York Tokyo, pp 22–30
- 1999 Tejado A, Chen WC, Alam MN, van de Ven TGM (2014) Superhydrophobic foam-like cellulose made
2000 of hydrophobized cellulose fibres. *Cellulose* 21:1735-1743
- 2001 Trygg J, Fardim P, Gericke M, Mäkilä E, Salonen J (2013) Physicochemical design of the morphology
2002 and ultrastructure of cellulose beads. *Carbohydrate Polymers* 93:291– 299
- 2003 Trygg J, Yildir E, Kolakovic R, Sandler N, Fardim P (2014) Anionic cellulose beads for drug
2004 encapsulation and release. *Cellulose* 21:1945–1955
- 2005 Tsiptsias C, Stefopoulos A, Kokkinomalis I, Papadopoulou L, Panayiotou C (2008) Development of
2006 micro- and nano-porous composite materials by processing cellulose with ionic liquids and
2007 supercritical CO₂. *Green Chem.* 10:965–971
- 2008 Veronovski A, Tkalec G. Knez Z. Novak Z (2014) Characterisation of biodegradable pectin aerogels and
2009 their potential use as drug carriers. *Carbohydrate Polymers* 113:272–278
- 2010 Voon LK, Pang SC, Chin SF (2016) Highly porous cellulose beads of controllable sizes derived from
2011 regenerated cellulose of printed paper wastes. *Materials Letters* 164:264-266
- 2012 Voon LK, Pang SC, Chin SF (2017) Porous Cellulose Beads Fabricated from Regenerated Cellulose as
2013 Potential Drug Delivery Carriers. *Journal of Chemistry* Volume 2017:1-11
- 2014 Wang H, Gong Y, Wang Y (2014a) Cellulose-based hydrophobic carbon aerogels as versatile and
2015 superior adsorbents for sewage treatment. *RSC Adv.* 4:45753-45759
- 2016 Wang H, Shao Z, Bacher M, Liebner F, Rosenau T (2013) Fluorescent cellulose aerogels containing
2017 covalently immobilized (ZnS)_x(CuInS₂)_{12x}/ZnS (core/shell) quantum dots. *Cellulose* 20:3007–3024
- 2018 Wang L, Schutz C, Salazar-Alvarez G, Titirici M-M (2014b) Carbon aerogels from bacterial
2019 nanocellulose as anodes for lithium ion batteries. *RSC Adv.* 4:17549-17554
- 2020 Wang Z, Liu S, Matsumoto Y, Kuga S (2012) Cellulose gel and aerogel from LiCl/DMSO solution.
2021 *Cellulose* 19:393–399
- 2022 Wan Ngah WS, Teong LC, Hanafiah MAKM (2011) Adsorption of dyes and heavy metal ions by
2023 chitosan composites: A review. *Carbohydrate Polymers* 83:1446–1456
- 2024 Weigold L, Reichenauer G (2014) Correlation between mechanical stiffness and thermal transport
2025 along the solid framework of a uniaxially compressed polyurea aerogel. *Journal of Non-Crystalline*
2026 *Solids* 406:73–78

- 2027 White RJ, Antonio C, Budarin VL, Bergstrom E, Thomas-Oates J, Clark JH (2010a) Polysaccharide-
2028 derived carbons for polar analyte separations. *Adv. Funct. Mater.* 20:1834–1841
- 2029 White RJ, Budarin V, Luque R, Clark JH, Macquarrie DJ (2009) Tuneable porous carbonaceous
2030 materials from renewable resources. *Chem. Soc. Rev.* 38:3401–3418
- 2031 White RJ, Budarin VL, Clark JH (2010b) Pectin-Derived Porous Materials. *Chem. Eur. J.* 16:1326 – 1335
- 2032 Wang R, Li G, Dong Y, Chi Y, Chen G (2013) Carbon Quantum Dot-Functionalized Aerogels for NO₂ Gas
2033 Sensing. *Anal. Chem.* 85:8065–8069
- 2034 Wong JCH, Kaymak H, Brunner S, Koebel MM (2014) Mechanical properties of monolithic silica
2035 aerogels made from Polyethoxydisiloxanes. *Microporous and Mesoporous Materials* 183:23–29
- 2036 Wu Z-S, Yang S, Sun Y, Parvez K, Feng X, Müllen K (2012) 3D Nitrogen-Doped Graphene Aerogel-
2037 Supported Fe₃O₄ Nanoparticles as Efficient Electrocatalysts for the Oxygen Reduction Reaction. *J.*
2038 *Am. Chem. Soc.* 134:9082–9085
- 2039 Wu Z-Y, Li C, Liang H-W, Chen J-F, Yu S-H (2013) Ultralight, Flexible, and Fire-Resistant Carbon
2040 Nanofiber Aerogels from Bacterial Cellulose. *Angew. Chem.* 125:2997 –3001
- 2041 Yang X, Fei B, Ma J, Liu X, Yang S, Tian G, Jiang Z (2018) Porous nanoplatelets wrapped carbon
2042 aerogels by pyrolysis of regenerated bamboo cellulose aerogels as supercapacitor electrodes.
2043 *Carbohydrate Polymers* 180:385–392
- 2044 Zhang DY, Zhang N, Song P, Hao JY, Wan Y, Yao XH, Chen T, Li L (2018) Functionalized cellulose beads
2045 with three dimensional porous structure for rapid adsorption of active constituents from *Pyrola*
2046 *incarnate*. *Carbohydr. Polym.* 181:560–569
- 2047 Zhang H, Li Y, Xu Y, Lu Z, Chen L, Huang L, Fan M (2016) Versatile fabrication of a superhydrophobic
2048 and ultralight cellulose-based aerogel for oil spillage clean-up. *Phys. Chem. Chem. Phys.* 18:28297-
2049 28306
- 2050 Zhang M, Dou M, Wang M, Yu Y (2017) Study on the solubility parameter of supercritical carbon
2051 dioxide system by molecular dynamics simulation. *J. Mol. Liq.* 248:322–329
- 2052 Zhang Z, Sèbe G, Rentsch D, Zimmermann T, Tingaut P (2014) Ultralightweight and Flexible Silylated
2053 Nanocellulose Sponges for the Selective Removal of Oil from Water. *Chem. Mater.* 26:2659–2668
- 2054 Zhou S, Chen G, Feng X, Wang M, Song T, Liu D, Lu F, Qi H (2018) In situ MnOx/N-doped carbon
2055 aerogels from cellulose as monolithic and highly efficient catalysts for the upgrading of bioderived
2056 aldehydes. *Green Chem.* 20:3593-3603
- 2057 Zhuo H, Hu Y, Tong X, Zhong L, Peng W, Sun R (2016) Sustainable hierarchical porous carbon aerogel
2058 from cellulose for high-performance supercapacitor and CO₂ capture. *Industrial Crops and Products*
2059 87:229–235
- 2060 Zu G, Shen J, Zou L, Wang F, Wang X, Zhang Y, Yao X (2016) Nanocellulose-derived highly porous
2061 carbon aerogels for supercapacitors. *Carbon* 99:203-211
- 2062

2063

Supporting Information

2064

2065

Cellulose II aerogels: a review

2066

2067

Tatiana Budtova

2068

MINES ParisTech, PSL Research University, Center for Materials Forming (CEMEF), UMR CNRS 7635, CS 10207, 06904 Sophia Antipolis, France

2069

2070

2071

Table S1. Main characteristics of cellulose II aerogels and some example of freeze-dried cellulose II with high specific surface area

cellulose type	cellulose solvent	cellulose concentration, wt%	density, g/cm ³	specific surface, m ² /g	compressive modulus, MPa	thermal conductivity in ambient conditions, W/m.K	comment	reference
	Indirect							
viscose				15 - 400			beads	Ookuna et al. 1993
cellulose carbamate	NaOH/water	3 - 5	0.06 - 0.22 (neat) and 0.21 - 0.27	361 - 433 and 492 - 661			monoliths and beads, neat and pyrolysed	Pinnow et al. 2008

			(pyrolysed)	(pyrolysed)				
NaOH based								
MCC	NaOH/water, gelled solutions	5 - 7	- 0.14 (0.06 (with surfactant))	200 - 240				Gavillon and Budtova 2008
filter paper	NaOH/urea/water	4 - 6	0.13 - 0.27	260 - 406				Cai et al. 2008
MCC mixed with organosolv lignin	NaOH/water, gelled solutions	5 - 6	0.1 - 0.135	200				Sescousse et al. 2010b
MCC	NaOH/water	5					beads of various shapes, with encapsulated iron and TiO ₂	Sescousse et al. 2011
dissolving pulp	NaOH/urea/water	4 - 6		340 - 470			beads	Trygg et al. 2013

from Whatman	NaOH/thiourea/water	1					with magnetic (Fe ₃ O ₄) nanoparticles, coated with TiO ₂ for oil absorption (25 g/g)	Chin et al. 2014
MCC	NaOH/ZnO/water, gelled solutions	5	0.12 (up to 0.27 with SiO ₂)	250 (down to 100 with SiO ₂ beads)			mixed with sodium silicate	Demilecamps et al. 2014
cellulose powder	NaOH/urea/ZnO/water	5	0.08 (up to 0.25 with ZnO)	341 - 407			beads 2 - 2.5 mm	Mohamed et al. 2015
MCC and tritylcellulose	NaOH/water and DMF	5	0.08 - 0.24	200 (up to 850 with SiO ₂ aerogels)	0.3 - 4	0.021 - 0.035	interpenetrated cellulose-silica aerogels, silica hydrophobised	Demilecamps et al. 2016
	LiOH based							
filter paper, cotton	LiOH/urea/water	0.5 - 7	0.01 - 0.4	291 - 485				Cai et al. 2008

linters, tunicate								
filter paper	LiOH/urea/water	4	0.12 (up to 0.17 with metal nanoparticles)	404 (360-406 with metal nanoparticles)			with metal (Ag, Au, Pt) nanoparticles	Cai et al. 2009
pulp	LiOH/urea/water	6	0.14 (up to 0.58 with SiO ₂)	356 (up to 664 with SiO ₂ aerogels)	7.9 - 12	0.025 - 0.045	interpenetrated cellulose-silica (TEOS) aerogels	Cai et al. 2012
cotton linters	LiOH/urea/water	5	0.2 - 0.228	270 - 330	49 - 204		composites with silica (sodium silicate)	Liu et al. 2013
cotton linters	LiOH/urea/water	5			3.5 - 104		interpenetrated cellulose/polymer	Shi et al. 2015
MCC	LiOH/urea/water	3	0.1 (0.12-0.21 with MnFe ₂ O ₄)	229 (236-288 with MnFe ₂ O ₄)			magnetic composites with MnFe ₂ O ₄	Cui et al. 2018

	NMMO monohydrate							
pulp			0.08			0.03		Innerlohinger et al. 2006b
various pulps			0.05 - 0.2	10 - 350			monoliths and spheres (2 - 4 mm)	Innerlohinger et al. 2006a
various pulps		3	0.12 - 0.13	260 - 280				Gavillon and Budtova 2008
various pulps		3 - 6	0.05 - 0.07	55 - 310	0.8 - 61.5			Liebner et al. 2009
cotton linters		3		220 - 290			composites with silica (TEOS)	Litschauer et al. 2011
cotton linters		3	around 0.06	240 - 270			cellulose phosphate aerogels as scaffolds and bone grafting	Liebner et al. 2012

hardwood prehydrolysis kraft pulp		3	0.05 - 0.06	280 - 290			cellulose phosphate aerogels as scaffolds and bone grafting	Liebner et al. 2012
hardwood sulfite pulp		3	around 0.06	280 - 350			cellulose phosphate aerogels as scaffolds and bone grafting	Liebner et al. 2012
cotton linters		3	0.06	250	4.3		thermoporosimetry used for pore size distribution	Pircher et al. 2016
	Ionic liquids							
softwood pulp	[Amim][Cl]	1.5	0.058	315			composites with hydroxyapatite and SiO ₂ particles	Tsioptsias et al. 2008
bleached softwood	[Bmim][Cl]	1.5	0.048	539				Aaltonen and

Kraft pulp								Jauhiainen 2009
cellulose pulp mixed with sodalignin and xylan	[Bmim][Cl]	2/0.7/1	0.114	213				Aaltonen and Jauhiainen 2009
spruce wood	[Bmim][Cl]	1.5	0.05	122				Aaltonen and Jauhiainen 2009
cellulose, lignin, hemicellulose, sucrose or starch	[Bmim][Cl], [Amim][Cl], [Emim][OAc]						neat and silylated aerogels	Rein and Cohen 2011
MCC	Emim][OAc], [Bmim][Cl]	3 - 15	0.06 - 0.22	130 - 230	0.6 - 40			Sescousse et al. 2011a
MCC	[Emim][OAc], [Emim][OAc]/DMSO	5 - 20	0.15 - 0.5	180 - 256				Rudaz 2013
eucalyptus	[Hmim][Cl]	1 - 3	0.037-	136-350 (up to 686	0.22-0.79		incorporation of	Wang et al. 2013

pulp			0.057	with quantum dots)			quantum dots	
cotton linters	[Emim][OAc]/DMSO	3	0.06	250	1.12		scaffolds (mixed with paraffin wax or PMMA spheres)	Pircher et al. 2015
pulp	[Emim][OAc]/DMSO	3	0.125 (neat) - 0.22 (with silica aerogel)	290 (neat) - 810 (with silica erogel)	2.8 (neat) - 11.5 (with silica aerogel)	0.33 (neat) - 0.26 (with silica aerogel)	neat and interpenetrated with silica aerogel	Demilecamps et al. 2015b
cotton linters	[Emim][OAc]/DMSO	1.5 - 3	0.04 - 0.055	246	0.26 - 1.12		thermoporosimetry used for pore size distribution	Pircher et al. 2016
MCC	[Emim][Cl]/DMSO	3 - 11	0.12 - 0.22	240 - 312				Buchtova and Budtova 2016
not specified	[Amim][Cl]	2	0.024 - 0.029	175 - 244	15.2 - 27.3		solvent exchange in [Amim][Cl]-	Mi et al. 2016

							water, then ethanol	
cellulose from paper waste	[Amim][Cl]	4		101-478			beads of diameter 0.8 - 4.6 mm, delivery of curcumin	Voon et al. 2017
	calcium thiocyanate based							
not specified	Ca(SCN) ₂ ·6H ₂ O	0.5 - 3	0.01 - 0.057	210				Hoepfner et al. 2008
cellulose fiber powder	Ca(SCN) ₂ ·6H ₂ O	2 - 6	0.01 - 0.14	156 - 222 (monoliths) 120 - 160 (fibers)	2.0 - 16	0.04 - 0.075	monoliths and fibers	Karadagli et al. 2015
cotton linters	Ca(SCN) ₂ /8H ₂ O/LiCl	1.5	0.03	190	2			Pircher et al. 2015
MCC	Ca(SCN) ₂ ·6H ₂ O	2 - 5	0.02 - 0.09		2.0 - 10		mechanical modelling	Rege et al. 2016

MCC	$\text{Ca}(\text{SCN})_2 \cdot 6\text{H}_2\text{O}$	4	0.06 - 0.12	290 - 300	1.9 - 15		surfactant added for additional porosity	Ganesan et al. 2016
cotton linters	$\text{Ca}(\text{SCN})_2 / 8\text{H}_2\text{O} / \text{LiCl}$	1.5 - 2	0.03 - 0.048	190	2 - 3.3		thermoporosimetry used for pore size distribution	Pircher et al. 2016
cellulose powder from cotton	$\text{Ca}(\text{SCN})_2 \cdot 6\text{H}_2\text{O}$	2 - 3, with silica aerogel particles added	0.041 - 0.113 (0.08 - 0.16 with silica aerogel)	799 with silica aerogels from sodium silicate, 433 with silica from TMOS	1 (up to 4.2 with silica aerogels)	0.044 - 0.055 (0.04 - 0.05 with silica aerogels)		Laskowski et al. 2016
cellulose fiber powder	$\text{Ca}(\text{SCN})_2 \cdot 6\text{H}_2\text{O}$	3	0.057 (0.093 with Ag particles)	170 (166 with Ag particles)			catalytic applications	Schestakow et al. 2016b
	$\text{ZnCl}_2 \cdot 4\text{H}_2\text{O}$							

MCC		2 - 5	0.06 - 0.3		5.0 - 95		mechanical modelling	Rege et al. 2016
MCC		1 - 5	0.1 - 0.3	212 - 340	5 - 120		coagulation in different non-solvents	Schestakow et al. 2016a
	TBAF/DMSO·3H₂O							
cotton linters		3	0.067	328	5.1		thermoporosimetry used for pore size distribution	Pircher et al. 2016
freeze-dried								
	solvent							
Whatman CF11	Ca(SCN) ₂ ·4H ₂ O	0.5 - 3	0.02 - 0.1 (freeze-drying)	150 - 190 (solvent exchange); 70 - 100 (freeze-drying)				Jin et al. 2004

Whatman CF11	LiCl/DMSO	3 - 7	0.07 - 0.14	190 - 213				Wang et al. 2012
filter paper	LiCl/DMSO	3	0.075	185				Wang et al. 2012
cotton linters	NaOH/thiourea/water	2 - 5	0.23 - 0.3			0.03 - 0.033 (hydrophobised)	hydrophobic treatment with plasma, thermal cond vs humidity	Shi et al. 2013a
cotton linters	NaOH/thiourea/water	2 - 5, mixed with TEOS	0.23 - 0.45			0.026 - 0.031	hydrophobised	Shi et al. 2013b
recycled cellulose	NaOH/urea/water	2	0.04			0.029 - 0.032	hydrophobisation with water repellent spray (ReviveX®Nubuck) and with methyltrimethoxy silane, oil absorption	Nguyen et al. 2014
not	LiOH/urea/water	3		149 (500			absorption of organic solvents	Wang et al. 2014

specified				carbon)			and oil	
cotton linters	NaOH/urea/water			859 - 1364 (carbons)			activated carbons with high capacitance and adsorption of CO ₂	Zhuo et al. 2016
MCC	[Emim][Ac]	3 - 11	0.05 - 0.16	10 - 60				Buchtova and Budtova 2016
MCC	NaOH/water			299 (892 carbon)			carbons for supercapacitors	Zu et al. 2016
filter paper	LiOH/urea/water (drying from TBA)	2		261-333			with microalgae added, for Cd adsorption	Hwang et al. 2018
bamboo pulp	NaOH/urea/water		0.01 - 0.02	619 - 1085 (only carbons)			only carbons	Yang et al. 2018

2072

2073

2074